How many sabretooths? Reevaluating the number of carnivoran sabretooth lineages with total-evidence Bayesian techniques and a novel origin of the Miocene Nimravidae

PAUL Z. BARRETT,[1,2,*] SAMANTHA S. B. HOPKINS[1,2,3] and SAMANTHA A. PRICE[4]

[1]Department of Earth Sciences, University of Oregon, Eugene, Oregon 97403, U.S.A., pbarrett@uoregon.edu

[2]Museum of Natural and Cultural History, University of Oregon, Eugene, Oregon 97403, U.S.A.

[3]Clark Honors College, University of Oregon, Eugene, Oregon 97403, U.S.A., shopkins@uoregon.edu

[4]Department of Biological Sciences, Clemson University, Clemson, South Carolina 29634, U.S.A.

Journal of Vertebrate Paleontology

Character List

Characters 42 and 48 of Wesley-Hunt and Flynn (2005) modified as below to incorporate the unique conditions of derived feliforms and sabretooth carnivores. Additionally, characters 21, 43, 99, 140, 159, 165, 197, 198 and 214 were deleted for this analysis as advocated by Spaulding and Flynn (2012), or became invariant characters due to the removal of "creodonts" and other stem carnivoramorphans.

Institutional Acronyms: University of California Museum of Paleontology, Berkeley, California, USA (**UCMP**)

1. Lacrimal facial process: (0) broad rostral flange; (1) small, present on face; (2) not present on face; (3) orbital flange reduced to area around lacrimal foramen (Wesley-Hunt and Flynn (2005) character 1).

2. Ventral exposure of premaxilla; posterior extent of premaxilla, lateral to palatal foramen: (0) lateral to canine (1) anterior to canine (Wesley-Hunt and Flynn (2005) character 2).

3. Shape of infraorbital foramen: (0) elongate; (1) round (Wesley-Hunt and Flynn (2005) character 3).

4. Position of infraorbital foramen: (0) positioned above P3; (1) positioned above anterior edge of P4; (2) positioned above mid-posterior portion of P4 (Wesley-Hunt and Flynn (2005) character 4).

5. Length of palate – position of the posterior edge of palatine midline relative to tooth row: (0) posterior to upper tooth row; (1) anterior or equal to upper tooth row (Wesley-Hunt and Flynn (2005) character 5).

6. Palatine canal primary anterior opening: (0) opening through palatine; (1) at maxilla–palatine suture; (2) opening through maxilla (Wesley-Hunt and Flynn (2005) character 6).

7. Relative length of frontal and parietal atmidline: (0) parietal greater than frontal; (1) parietal equal or subequal to frontal; (2) frontal midline much longer than parietal (Wesley-Hunt and Flynn (2005) character 7).

8. Postorbital process: (0) prominent; (1) small, reduced (Wesley-Hunt and Flynn (2005) character 8).

9. Paroccipital process size: (0) well-developed; (1) reduced (Wesley-Hunt and Flynn (2005) character 9).

10. Paroccipital process shape: (0) simple process; (1) laterally flattened, thin, but is distinct process; (2) cupped around bulla, process not distinct; (3) absent (Wesley-Hunt and Flynn (2005) character 10).

11. Placement of postglenoid foramen: (0) medially placed; (1) more lateral, external, very near edge of skull (Wesley-Hunt and Flynn (2005) character 11).

12. Postglenoid foramen: (0) present; (1) greatly reduced, or missing (Wesley-Hunt and Flynn (2005) character 12).

13. Shape of mastoid process: (0) forming a distinct process, extending out farther than paroccipital process, or subequal; (1) blunt, rounded, does not protrude significantly, more a swelling of the mastoid; (2) thin plate, no distinct process (Wesley-Hunt and Flynn (2005) character 13).

14. Direction of mastoid process extention: (0) lateral – ventral; (1) ventral; (2) lateral; (3) none, or only swelling (Wesley-Hunt and Flynn (2005) character 14).

15. Condyloid (hypoglossal) foramen position relative to postlacerate foramen: (0) distant; (1) close (less than the diameter of the hypoglossal foramen away); (2) conjoined with posterior lacerate foramen (Wesley-Hunt and Flynn (2005) character 15).

16. Condyloid (hypoglossal) foramen position relative to groove between the occipital condyle and the paroccipital process: (0) inline or within groove; (1) anterior to groove (Wesley-Hunt and Flynn (2005) character 16).

17. Posterior lacerate foramen: (0) present as a vacuity between the promontorium and the basioccipital; (1) present as an individual foramen (Wesley-Hunt and Flynn (2005) character 17).

18. Fenestra cochleae (rotunda) position relative to mastoid tubercle: (0) posterior to mastoid tubercle; (1) anterior, subequal to mastoid tubercle (Wesley-Hunt and Flynn (2005) character 18).

19. Relative distance between the foramen ovale and the alisphenoid canal: (0) separated by at least the diameter of the alisphenoid canal; (1) separated only by a thin wall; (2) no alisphenoid canal present (Wesley-Hunt and Flynn (2005) character 19).

20. Ossification of tegmen tympani: (0) facial nerve exposed ventrally; (1) facial nerve partially embedded within tegmen tympani and floored in anteromedial segment; (2) facial nerve beneath a bony sheath that defines the fossa for tensor tympani muscle (Wesley-Hunt and Flynn (2005) character 20).

21. Composition of mastoid tubercle: (0) mastoid tubercle formed by petrosal; (1) mastoid tubercle formed by squamosal (Wesley-Hunt and Flynn (2005) character 22).

22. Anterior loop of internal carotid artery: (0) lack of an anterior loop of the internal carotid artery; (1) presence of the loop – excavation in basisphenoid; (2) presence of loop – but extrabullar (Wesley-Hunt and Flynn (2005) character 23).

23. Suprameatal fossa (fossa on squamosal anterior to mastoid): (0) absent; (1) small; (2) large, well developed (Wesley-Hunt and Flynn (2005) character 24).

24. Position of internal carotid artery: (0) internal carotid artery laterally positioned, transpromontorial, runs close to margin of fenestra cochlea, presence of a promontory

artery, groove for stapedial artery may or may not be present; (1) internal carotid artery transpromontorial but medially positioned, course far from fenestra cochlea; (2) internal carotid artery medial, extrabullar, inside a bony canal formed by the caudal entotympanic (Wesley-Hunt and Flynn (2005) character 25).

25. Apron shelf on promontorium posterior to fenestra cochleae for entotympanic attachment: (0) absent; (1) blunt – surface present posterior to fenestra cochleae, but no extensive attachment possible; (2) extended, large area for attachment, may roof posterior bullar chamber (Wesley-Hunt and Flynn (2005) character 26).

26. Ventral process of promontorium: (0) absent; (1) present, medially positioned on promontorium; (2) present, anteriorly positioned (Wesley-Hunt and Flynn (2005) character 27).

27. Shape of the promontorium, anterior extension: (0) elongate, apron extension tapers to a point anteriorly, almondlike in appearance; (1) elongate, rounded anteriorly; (2) blunt, quickly truncating; (3) elongate, apron is broad, flat extension, not almond-shaped and not blunt (Wesley-Hunt and Flynn (2005) character 28).

28. Facet on promontorium indicative of ectotympanic contact: (0) absent; (1) present (Wesley-Hunt and Flynn (2005) character 29).

29. Surface of the anterior-medial promontorium or tympanic wing of basisphenoid: (0) smooth; (1) roughened surface associated with attachment of rostral entotympanic, or rostral entotympanic present (Wesley-Hunt and Flynn (2005) character 30).

30. Inferior petrosal sinus: (0) inferior petrosal sinus small; (1) inferior petrosal sinus greatly enlarged; (2) excavation into basioccipital extremely deep (Wesley-Hunt and Flynn (2005) character 31).

31. A deep, well developed fossa or pit on the squamosal/alisphenoid recording the contact with the anterior crus or anterior face of the ectotympanic: (0) absent, may have slight/shallow indentation; (1) present, well developed, or bulla present and fully ossified (Wesley-Hunt and Flynn (2005) character 32).

32. Shelf between mastoid process and paroccipital process: (0) laterally wide, curved trough with smooth surface; (1) laterally wide, could have flat surface, rugose or bulbous, no smoothed out trough; (2) very thin, outside edge could be raised; (3) no shelf present (Wesley-Hunt and Flynn (2005) character 33).

33. Extent of flange on basiocciptal lateral edge bordering auditory region: (0) absent; (1) small, nascent; (2) well developed when compared to basal ‘miacids’ (Wesley-Hunt and Flynn (2005) character 34).

34. Evidence on basisphenoid and basioccipital for marked medial inflation of the entotympanic: (0) absent; (1) present – inflation of entotympanic pushing medially onto and over the basioccipital (Wesley-Hunt and Flynn (2005) character 35).

35. Evidence of marked posterior inflation of the entotympanic; entotympanic attached during life to paroccipital process or to extensive area posterior to the petrosal: (0) absent; (1) present (Wesley-Hunt and Flynn (2005) character 36).

36. Fossa for the stapedius muscle: (0) borders tightly defined and anteriorly bound by the mastoid; (1) general area of muscle insertion, open, less defined (Wesley-Hunt and Flynn (2005) character 37).

37. Epitympanic wing of the petrosal forms ventral floor to the anterior medial corner of the fossa for the tensor tympani muscle: (0) absent; (1) present, but relatively flat and horizontal; (2) ventral floor present, but not horizontal, instead it forms a delicate 'tube', the bony floor is not an extension of the petrosal (Wesley-Hunt and Flynn (2005) character 38).

38. Fossa for the tensor tympani muscle, defined and deep, excavating well dorsal of the level of the fenestra vestibuli: (0) absent, fossa for the tensor tympani muscle shallow, not strongly defined; (1) present, defined and deep; (2) shallow/absent – tensor tympani inserts on eustachian canal (Wesley-Hunt and Flynn (2005) character 39).

39. Placement of middle lacerate foramen: (0) foramen a vacuity – not defined anteriorly nor posteriorly, positioned directly anterior to petrosal; (1) foramen anteriorly defined, posteriorly bordered by petrosal – positioned equal or posterior to basisphenoid/basioccipital suture; (2) foramen defined anteriorly, petrosal may be undefined posterior border, foramen positioned in basisphenoid (or edge of alisphenoid) just anterior to basisphenoid/basioccipital suture; (3) foramen defined anteriorly and posteriorly completely bordered by basisphenoid, foramen positioned far anterior to basisphenoid/basioccipital suture (Wesley-Hunt and Flynn (2005) character 40).

40. M1 a defined cingulum continuous around the lingual face of the protocone: (0) absent; (1) complete cingulum present; (2) anterior segment of cingulae absent or smaller than posterior cingulae (Wesley-Hunt and Flynn (2005) character 41).

41. M1 protocone height relative to paracone: (0) protocone shorter than paracone; (1) protocone equal or subequal to height of paracone; (2) protocone absent or lacks a cusp associated with the root (Wesley-Hunt and Flynn (2005) character 42).

42. M1 parastyle projects farther labially than metastyle: (0) absent; (1) present (Wesley-Hunt and Flynn (2005) character 44).

43. M1 parastyle direction: (0) buccally with anterior direction; (1) buccally; (2) no parastyle present (Wesley-Hunt and Flynn (2005) character 45).

44. M1 size: (0) well-developed; (1) markedly reduced (Wesley-Hunt and Flynn (2005) character 46).

45. M1 size of posterior lingual cingular shelf at base of protocone: (0) posterior lingual cingular shelf equal or subequal to anterior cingulum; (1) posterior lingual cingular shelf more pronounced, larger than anterior cingulum (Wesley-Hunt and Flynn (2005) character 47).

46. M1 relative height of paracone and metacone: (0) paracone equals metacone in height; (1) paracone greater than metacone; (2) metacone absent (modified from Wesley-Hunt and Flynn (2005) character 48).

47. M1 relative height of paraconule and metaconule: (0) paraconule greater than metaconule; (1) paraconule equal or subequal to metaconule; (2) both absent; (3) metaconule enlarged, greater than paraconule (Wesley-Hunt and Flynn (2005) character 49).

48. M1 presence of hypocone: (0) absent; (1) present (distinct cusp); (2) present, formed by swelling of entire cingulum ridge (Wesley-Hunt and Flynn (2005) character 50).

49. M1 width of parastylar shelf: (0) lack of a shelf; (1) broad; (2) narrow, consisting mainly of ridge (Wesley-Hunt and Flynn (2005) character 51).

50. Presence of M2: (0) present; (1) residual or reduced, simplified morphology, less than half the size of M1; (2) absent (Wesley-Hunt and Flynn (2005) character 52).

51. Presence of M3: (0) present; (1) absent (Wesley-Hunt and Flynn (2005) character 53).

52. P4/m1 carnassial shear: (0) absent; (1) present (Wesley-Hunt and Flynn (2005) character 54).

53. P4 size of parastyle cusp: (0) absent; (1) well-developed, defined cusp; (2) present as bulge on cingulum, reduced (Wesley-Hunt and Flynn (2005) character 55).

54. P4 protocone: (0) large, well-developed; (1) reduced or absent (Wesley-Hunt and Flynn (2005) character 56).

55. P4 size of metastylar blade: (0) short; (1) elongate (Wesley-Hunt and Flynn (2005) character 57).

56. Posterior accessory cusps on P3: (0) one cusp present; (1) two cusps present; (2) absent (Wesley-Hunt and Flynn (2005) character 58).

57. m2 talonid morphology: (0) high trigonid with extremely elongate talonid due to large hypoconulid, tooth elongate oval outline; (1) talonid not elongate, tooth oval outline, no enlarged hypoconulid; (2) low trigonid, extremely elongate with low, well developed talonid cusps; (3) absent (Wesley-Hunt and Flynn (2005) character 59).

58. Palatine, relative size: (0) midline length of palatine less than midline length of maxilla; (1) midline length greater than midline length of maxilla (Wesley-Hunt and Flynn (2005) character 60).

59. Posterior width of palate (versus width between canines): (0) wider than width at canines; (1) nearly equal (resulting in nearly parallel tooth rows) (Wesley-Hunt and Flynn (2005) character 61).

60. Turbinal bones: (0) simple development of maxilloturbinals in nasal cavity; (1) maxilloturbinals large and branching, excluding nasoturbinals from narial opening (Wesley-Hunt and Flynn (2005) character 62).

61. Posterior projection of nasals: (0) nasals terminate anterior to, or in extreme anterior region of, orbit, projecting at most slightly between frontals; (1) nasals project deeply between frontals, far posterior of anterior orbital rim; (2) nasals with W-shaped termination; (3) nasals with flat termination (Wesley-Hunt and Flynn (2005) character 63).

62. Jugal: (0) jugal reaches lacrimal, or is separated from it by only thin sliver of maxilla; (1) jugal widely separated from lacrimal, maxilla broadly laps posteriorly over anterior orbital rim (Wesley-Hunt and Flynn (2005) character 64).

63. Anterior extent of palatine in orbit: (0) broadly contacts lacrimal; (1) fails to contact lacrimal (Wesley-Hunt and Flynn (2005) character 65).

64. Postorbital constriction: (0) just anterior of frontoparietal suture, ear posterior margin of frontal; (1) braincase expanded, with frontals making much greater contribution; fronto–parietal suture located more anteriorly in frontal (Wesley-Hunt and Flynn (2005) character 66).

65. Posterior entrance of carotid artery into auditory capsule: (0) posterior entry, artery not enclosed in osseous tube; (1) posterior entry, artery enclosed in tube; (2) anterior entry, artery enclosed in osseous tube; (3) anterior entry, artery not enclosed in tube (Wesley-Hunt and Flynn (2005) character 67).

66. Entotympanic: (0) fails to ossify, or is only weakly attached to auditory capsule; (1) ossified at least partially, and firmly fused to the skull (Wesley-Hunt and Flynn (2005) character 68).

67. Ectotympanic contributes to external auditory meatal tube: (0) no; (1) yes (Wesley-Hunt and Flynn (2005) character 69).

68. Ectotympanic septum: (0) absent; (1) present (Wesley-Hunt and Flynn (2005) character 70).

69. Entotympanic septum: (0) absent; (1) present (Wesley-Hunt and Flynn (2005) character 71).

70. Fenestra cochleae: (0) approximately equal in size to fenestra ovalis, cochlear fossula not developed; (1) at least three times the area of oval window, cochlear fossula well developed (Wesley-Hunt and Flynn (2005) character 72).

71. Malleus, muscular process: (0) present; (1) absent (Wesley-Hunt and Flynn (2005) character 73).

72. Malleus, processus gracilis and anterior lamina: (0) well developed; (1) reduced (Wesley-Hunt and Flynn (2005) character 74).

73. Major a2 arterial shunt: (0) small; (1) large, intracranial rete (Wesley-Hunt and Flynn (2005) character 75).

74. Major a4 arterial shunt: (0) absent; (1) present (Wesley-Hunt and Flynn (2005) character 76).

75. Major anastomosis x: (0) absent; (1) present (Wesley-Hunt and Flynn (2005) character 77).

76. i1: (0) present; (1) absent (Wesley-Hunt and Flynn (2005) character 78).

77. P1: (0) present; (1) absent (Wesley-Hunt and Flynn (2005) character 79).

78. P3 lingual cusp: (0) absent; (1) present (Wesley-Hunt and Flynn (2005) character 80).

79. P4 metastyle: (0) V- or slit-shaped notch; (1) notch absent (Wesley-Hunt and Flynn (2005) character 81).

80. P4 protocone: (0) medial or posterior to paracone; (1) anterior to paracone (Wesley-Hunt and Flynn (2005) character 82).

81. P4 hypocone: (0) absent; (1) present (Wesley-Hunt and Flynn (2005) character 83).

82. p1: (0) present; (1) absent (Wesley-Hunt and Flynn (2005) character 84).

83. m1 talonid: (0) present; (1) absent (Wesley-Hunt and Flynn (2005) character 85).

84. Lower molars: (0) subequal in size; (1) m1 much larger than m2–3 and progressive decrease in size from m1–3 (Wesley-Hunt and Flynn (2005) character 86).

85. M2 hypocone: (0) absent; (1) present (Wesley-Hunt and Flynn (2005) character 87).

86. m3: (0) present; (1) absent (Wesley-Hunt and Flynn (2005) character 88).

87. Baculum: (0) small and simple or absent; (1) long, stylized (Wesley-Hunt and Flynn (2005) character 89).

88. Scapula, postscapular fossa: (0) absent; (1) present (Wesley-Hunt and Flynn (2005) character 90).

89. Tail: (0) long; (1) reduced (Wesley-Hunt and Flynn (2005) character 91).

90. Scaphoid and lunate: (0) unfused; (1) fused (Wesley-Hunt and Flynn (2005) character 92).

91. Hallux: (0) present; (1) greatly reduced or absent (Wesley-Hunt and Flynn (2005) character 93).

92. Femur, third trocanter: (0) present; (1) absent (Wesley-Hunt and Flynn (2005) character 94).

93. Cowper's (bulbourethral) gland: (0) present; (1) absent (Wesley-Hunt and Flynn (2005) character 95).

94. Prostate gland: (0) small/vestigial; (1) large, ampulla bilobed (Wesley-Hunt and Flynn (2005) character 96).

95. Kidneys: (0) simple; (1) conglomeratic (Wesley-Hunt and Flynn (2005) character 97).

96. Anal glands: (0) simple; (1) enlarged and having enlarged anal sac (Wesley-Hunt and Flynn (2005) character 98).

97. Scapula – supraglenoid tubercle morphology: (0) expands out over the glenoid fossa; (1) blunt, does not extend over the glenoid fossa (Spaulding and Flynn (2012), character 100).

98. Scapula – acromion process angle: Either or a short or a long process can be dorsally directed at the acromion process apex, or remain in the same plane as the scapular spine: (0) process angles dorsally; (1) process remains in same plane as the scapular spine (Spaulding and Flynn (2012), character 101).

99. Scapula – acromion process length: The acromion process can terminate far distally to the glenoid fossa or terminate at or before the border. A long acromion can be used as a proxy for the presence of clavicles in extinct taxa. (0) process extends past glenoid fossa; (1) process terminates before or at glenoid fossa (Spaulding and Flynn (2012), character 102).

100. Scapula – coracoid process: (0) present, as a large clearly projecting process; (1) extremely small or absent (Spaulding and Flynn (2012), character 103).

101. Scapula – scapular spine morphology: Coded while viewing the spine from a ventral view of the scapula. (0) spine forms one continuous, smooth, downward curve; (1) spine has a dip or embayment in the curve; (2) spine has a sharply angled drop rather than a smooth downward slope (Spaulding and Flynn (2012), character 104).

102. Scapula – metacromion process: (0) present and well developed; (1) weak or absent (Spaulding and Flynn (2012), character 105).

103. Humerus – indentation on the anterior surface of the capitulum : (0) present; (1) absent (Spaulding and Flynn (2012), character 106).

104. Humerus – olecranon fossa shape (Matthew 1909): (0) shallow and round; 1: deep and slot-like; (2) perforated (Spaulding and Flynn (2012), character 107).

105. Humerus – medial edge of posterior trochlea (new): (0) vertical; (1) slanted (Spaulding and Flynn (2012), character 108).

106. Humerus – delto-pectoral crest: (0) present; (1) absent (Spaulding and Flynn (2012), character 109).

107. Humerus – medial epicondyle: (0) ends with a well rounded head; (1) poorly defined, appearing more like a blunt tubercle (Spaulding and Flynn (2012), character 110).

108. Humerus – medial epicondyle orientation: (0) lacks curvature (is straight); (1) curves anteriorly; (2) curves posteriorly (Spaulding and Flynn (2012), character 111).

109. Humerus – greater tuberosity height: (0) extends past head; (1) flush with head in height (Spaulding and Flynn (2012), character 112).

110. Humerus – posterior trochlea: (0) not bound by high ridges; (1) bound by high ridges (Spaulding and Flynn (2012), character 113).

111. Humerus – brachial flange: (0) present and large, extending out from the body of the bone as a flat surface; (1) small, nothing but a small raised line of bone (Spaulding and Flynn (2012), character 114).

112. Humerus – lesser tuberosity with a crest or ridge of bone leading from this feature down the shaft: (0) present; (1) absent (Spaulding and Flynn (2012), character 115).

113. Humerus – trochlea extent: (0) extends distally past capitulum when viewed anteriorly; (1) two articular surfaces are more inline (Spaulding and Flynn (2012), character 116).

114. Humerus – epicondylar foramen: (0) absent; (1) present and round; (2) present and elongated (Spaulding and Flynn (2012), character 117).

115. Humerus – distal L-shaped ridge of bone on capitulum in distal view: (0) present; (1) absent (Spaulding and Flynn (2012), character 118).

116. Humerus – orientation of bone on the lateral distal margin: (0) faces laterally; (1) faces posteriorly (Spaulding and Flynn (2012), character 119).

117. Humerus – ulnar collateral ligament insertion site size; (0) very large, forming a distinct circular pit; (1) small, forming only a shallow depression (Spaulding and Flynn (2012), character 120).

118. Humerus – greater tuberosity angle: (0) greater tuberosity angled away from head; smooth arch is not formed with lesser tuberosity; (1) greater tuberosity more flush with head (Spaulding and Flynn (2012), character 121).

119. Humerus – prominence of bicipital groove: (0) groove is very noticeable and deep; (1) groove is very subtle if noticeable at all (Spaulding and Flynn (2012), character 122).

120. Humerus – capitulum shape: (0) flat for the whole length with a uniform distal margin; (1) rounded (Spaulding and Flynn (2012), character 123).

121. Humerus - tricipital line: (0) large and distinctive; (1) reduced (Spaulding and Flynn (2012), character 124).

122. Ulna – semi-lunar notch distal border morphology: (0) W-shaped distal border; an indentation occurs between the articular surface with the radius and the rest of the facet; (1) indentation lacking (Spaulding and Flynn (2012), character 125).

123. Ulna – semi-lunar notch proximal border extent: (0) proximal ridge extends far from shaft surface; (1) proximal ridge flush with shaft surface (Spaulding and Flynn (2012), character 126).

124. Ulna – m. bracialis insertion site: (0) present; (1) absent (Spaulding and Flynn (2012), character 127).

125. Ulna – m. bracialis insertion site position: (0) on anterior surface of ulna; (1) on the lateral margin of the shaft (Spaulding and Flynn (2012), character 128).

126. Ulna – radial notch curvature: (0) absent; (1) present (Spaulding and Flynn (2012), character 129).

127. Ulna – flange presence on distal region of the shaft: (0) two flanges present and well defined; (1) flanges absent (Spaulding and Flynn (2012), character 130).

128. Ulna – deep tendon groove on proximal end of ulna; (0) present; (1) absent (Spaulding and Flynn (2012), character 131).

129. Ulna – olecranon process shape: (0) mediolaterally robust, square in shape; (1) mediolaterally compressed (Spaulding and Flynn (2012), character 132).

130. Ulna – anconeal process extent: (0) projecting from the shaft, shelf like; (1) flush with shaft (Spaulding and Flynn (2012), character 133).

131. Ulna – proximal border of semi-lunar notch, position: (0) lateral to the shaft; (1) centered with respect to the shaft (Spaulding and Flynn (2012), character 134).

132: Ulna – anteriormedial protuberuance development: (0) well developed; (1) small (Spaulding and Flynn (2012), character 135).

133. Ulna – groove on lateral side of shaft: (0) present; (1) absent (Spaulding and Flynn (2012), character 136).

134. Ulna shape – sigmoidal; the ulna is used as a proxy for the curved nature of all forelimb bones: (0) sigmoidal; (1) straight (Spaulding and Flynn (2012), character 137).

135. Ulna – radial notch orientation: (0) faces anteriorly; (1) faces more laterally (Spaulding and Flynn (2012), character 138).

136. Radius – radial head shape: (0) round; (1) oval (Spaulding and Flynn (2012), character 139).

137. Radius – large scaphoid articulation surface: (0) present; (1) surface small (Spaulding and Flynn (2012), character 141).

138. Radius – capitular eminence of radial head development: (0) small; (1) large, disrupts radial rim (Spaulding and Flynn (2012), character 142).

139. Radius – distal articulation surface shape: (0) with a deep sulcus; (1) smooth, lacks a deep sulcus (Spaulding and Flynn (2012), character 143).

140. Carpus – cuneiform shape in proximal view: (0) triangular; (1) rectangular (Spaulding and Flynn (2012), character 144).

141. Carpus – proximal surface of scapholunar, curvature: (0) fully convex; (1) convex and concave (Spaulding and Flynn (2012), character 145).

142. Carpus – uniciform width: (0) as wide as trapezoid and magnum combined; (1) small, only as wide as magnum alone (Spaulding and Flynn (2012), character 146).

143. Carpus – trapezium position: (0) on the posterior surface of the trapezoid ; (1) on the radial surface of the trapezoid (Spaulding and Flynn (2012), character 147).

144. Carpus – metacarpal III overlaps IV proximally: (0) absent; (1) present (Spaulding and Flynn (2012), character 148).

145. Carpus – distal surface of scapholunar shape: (0) relatively smooth/even; (1) a sharp projection exists between the magnum and trapezoid (Spaulding and Flynn (2012), character 149).

146. Carpus – cuneiform articulation with ulna, position: (0) on medial (radial) margin; (1) on distal surface of ulna (Spaulding and Flynn (2012), character 150).

147. Carpus –metacarpal II strongly overlaps III proximally: (0) overlap small or absent; (1) overlap present and substantial (Spaulding and Flynn (2012), character 151).

148. Carpus – metacarpal length: (0) metacarpal lengths are equivalent to sum of phalanges; (1) metacarpals are much longer than sum of phalangeal lengths; (2) phalanges are longer than metacarpals (Spaulding and Flynn (2012), character 152).

149. Carpus – medial phalanx distal articular surface symmetry: (0) symmetrical; (1) asymmetrical (Spaulding and Flynn (2012), character 153).

150. Carpus – proximal phalanges compressed dorsoventrally: (0) absent; (1) present (Spaulding and Flynn (2012), character 154).

151. Carpus – lateral excavation of the medial phalanx: (0) absent; (1) present (Spaulding and Flynn (2012), character 155).

152. Femur – lesser trochanter orientation: (0) projects posteriorly; (1) projects medially (Spaulding and Flynn (2012), character 156).

153. Femur – intertrochanteric crest extent: (0) extends to lesser trochanter; (1) becomes flush with shaft before reaching the lesser trochanter (Spaulding and Flynn (2012), character 157).

154. Femur – position of lesser trochanter relative to the third trochanter: (0) third trochanter is lower; (1) third trochanter is roughly at the same level (Spaulding and Flynn (2012), character 158).

155. Femur – supracondylar tuberosities: (0) absent; (1) presence of two or more raised tuberosities just proximal to the condyles of the femur on the posterior shaft (Spaulding and Flynn (2012), character 160).

156. Femur – height of greater trochanter relative to head of femur: (0) greater trochanter is higher or sub-equal; (1) greater trochanter is lower than head of femur (Spaulding and Flynn (2012), character 161).

157. Femur – medial condyle morphology: (0) proximal edge of the articular surface of condyles are flush with the shaft, due to the lack of development of a condylar neck; (1) proximal edge of the articular surface of condyles are not flush with the shaft, due to the development of a condylar neck (Spaulding and Flynn (2012), character 162).

158. Femur – lesser trochanter development: (0) strong, prominently projecting feature; (1) small, barely more than a small bump or ridge on the shaft (Spaulding and Flynn (2012), character 163).

159. Femur – greater trochanter broadest surface, orientation: (0) faces laterally; (1) faces posteriorly (Spaulding and Flynn (2012), character 164).

160. Femur – patellar groove shape: (0) deep and narrow; (1) wide and flat (Spaulding and Flynn (2012), character 166).

161. Femur – position of greater trochanter relative to shaft: (0) greater trochanter over distal midline; (1) greater trochanter lateral to midline (Spaulding and Flynn (2012), character 167).

162. Tibia – tibia and fibula fusion: (0) fusion present; (1) fusion absent (Spaulding and Flynn (2012), character 168).

163. Tibia – deep groove on the posterior surface of the tibia: (0) present; (1) absent (Spaulding and Flynn (2012), character 169).

164. Tibia – posterior bone spur on distal tibia: (0) presence of a prominent bone spur on the posterior margin; (1) spur absent (Spaulding and Flynn (2012), character 170).

165. Tibia – contact of inner borders of condyles: (0) in contact; (1)separate (Spaulding and Flynn (2012), character 171).

166. Tibia – internal malleolus morphology: (0) forms a clear and distinct well-defined point; (1) indistinct, forming a general extension of the medial surface of the tibia (Spaulding and Flynn (2012), character 172).

167. Pes – astragalus – length of medial border of astragalar tibial trochlea: (0) shorter than lateral; (1) longer than lateral (Spaulding and Flynn (2012), character 173).

168. Pes – dorsal surface of astragalus, shape: (0) smooth; (1) grooved (Spaulding and Flynn (2012), character 174).

169. Pes – astragalus – height of fibular facet: (0) height subequal to length, resulting in a roughly square shaped facet; (1) height much less than length, resulting in a more crescent shaped feature (Spaulding and Flynn (2012), character 175).

170. Pes – astragalar head shape when viewed dorsally: (0) rounded; (1) flattened (Spaulding and Flynn (2012), character 176).

171. Pes – height of astragalar head when viewed distally: (0) apex of astragalar head even with or higher than articular surface; (1) apex of astragalar head very low, does not rise above astragalar neck (head flattened); (2) apex of astragalar head rises in between astragalar neck and articular surface of astragalar body (Spaulding and Flynn (2012), character 177).

172. Pes – astragalus fossa, on the lateral edge, posterior ventral quadrant: (0) present; (1) absent (Spaulding and Flynn (2012), character 178).

173. Pes – astragalus lateral margin, anterior ventral edge expansion: (0) lateral expansion present; (1) expansion absent, creating a much smoother margin. (Spaulding and Flynn (2012), character 179).

174. Pes – astragalar head medial articulation surface extent: (0) extends backwards a great distance, past the border of the sustentacular facet; (1) short, does not extend past the start of the neck. (Spaulding and Flynn (2012), character 180).

175. Pes – astragalus sustentacular facet shape: (0) has clear edges, is somewhat convex, and does not extend into gully; (1) is more flat than convex and extends into gully (Spaulding and Flynn (2012), character 181).

176. Pes – astragalar foramen; (0) present and dorsally positioned; (1) present and posteriorly positioned; (2) absent (Spaulding and Flynn (2012), character 182).

177. Pes – astragalus, posterior ridge for ligament attachments, presence: (0) present, high; (1) low or absent (Spaulding and Flynn (2012), character 183).

178. Pes – astragalus, orientation of posterior ridge for ligament attachments: (0) orientated at an oblique angle relative to the long axis of the astragalar trochlea; (1) orientated in line with the trochlea (Spaulding and Flynn (2012), character 184).

179. Pes – astragalus-tibia articulation surface, extent: (0) covers entire posterior dorsal surface; (1) restricted, fails to cover entire posterior dorsal surface, leaving a gap in the lateral posterior quadrant (Spaulding and Flynn (2012), character 185).

180. Pes – astragalus border heights: (0) lateral border subequal in height to medial border; (1) lateral border raised relative to medial border; (2) medial border higher (Spaulding and Flynn (2012), character 186).

181. Pes – astragalus, cotylar fossa presence: (0) present; (1) absent (Spaulding and Flynn (2012), character 187).

182. Pes – Calcaneus, sustentaculum position: (0) far from anterior border, roughly in the middle of the calcaneus; (1) close to anterior border (Spaulding and Flynn (2012), character 188).

183. Pes – Calcaneus, peroneal tubercle development: (0) weakly developed, little more than a ridge; (1) well developed (Spaulding and Flynn (2012), character 189).

184. Pes – astragalus neck development: (0) absent (lacks a clearly defined neck of astragalus); (1) present (Spaulding and Flynn (2012), character 190).

185. Pes – calcaneus, cuboid facet shape: (0) irregularly shaped; (1) round (Spaulding and Flynn (2012), character 191).

186. Pes – calcaneus, cuboid facet orientation: (0) angled dorsally; (1) in planes other than dorsal (Spaulding and Flynn (2012), character 192).

187. Pes – calcaneus, fibular facet: (0) present; (1) absent (Spaulding and Flynn (2012), character 193).

188. Pes – calcaneus –dorsal facet morphology: (0) smooth; (1) clearly defined, sharp corner (rather than a smooth curve) (Spaulding and Flynn (2012), character 194).

189. Pes – cuboid, contact with metatarsal V: (0)small (less than 40%) articular surface for metatarsal V; (1) large, articular surface for metatarsal V at least 40% of distal surface (Spaulding and Flynn (2012), character 195).

190. Pes – cuboid shape: (0) relatively rectangular; (1) wider proximally than distally (Spaulding and Flynn (2012), character 196).

191. Pes – navicular height: (0) height less than width; (1) height roughly equal to or greater than width (Spaulding and Flynn (2012), character 199).

192. Pelvis – ilium, anterior expansion: (0) not expanded; (1) expanded dorsoventrally (Spaulding and Flynn (2012), character 200).

193. Pelvis – ischial spine position: (0) located just posterior of the border of the acetabulum; (1) far posterior from acetabulum; (2) spine absent (Spaulding and Flynn (2012), character 201).

194. Pelvis – dorsal margin of acetabulum, position: (0) even with or above dorsal surface of pelvis; (1) ventral to dorsal surface of pelvis (Spaulding and Flynn (2012), character 202).

195. Pelvis – angle at pubic symphysis: (0) 'U' like (*Canis*); (1) 'V' like (*Felis*) (Spaulding and Flynn (2012), character 203).

196. Pelvis – ilium, anterior region morphology: (0) broad and flat (*Canis*); (1) divided by a distinct ridge running antero-posteriorly (*Vulpavus*) (Spaulding and Flynn (2012), character 204).

197. Pelvis – ilium, ventral surface morphology: (0) broad and flat; (1) narrow (Spaulding and Flynn (2012), character 205).

198. Atlas – posterior transverse foramen position: (0) dorsal to the transverse processes (1) in line with or ventral to the transverse processes (Spaulding and Flynn (2012), character 206).

199. Atlas – alar foramen: (0) absent, only a notch is present; (1) present, confluent with lateral vertebral foramen; (2) present, separate from lateral vertebral foramen (Spaulding and Flynn (2012), character 207).

200. Atlas – transverse processes, orientation: (0) projects at right angle from the body; (1) extends posteriorly at an acute angle to the body (Spaulding and Flynn (2012), character 208).

201. Atlas – ventral arch length: (0) equal to or shorter than dens of axis; (1) longer than dens of axis (Spaulding and Flynn (2012), character 209).

202. Axis – body length: (0) roughly as long as it is wide; (1) elongated relative to its width (Spaulding and Flynn (2012), character 210).

203. Cervical vertebrae – keel: (0) large ventral keel present; (1) ventral keel absent (Spaulding and Flynn (2012), character 211).

204. Cervical vertebrae – spinous processes, size: (0) large; (1) small (Spaulding and Flynn (2012), character 212).

205. Cervical vertebrae – dorsal lateral margin shape: (0) concave; (1) convex (Spaulding and Flynn (2012), character 213).

206. Sacrum – size compared to pelvis: (0) small, does not reach border of acetabulum; (1) large, reaches border of acetabulum (Spaulding and Flynn (2012), character 215).

207. Sacrum – neural spines: (0) clear and distinct from one another; (1) fused to one another, appearing as one long keel; (2) spines very small, hardly more than small bumps on the sacrum (Spaulding and Flynn (2012), character 216).

208. Ventral flange on the anterior part of the dentary: (0) absent; (1) present. The genial flange is a common feature amongst sabertooth carnivores, and as noted by Solé *et al.* (2014), also present in *Uintacyon* and *Tapocyon*.

209. Tooth serrations on upper canines: (0) absent; (1) present. Crenulations or denticles on the posterior or anterior edge of the upper canine are not a universal feature of sabretooth taxa, *Megantereon* lacks them, but are extremely common amongst most species.

210. p3: (0) similar height to p4; (1) substantially reduced crown height compared to p(4) see Barrett (2016) character # 26; (2) absent. Reduction or loss of the lower p3 is a common feature of the more-derived sabertooth taxa, such as *Smilodon* or *Hoplophoneus cerebralis*. However, no reported barbourofeline taxon loses this tooth, even the most-derived, *Barbourofelis fricki*.

211. P3: (0) crown height similar to P4; (1) crown height of P3 70% or less of P4.

212. C1 vertical grooves: (0) absent; (1) present. Two of the ingroup taxa of this analysis possess this feature, the barbourofelids which all display an hourglass-shape cross-section, and *Ailurus fulgens* which possess the diagnostic ailurid lateral groove (Wallace, 2011).

213. P4 nimravid "parastyle": (0) absent; (1) present. Flynn and Galiano (1982) viewed this cusp on the P4 of nimravids (inclusive of barbourofelines) to not be homologous with the feliform parastyle (deriving from the cingular base of the tooth). Instead, the prior authors viewed this structure as an elaboration of a strong anterior ridge of the paracone. After surveying numerous stem and derived nimravid specimens, we concur with the findings of Flynn and Galiano (1982). The nimravid "parastyle" is formed at the juncture of three cristae on the anterior edge of the paracone, emanating from the buccal-cingular, medial-cingular, and ventral apices (see Figure S1). In *Nimravus* and *Pogonodon* this triple-juncture is present, but lacking in a cusp (though UCMP 76603) *Nimravus brachyops*, possesses a nascent cusp in this area). However, *Hoplophoneus* specimens develop a distinct ventral projecting cusp at this location, simple at first as shown in the below figure, but substantially developed (comparable to basal barbourofelines) in the more-derived Oligocene taxa (*e.g*. *Hoplophoneus cerebralis*).

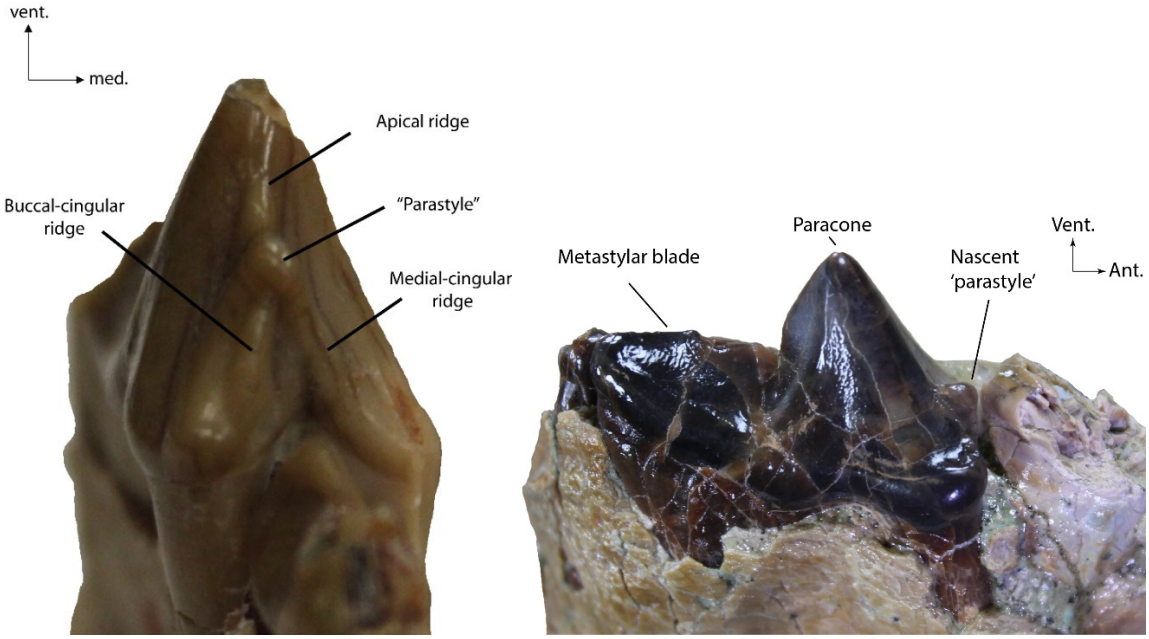

Figure S1. Left: P4 of UCMP 28019, *Hoplophoneus primaevus*. Note the triple-juncture of cristae, which at their intersection form the nimravid "parastlye". Right: P4 of UCMP 76603 *Nimravus brachyops.* Note the nascent 'parastyle' near the cingulum at the anterior of the paracone.

214. P4 preparastyle: (0) absent; (1) present. This feature is likely analogous to the ectostyle of the most-derived machairodontine felids (e.g. *Smilodon*), and similarly restricted to the most-derived members of the Barbourofelinae (Geraads and Güleç, 1997; Morlo et al., 2004; Robles et al., 2013).

215. P2: (0) double-rooted; (1) single-rooted; (2) absent.

216. c1: (0) larger than i3; (1) same size. Reduction in size of the lower canine relative to the adjacent incisors has been noted as a synapomorphy for the Machairodontinae and a more diagnostic character than saber teeth for the clade (Christiansen, 2013). However, this feature is also seen in both nimravid and barbourofeline lineages.

217. m1 metaconid: (0) present; (1) absent.

218. Caniform incisors: (0) absent; (1) present.

219. Procumbent incisors: (0) absent; (1) present.

220. p3 posterior cusps: (0) one cusp (posterior cingular cusp); 1: two cusps (Posterior cingular cusp and posterior accessory cusp).

221. p4 posterior cusps. 0: one cusp (posterior cingular cusp); 1: two cusps (Posterior cingular cusp and posterior accessory cusp).

222. Basicranial foramina: (0) petrobasilar venous sinus and sigmoid sinus merge intracranially and exit the posterior lacerate (jugular) foramen; (1) veins merge

extracranially, passing through the petrobasilar and posterior lacerate foramina respectively.

223. Rostral entotympanic septum: (0) absent; (1) present. The Eocene-Oligocene Nimravidae are united by this derived feature, a condition differential from all other Carnivoramorpha. The condition of "barbourofeline" taxa is unknown due to lack of visible sutures between the tympanic elements of any known specimen. Wang et al. (2020)'s description of a rostral entotympanic element in the bullar capsule of *Oriensmilus liupanensis* is at odds with the body of literature describing the anatomical associations of carnivoran bullar elements, especially those of nimravid taxa (Hunt, 1974 1989, 2001; Ivanoff, 2001 2019; Joeckel et al., 2002). However, it can be said that the barbourofeline condition is different from the aeluroid, cynoid or arctoid condition (Ivanoff, 2001), and either an elaboration of the nimravid condition or unique unto themselves (Neff, 1983; Hunt, 1987). Thus, barbourofelines were scored as "?" for this study.

REFERENCES

Barrett, P. Z. 2016. Taxonomic and systematic revisions to the North American Nimravidae (Mammalia, Carnivora). PeerJ 4:e1658.

Christiansen, P. 2013. Phylogeny of the sabertoothed felids (Carnivora: Felidae: Machairodontinae). Cladistics 29:543–559.

Flynn, J. J., and H. Galiano. 1982. Phylogeny of early Tertiary Carnivora, with a description of a new species of Protictis from the middle Eocene of northwestern Wyoming. American Museum Novitates 2725:1–64.

Geraads, D., and E. Güleç. 1997. Relationships of Barbourofelis piveteaui (Ozansoy, 1965), a late miocene nimravid (Carnivora, Mammalia) from Central Turkey. Journal of Vertebrate Paleontology 17:370–375.

Hunt, R. M. 1974. The auditory bulla in Carnivora: an anatomical basis for reappraisal of carnivore evolution. Journal of Morphology 143:21–75.

Hunt, R. M. 1987. Evolution of the aeluroid Carnivora: significance of auditory structure in the nimravid cat Dinictis. American Museum Novitates 2886:1–74.

Hunt, R. M. 1989. Evolution of the Aeluroid Carnivora: Significance of the Ventral Promontorial Process of the Petrosal, and the Origin of Basicranial Patterns in the Living Families. American Museum Novitates 2930:1–32.

Hunt, R. M. 2001. Basicranial anatomy of the living linsangs Prionodon and Poiana (Mammalia, Carnivora, Viverridae), with comments on the early evolution of aeluroid carnivorans. American Museum Novitates 3330.

Ivanoff, D. V. 2019. Composition of the canid auditory bulla and a new look at the evolution of carnivoran entotympanics. Organisms Diversity and Evolution 363–375.

Ivanoff, D. V. 2001. Partitions in the carnivoran auditory bulla: their formation and significance for systematics. Mammal Review 31:1–16.

Joeckel, R. M., S. Peigné, R. M. Hunt Jr., and R. I. Skolnick. 2002. The auditory region and nasal cavity of Oligocene Nimravidae (Mammalia: Carnivora). Journal of Vertebrate Paleontology 22:830–847.

Morlo, M., S. Peigné, and D. Nagel. 2004. A new species of Prosansanosmilus: implications for the systematic relationships of the family Barbourofelidae new rank (Carnivora, Mammalia). Zoological Journal of the Linnean Society 140:43–61.

Neff, N. A. 1983. The basicranial anatomy of the Nimravidae (Mammalia: Carnivora) : character analyses and phylogenetic inferences. City University of New York, 642 pp.

Robles, J. M., D. M. Alba, J. Fortuny, S. De Esteban-Trivigno, C. Rotgers, J. Balaguer, R. Carmona, J. Galindo, S. Almecija, J. V Berto, and S. Moya-Sola. 2013. New craniodental remains of the barbourofelid Albanosmilus jourdani (Filhol, 1883) from the Miocene of the Valles-Penedes Basin (NE Iberian Peninsula) and the phylogeny of the Barbourofelini. Journal of Systematic Palaeontology 11:993–1022.

Solé, F., R. Smith, T. Coillot, E. de Bast, and T. Smith. 2014. Dental and tarsal anatomy of Miacis latouri and a phylogenetic analysis of the earliest carnivoraforms (Mammalia, Carnivoramorpha). Journal of Vertebrate Paleontology 34:1–21.

Spaulding, M., and J. J. Flynn. 2012. Phylogeny of the Carnivoramorpha: The impact of postcranial characters. Journal of Systematic Palaeontology 10:653–677.

Wallace, S. C. 2011. Advanced Members of the Ailuridae (Lesser or Red Pandas - Subfamily Ailurinae); pp. 43–60 in A. R. Glatston (ed.), Red Panda: Biology and Conservation of the First Panda. Elsevier, London, UK.

Wang, X., S. C. White, and J. Guan. 2020. A new genus and species of sabretooth , Oriensmilus liupanensis (Barbourofelinae, Nimravidae, Carnivora), from the middle Miocene of China suggests barbourofelines are nimravids, not felids. Journal of Systematic Palaeontology 18:783–803.

Wesley-Hunt, G. D., and J. J. Flynn. 2005. Phylogeny of the Carnivora: basal relationships among the carnivoramorphans, and assessment of the position of “Miacoidea” relative to Carnivora. Journal of Systematic Palaeontology 3:1–28.

Source Material for Character Scoring

American Museum of Natural History (**AMNH**)

American Museum of Natural History – Frick Collection (**F:AM**)

Field Museum of Natural History, Chicago, Illinois, USA **(FMNH**)

John Day Fossil Beds National Monument, Oregon, USA (**JODA**)

University of California Museum of Paleontology, Berkeley, California (**UCMP**)

University of Oregon, Museum of Natural and Cultural History-Modern Collection (**B**)

Los Angeles County Museum, George C. Page Museum (Hancock Collection) (**LACMHC**)

National Museum of Kenya, Nairobi, Osteology Department (**OM**)

Institute of Vertebrate Paleontology and Paleoanthropology, Chinese Academy of Sciences Beijing, China (**IVPP**)

Beijing Natural History Museum, Beijing, China (**BNHM**)

Barbourofelis morrisi

AMNH 79999; F:AM 61876, 61900, 80000, 61895, 25204, 69359, 61893, 61976, 61898, 61970, 125665, 61882

Barbourofelis fricki

(Schultz et al., 1970)

AMNH 108193; F:AM 61986, 61994, 61997, 99258, 68234, 2672, 61984, 61983, 125670, 116854, 61991

Albanosmilus whitfordi

AMNH 14308; F:AM 61856, 61858, 61861, 61864, 61849, 61680, 61885

Sansanosmilus palmidens

(Filhol, 1890; Ginsburg, 1961; Morlo et al., 2004; Peigné, 2012)

Nimravus brachyops

(Merriam, 1906; Scott and Jepsen, 1936; Toohey, 1959; Joeckel et al., 2002)

JODA 1312; AMNH 6930, 6993, 6940; F:AM 62020, 62151; UCMP 1681, 2256, 260156, 76111

Smilodon fatalis

(Matthew, 1910; Stock and Merriam, 1932)

LACMHC 2002-R-289, R10864, R10688, A-3708, K-65, K-876, K-1541, K-2281, Q-1609, Q-2965, 36960, 37415, 37873, 38504, 38731, 39221, U-3585, R-423, R-6739, 40416, K-3309, K-4507, K-4671, J-6083, T-5113, T-3068, Q-5192, Q-3903, 46699, K-2768, N-1219, N-1737, 133528, 60175

Panthera leo

(Hunt, 1987; Salles, 1992; Hsieh and Takemura, 1994; Mattern and McLennan, 2000; Lueders et al., 2012; De Schepper, 2016)

B 8707; FMNH 31121; OM 7713, 7477

Pseudaelurus validus

(Hunt, 1998; Rothwell and McKenna, 2001; Rothwell, 2003)

AMNH 62128, 62167; F:AM 61847

Megantereon cultridens

(Vekua, 1995; Antón and Werdelin, 1998; Qiu et al., 2004; Christiansen and Adolfssen, 2007; Palmqvist et al., 2007; Christiansen, 2013)

AMNH 105446, 113842, 113848, 101471, 105087

Machairodus catocopis

F:AM 104044

Dinofelis diastemata

(Werdelin and Lewis, 2001)

F:AM 50445, 50446

Paramachaerodus ogygia

(Salesa et al., 2005, 2010b, 2010a; Siliceo et al., 2014)

Ginsburgsmilus napakensis

(Morales et al., 2001, 2008; Morlo et al., 2004; Morales and Pickford, 2018)

Prosansanosmilus eggeri

(Morlo et al., 2004)

Prosansanosmilus peregrinus

(Heizmann et al., 1980; Morlo, 2006)

Afrosmilus hispanicus

(Belichón and Morales, 1989; Morales et al., 2001)

Afrosmilus africanus

(Andrews, 1914; Savage, 1965; Morales et al., 2001)

Maofelis cantonensis

(Averianov et al., 2016)

Dinailurictis bonali

(Piveteau, 1931; Peigné and De Bonis, 2003)

Metailurus minor
AMNH 131854 (cast of IVPP 5679), AMNH 26379

Nimravides pedionomus
F:AM 61855, 61852, 25205, 25206, 62156-B, 62156-C, 62154, 62153-A, 62155, 62174, 62158, 62157-B

Oriensmilus liupanensis

(Wang et al., 2020)

AMNH 144755 (cast of an uncatalogued BNHM specimen)

REFERENCES

Andrews, C. W. 1914. On the Lower Miocene vertebrates from British East Africa, collected by Dr. Felix Oswald. Quarterly Journal of the Geological Society of London 70:163–186.

Antón, M., and L. Werdelin. 1998. Too well restored? The case of the Megantereon skull from Seneze. Lethaia Seminar 31:158–160.

Averianov, A., E. Obraztsova, I. Danilov, P. Skutschas, and J. Jin. 2016. First nimravid skull from Asia. Scientific Reports 6:1–8.

Belichón, M., and J. Morales. 1989. Los Carnívoros del Mioceno inferior de Buñol (Valencia, España). Revista Espanola de Paleontologia 4:3–8.

Christiansen, P. 2013. Phylogeny of the sabertoothed felids (Carnivora: Felidae: Machairodontinae). Cladistics 29:543–559.

Christiansen, P., and J. S. Adolfssen. 2007. Osteology and ecology of Megantereon cultridens SE311 (Mammalia; Felidae; Machairodontinae), a sabrecat from the Late Pliocene – Early Pleistocene of Senéze, France. Zoological Journal of the Linnean Society 151:833–884.

Filhol, H. 1890. Études sur les Mammifères Fossiles de Sansan. Bibliothèque Des Hautes Études Section Des Sciences Naturelles 37:1–319.

Ginsburg, L. 1961. La faune des carnivores miocènes de Sansan (Gers). Mémoires Du Muséum National d'Histoire Naturelle, Sér. C - Sciences de La Terre 9:1–190.

Heizmann, E. P. J., L. Ginsburg, and C. Bulot. 1980. Prosansanosmilus peregrinus, ein neuer machairodontider Felide aus dem Miocän Deutschlands und Frankreichs. Stuttgarter Beiträge Zur Naturkunde B 58:1–27.

Hsieh, H.-M., and A. Takemura. 1994. The Rete Mirabile of the Maxillary Artery in the Lion (Panthera leo). Okajimas Folia Anatomica Japonica 71:1–12.

Hunt, R. M. 1987. Evolution of the aeluroid Carnivora: significance of auditory structure in the nimravid cat Dinictis. American Museum Novitates 2886:1–74.

Hunt, R. M. 1998. Evolution of the aeluroid Carnivora. Diversity of the earliest aeluroids from Eurasia (Quercy, Hsanda-Gol) and the origin of felids. American Museum Novitates 3252.

Joeckel, R. M., S. Peigné, R. M. Hunt Jr., and R. I. Skolnick. 2002. The auditory region and nasal cavity of Oligocene Nimravidae (Mammalia: Carnivora). Journal of Vertebrate Paleontology 22:830–847.

Lueders, I., I. Luther, G. Scheepers, and G. van der Horst. 2012. Improved semen collection method for wild felids: Urethral catheterization yields high sperm quality in African lions (Panthera leo). Theriogenology 78:696–701.

Mattern, M. Y., and D. A. McLennan. 2000. Phylogeny and Speciation of Felids. Cladistics 16:232–253.

Matthew, W. D. 1910. The phylogeny of the Felidae. Bulletin of the American Museum of Natural History 28:289–316.

Merriam, J. C. 1906. Carnivora from the Tertiary formations of the John Day Region. Bulletin of the Department of Geology 5:1–64.

Morales, J., and M. Pickford. 2018. A new barbourofelid mandible (Carnivora, Mammalia) from the Early Miocene of Grillental-6, Sperrgebiet, Namibia. Communications of the Geological Survey of Namibia 18:113–123.

Morales, J., M. Pickford, and M. J. Salesa. 2008. Creodonta and Carnivora from the Early Miocene of the Northern Sperrgebiet, Namibia. Memoirs of the Geological Survey of Namibia 20:291–310.

Morales, J., M. J. Salesa, M. Pickford, and D. Soria. 2001. A new tribe, new genus and two new species of Barbourofelinae (Felidae, Carnivora, Mammalia) from the early Miocene of East Africa and Spain. Transactions of the Royal Society of Edinburgh: Earth Sciences 92:97–102.

Morlo, M. 2006. New remains of Barbourofelidae (Mammalia, Carnivora) from the Miocene of Southern Germany: implications for the history of barbourofelid migrations. Beiträge Zur Paläontologie 30:339–349.

Morlo, M., S. Peigné, and D. Nagel. 2004. A new species of Prosansanosmilus: implications for the systematic relationships of the family Barbourofelidae new rank (Carnivora, Mammalia). Zoological Journal of the Linnean Society 140:43–61.

Palmqvist, P., V. Torregrosa, J. A. Pérez-Claros, B. Martínez-Navarro, and A. Turner. 2007. A re-evaluation of the diversity of Megantereon (Mammalia, Carnivora, Machairodontinae) and the problem of species identification in extinct carnivores. Journal of Vertebrate Paleontology 27:160–175.

Peigné, S. 2012. Les Carnivora de Sansan; pp. 559–660 in S. E. N. S. (ed.), Mammifères de Sansan. Muséum national d'Histoire naturelle, Paris.

Peigné, S., and L. De Bonis. 2003. Juvenile cranial anatomy of Nimravidae (Mammalia, Carnivora): biological and phylogenetic implications. Zoological Journal of the Linnean Society 138:477–493.

Piveteau, J. 1931. Les Chats des Phosphorites du Quercy. Annales de Paléontologie 20:107–163.

Qiu, Z. -x., T. Deng, and B. -y. Wang. 2004. Early Pleistocene mammalian fauna from Longdan, Dongxiang, Gansu, China. Palaeontologia Sinica, New Series C 191:1–198.

Rothwell, T. P. 2003. Phylogenetic systematics of North American Pseudaelurus (Carnivora, Felidae). American Museum Novitates 3403.

Rothwell, T. P., and M. McKenna. 2001. Phylogenetic systematics of North American Pseudaelurus (Carnivora: Felidae). Columbia University, Ann Arbor, 358 pp.

Salesa, M. J., M. Antón, A. Turner, and J. Morales. 2005. Aspects of the functional morphology in the cranial and cervical skeleton of the sabre-toothed cat Paramachairodus ogygia (Kaup, 1832) (Felidae, Machairodontinae) from the Late Miocene of Spain: implications for the origins of the machairodont killing bit. Zoological Journal of the Linnean Society 144:363–377.

Salesa, M. J., M. Anton, A. Turner, and J. Morales. 2010a. Functional anatomy of the forelimb in Promegantereon* ogygia (Felidae, Machairodontinae, Smilodontini) from the Late Miocene of Spain and the origins of the sabre-toothed felid model. Journal of Anatomy 216:381–396.

Salesa, M. J., M. Antón, A. Turner, L. Alcalá, P. Montoya, and J. Morales. 2010b. Systematic revision of the late Miocene sabre-toothed felid Paramachaerodus in Spain. Palaeontolgy 53:1369–1391.

Salles, L. O. 1992. Felid Phylogenetics: Extant Taxa and Skull Morphology (Felidae, Aeluroidea). American Museum Novitates 3047:67.

Savage, R. J. G. 1965. Fossil Mammal of Africa: The Miocene Carnivora of East Africa. Bulletin of the British Museum (Natural History) 10:239–316.

De Schepper, M. 2016. A comparative study in morphological defects of semen from African Lions (Panthera leo) and Caracal (Caracal caracal): collected by urethral catheterization and electro-ejaculation. Ghent University, 31 pp.

Schultz, C. B., M. R. Schultz, and L. D. Martin. 1970. A new tribe of saber-toothed cats (Barbourofelini) from the Pliocene of North America. Bulletin of the University of Nebraska State Museum 9:1–31.

Scott, W. B., and G. L. Jepsen. 1936. The mammalian fauna of the white river oligocene.

Transactions of the American Philosophical Society 108–153.

Siliceo, G., M. J. Salesa, M. Antón, M. F. G. Monescillo, and J. Morales. 2014. Promegantereon ogygia (Felidae, Machairodontinae, Smilodontini) from the Vallesian (late Miocene, MN 10) of Spain: morphological and functional differences in two noncontemporary populations. Journal of Vertebrate Paleontology 34:407–418.

Stock, C., and J. C. Merriam. 1932. The Felidae of Ranch La Brea. The Carnegie Institution, Washington, pp.

Toohey, L. 1959. The Species of Nimravus (Carnivora, Felidae). Princeton University, New York, 130 pp.

Vekua, A. 1995. Die Wirbeltierfauna des Villafranchium von Dmanisi und ihre biostratigraphische Bedeutung. Jahrbuch Des Romisch-Germanischen Zentralmuseums Mainz 42:77–180.

Wang, X., S. C. White, and J. Guan. 2020. A new genus and species of sabretooth , Oriensmilus liupanensis (Barbourofelinae, Nimravidae, Carnivora), from the middle Miocene of China suggests barbourofelines are nimravids, not felids. Journal of Systematic Palaeontology 18:783–803.

Werdelin, L., and M. E. Lewis. 2001. A revision of the genus Dinofelis (Mammalia, Felidae). Zoological Journal of the Linnean Society 132:147–258.

Table S3. Stratigraphic Ranges of Taxa

Taxa	FAD	LAD
Afrosmilus_africanus	18	17.5
Afrosmilus_hispanicus	16.7	16.6
Ailurus_fulgens	0	0
Albanosmilus_whitfordi	12	7
Barbourofelis_morrisi	12	9.5
Barbourofelis_fricki	8.9	6.9
Canis_latrans	2.588	0
Civettictis_civetta	3.2	0
Daphoenus	38.39	25.03
Dinailurictis_bonali	30.83	27.24
Dinictis_felina	35.5	23.03
Dinofelis_diastemata	4.7	4.2
Echinosorex_gymnura	0	0
Erinaceus_europaeus	1	0
Ginsburgsmilus_napakensis	20.5	19.2
Gulo_gulo	1.3	0
Herpestes_edwardsii	0	0
Herpestides_antiquus	23.03	20.44
Hesperocyon_gregarius	40.4	30.8
Hoplophoneus_primaevus	35.5	30.25
Hyaena_hyaena	2.58	0
Leptictis_dakotensis	37.2	30.8
Maofelis_cantonensis	37.2	33.9
Megantereon_cultridens	4.5	0.5
Mephitis_mephitis	1.8	0
Gustafsonia_cognita	37.47	36.62
Miacis_exiguus	54.68	52.83
Miacis_medius	45.65	44.61
Miacis_sylvestris	48.56	45.18
Miacis_uintensis	45.11	38.9
Miacis_washakius	45.65	44.61
Nandinia_binotata	0	0
Machairodus_catocopis	10.09	4.91
Nimravus_brachyops	30.5	25
Otarocyon_macdonaldi	33.9	33.3
Palaeoprionodon_lamandini	28.86	23.49
Panthera_leo	1.8	0
Paramachaerodus_ogygia	9.5	9
PM_3868	41.2	39.39
Proailurus_lemanensis	28.86	23.49

Procynodictis_vulpiceps	45.15	38.86
Procyon_lotor	2.6	0
Prosansanosmilus_eggeri	16.2	15.78
Prosansanosmilus_peregrinus	18	15.96
Pseudaelurus_validus	17.34	14.78
Pteronarctos_goedertae	20.44	11.61
Puma_concolor	2.588	0
Quercygale_angustidens	39.5	34.59
Sansanosmilus_palmidens	16.02	12.5
Smilodon_fatalis	1.8	0.01
Stenogale_julieni	23.03	20.44
Tapocyon_robustus	40.85	38.99
Ursus_americanus	2.58	0
Zalophus_californianus	0.781	0
Zodiolestes_daimonelixensis	24.8	20.43
Nimravides_pedionomus	13	9.07
Metailurus_major	8.2	4.7
Oriensmilus_liupanensis	16	15

Figure S2. 95% HPD of Node Ages of the MCC Tree

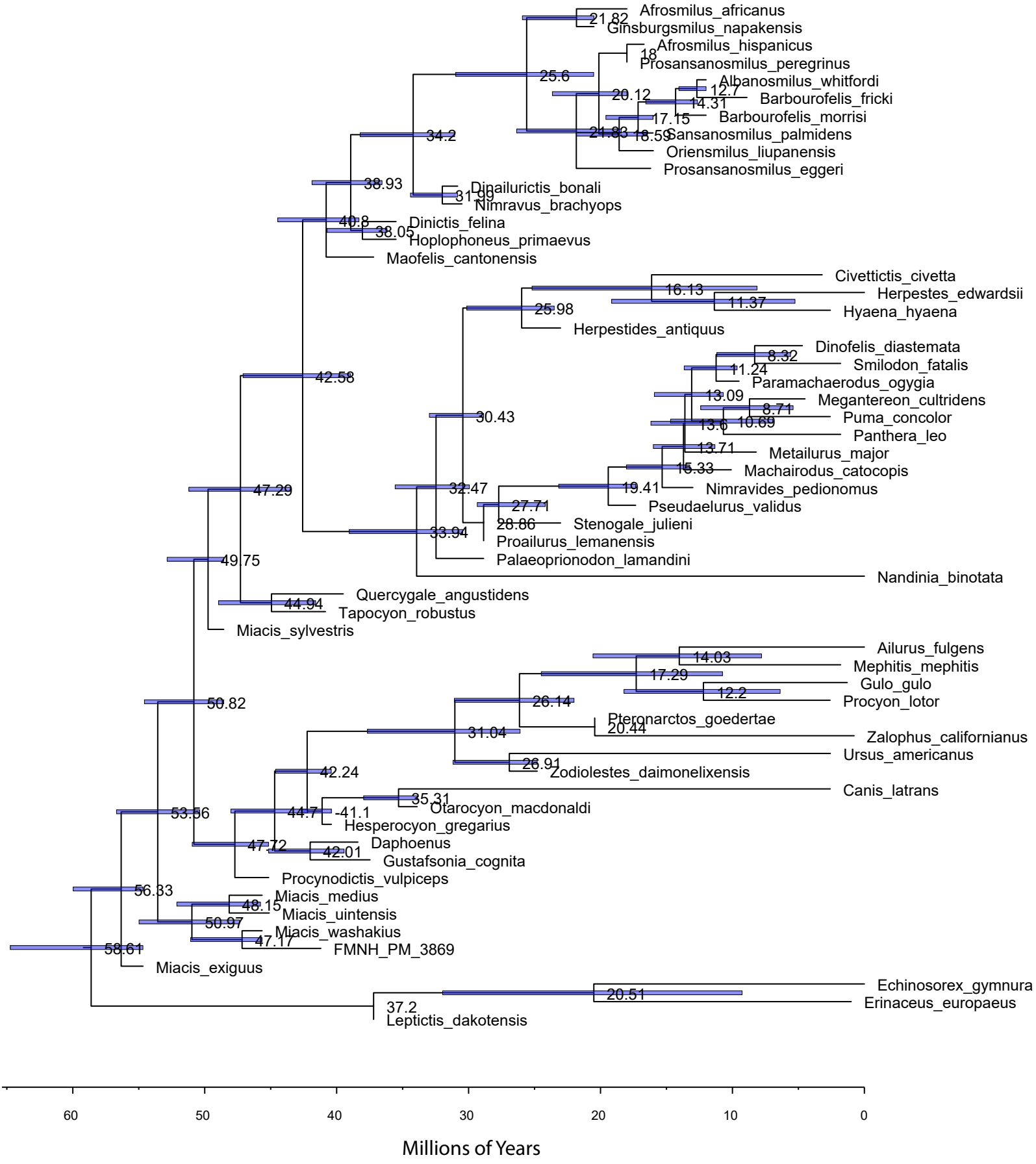

Figure S3. Synapomorphy 1

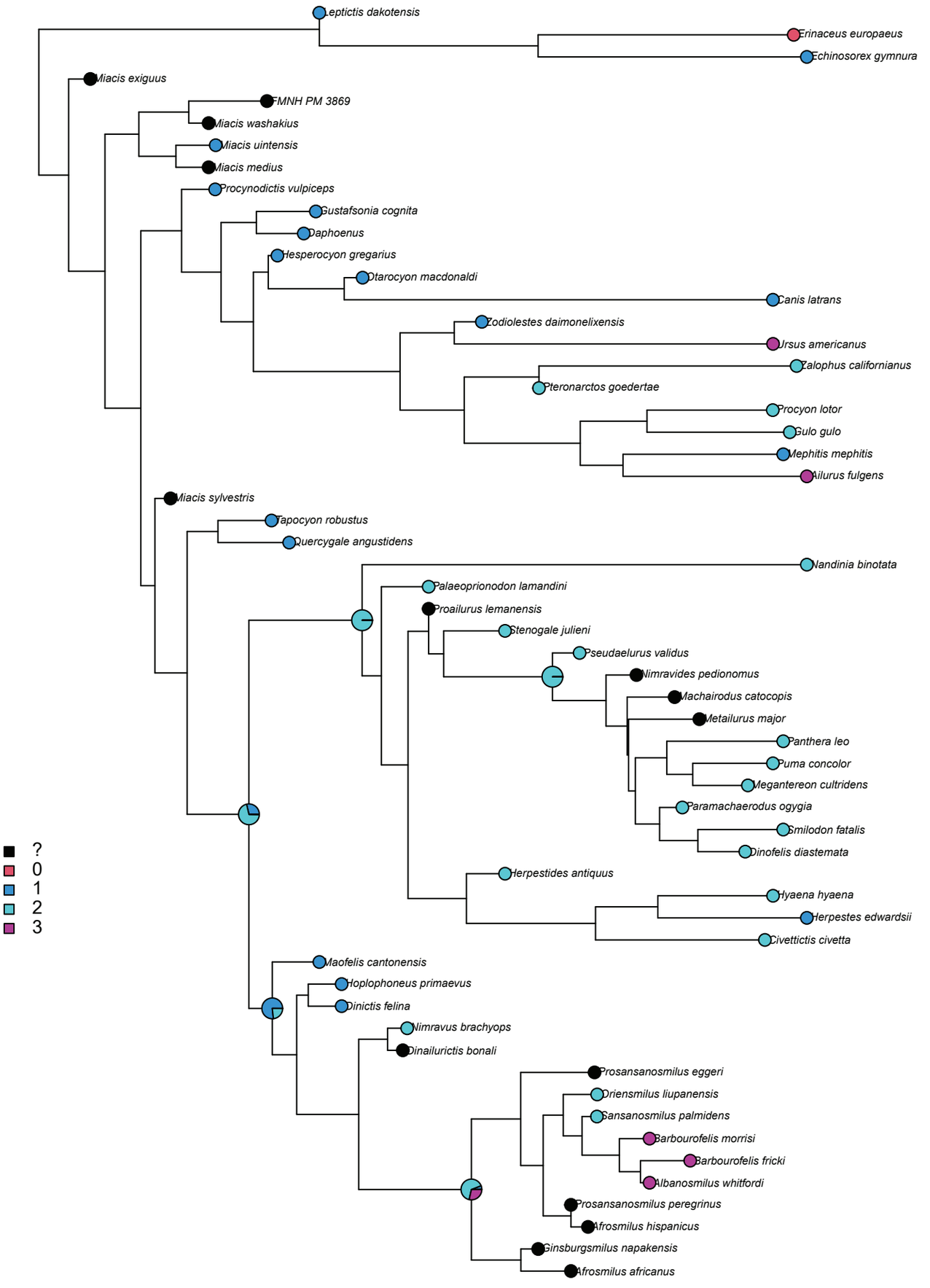

Figure S4. Synapomorphy 4

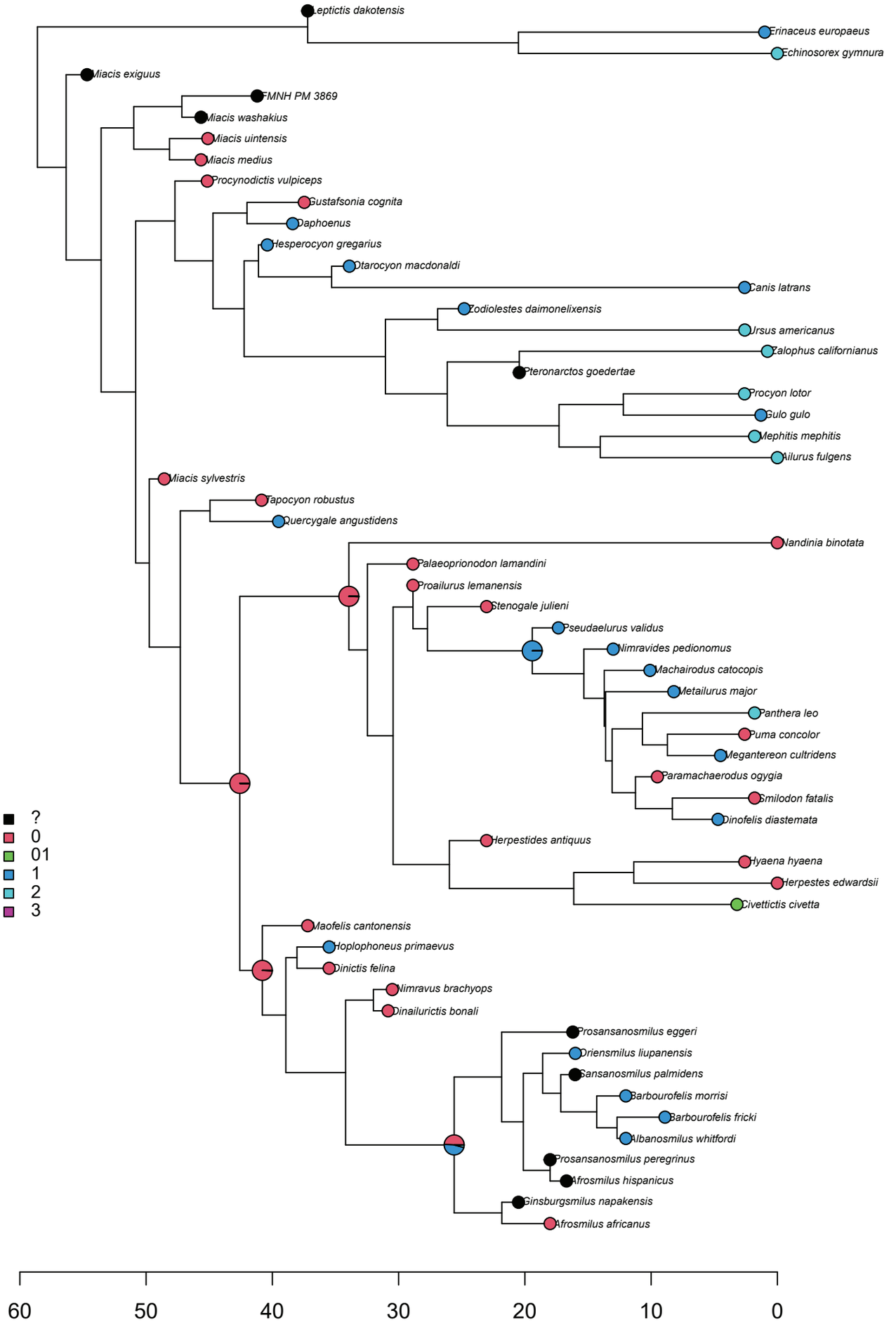

Figure S5. Synapomorphy 6

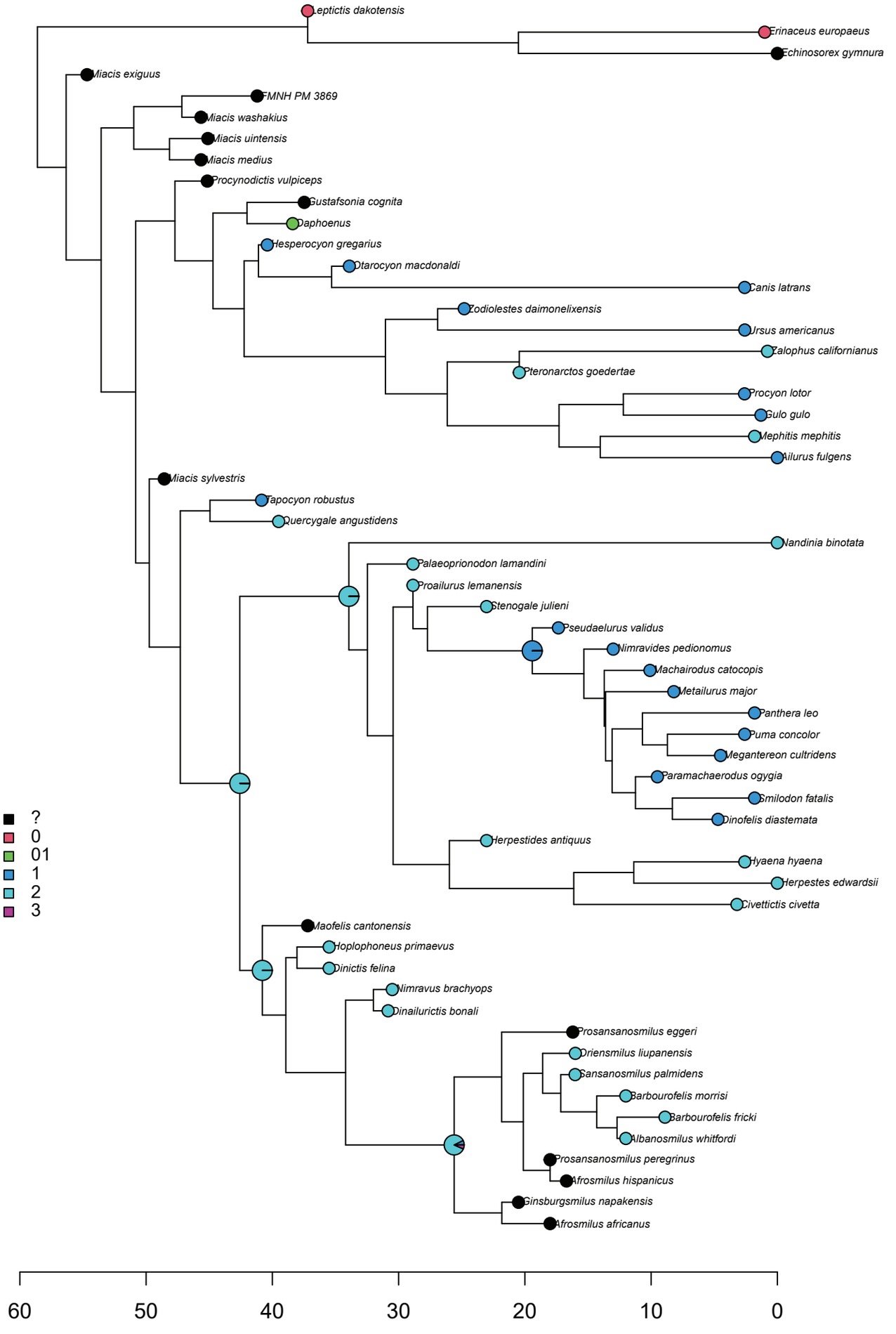

Figure S6. Synapomorphy 10

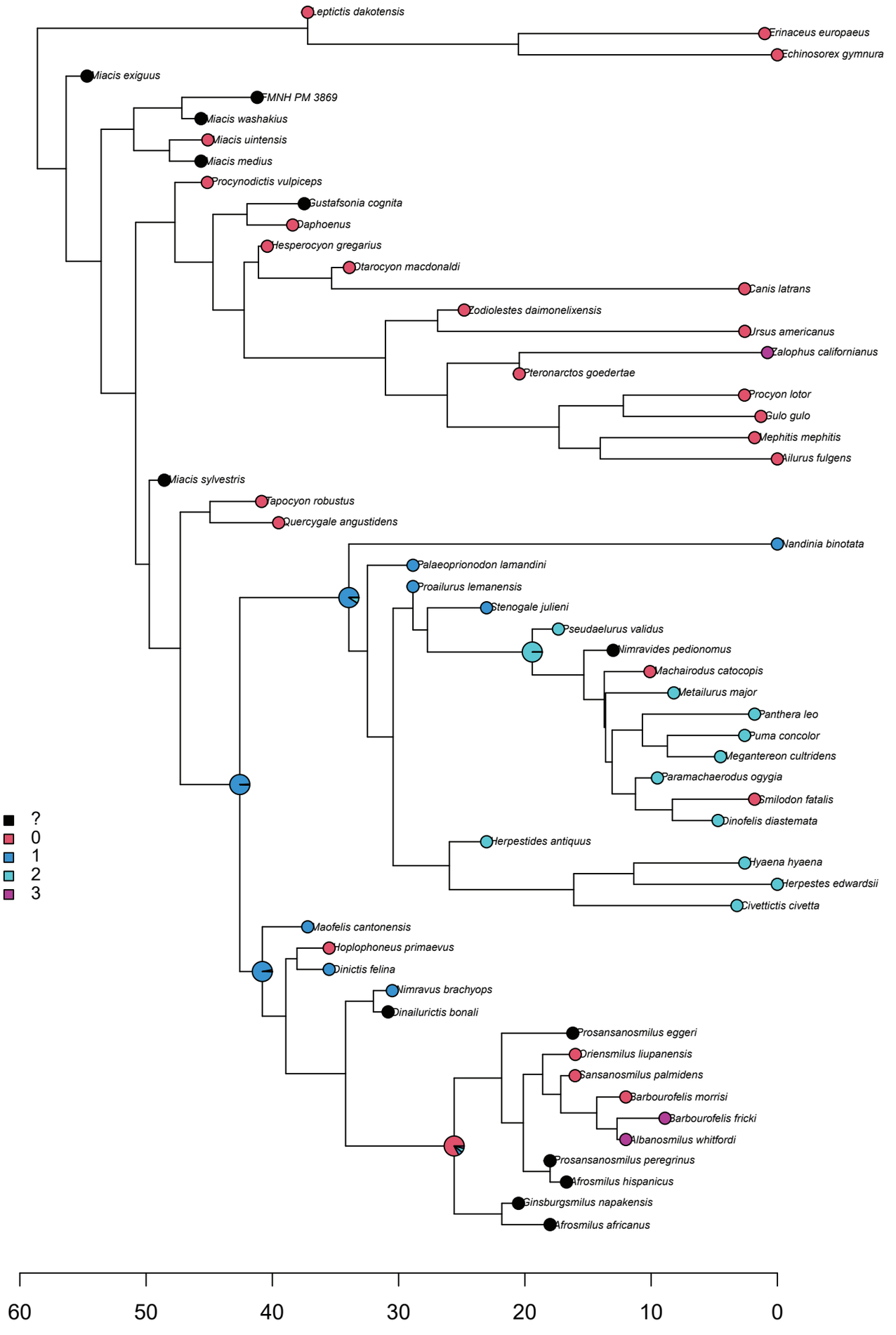

Figure S7. Synapomorphy 12

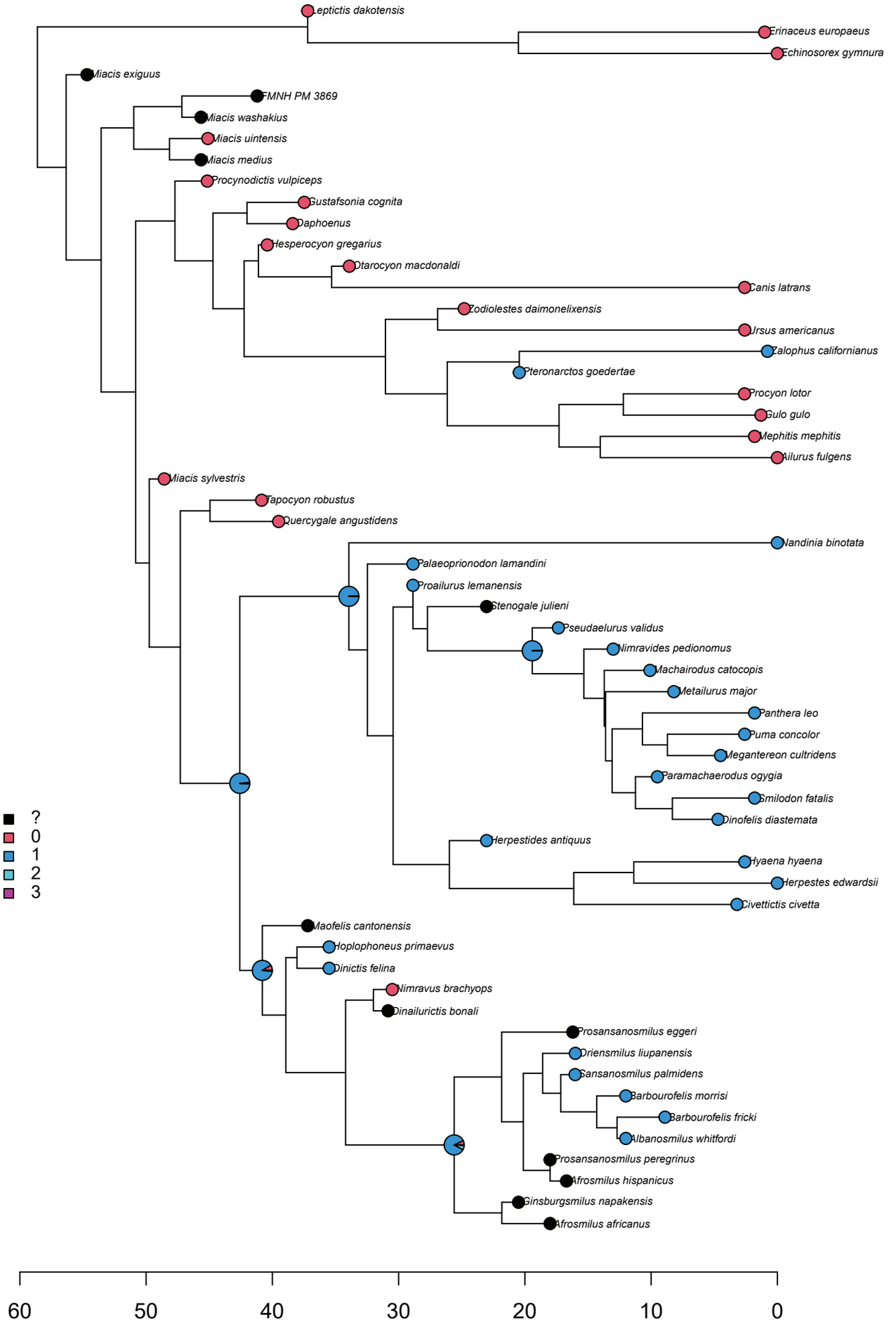

Figure S8. Synapomorphy 13

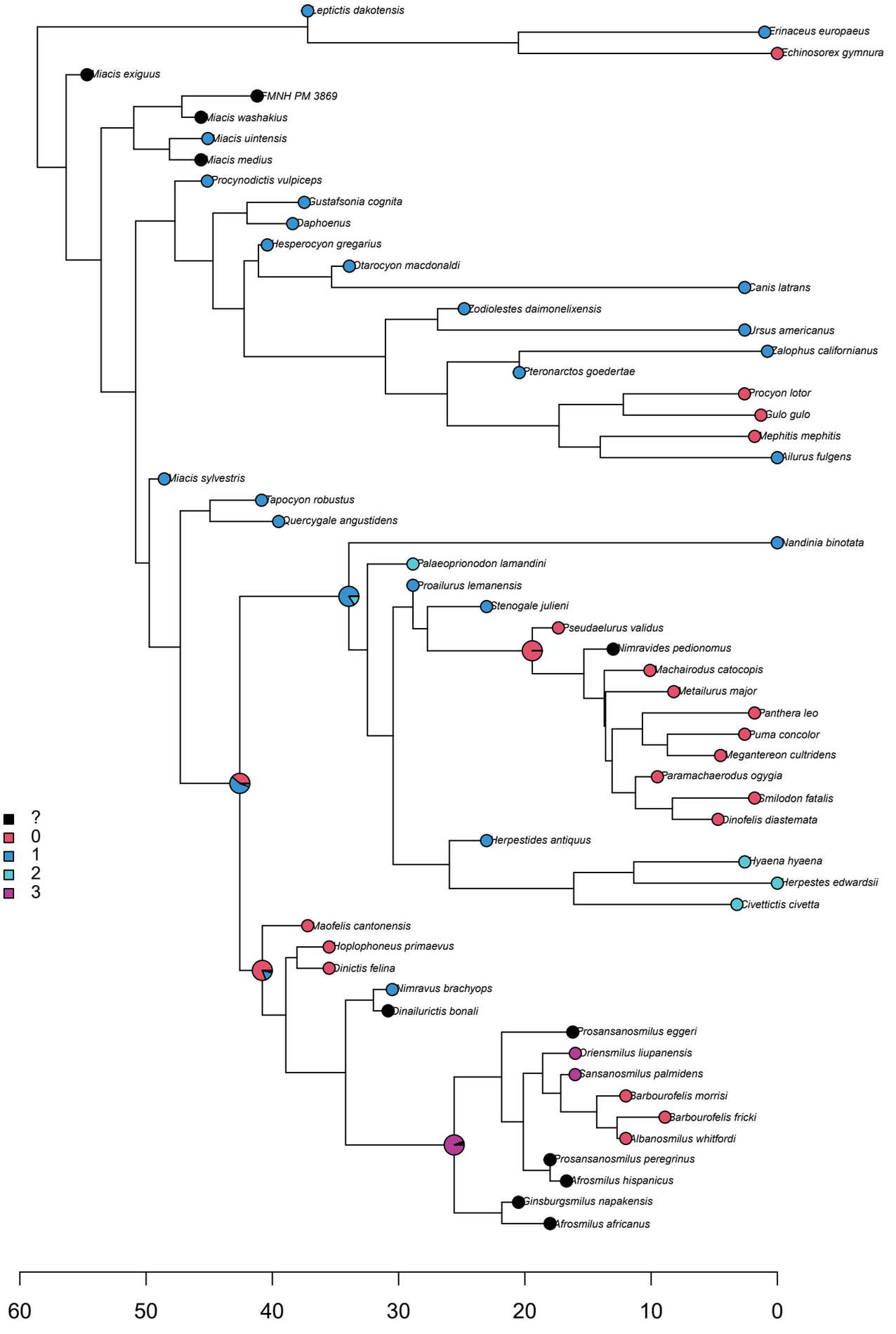

Figure S9. Synapomorphy 14

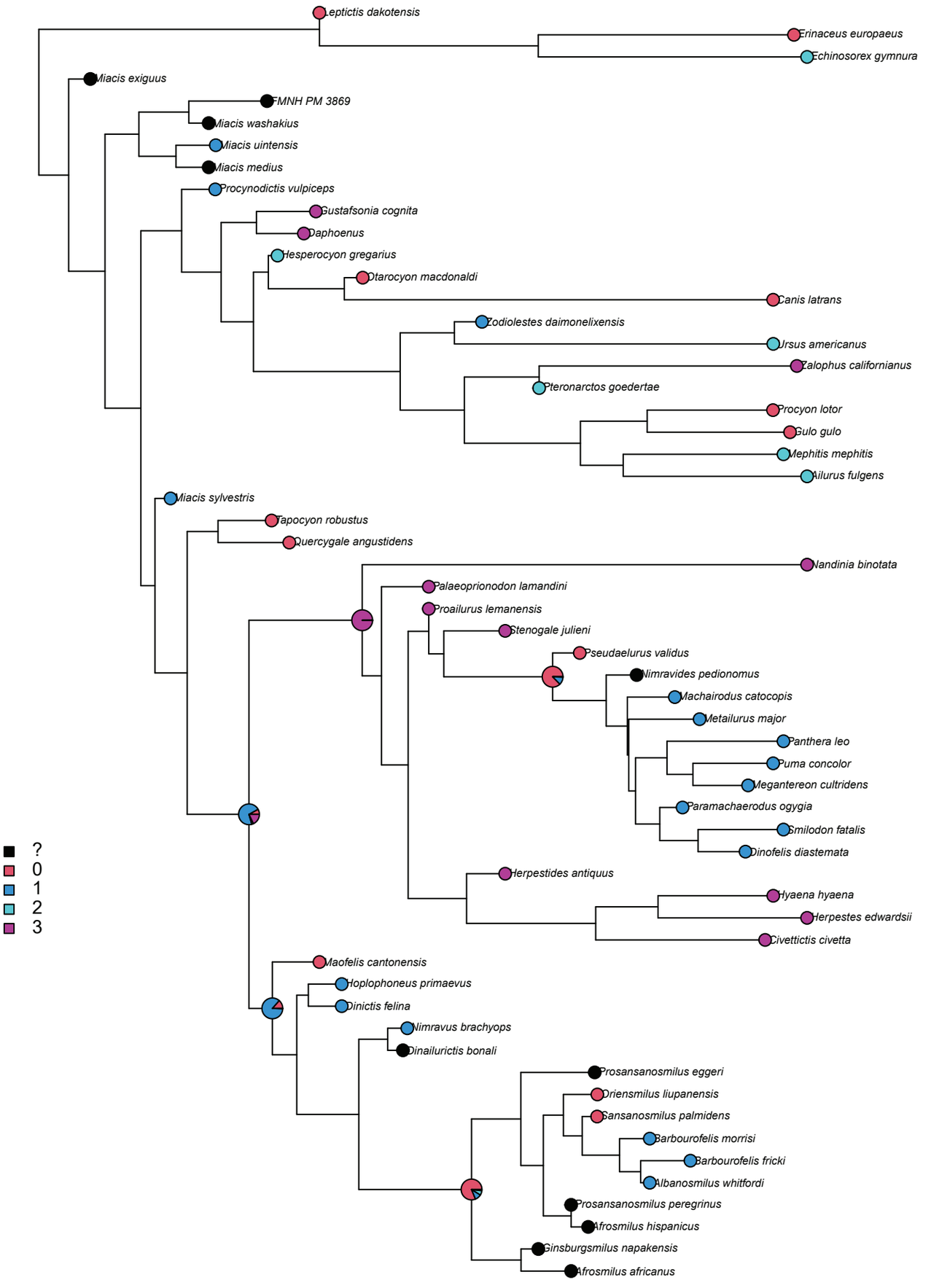

Figure S10. Synapomorphy 17

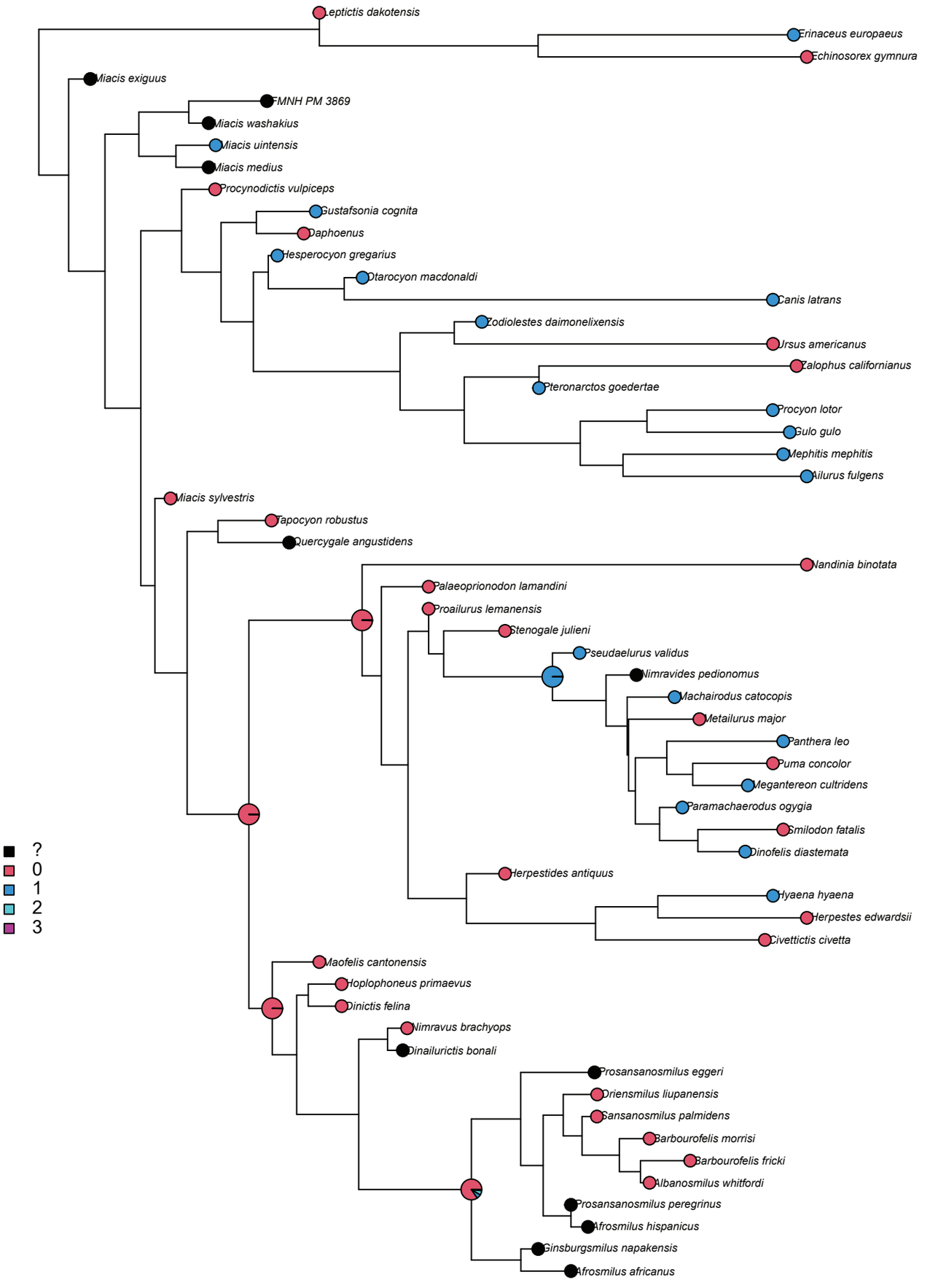

Figure S11. Synapomorphy 18

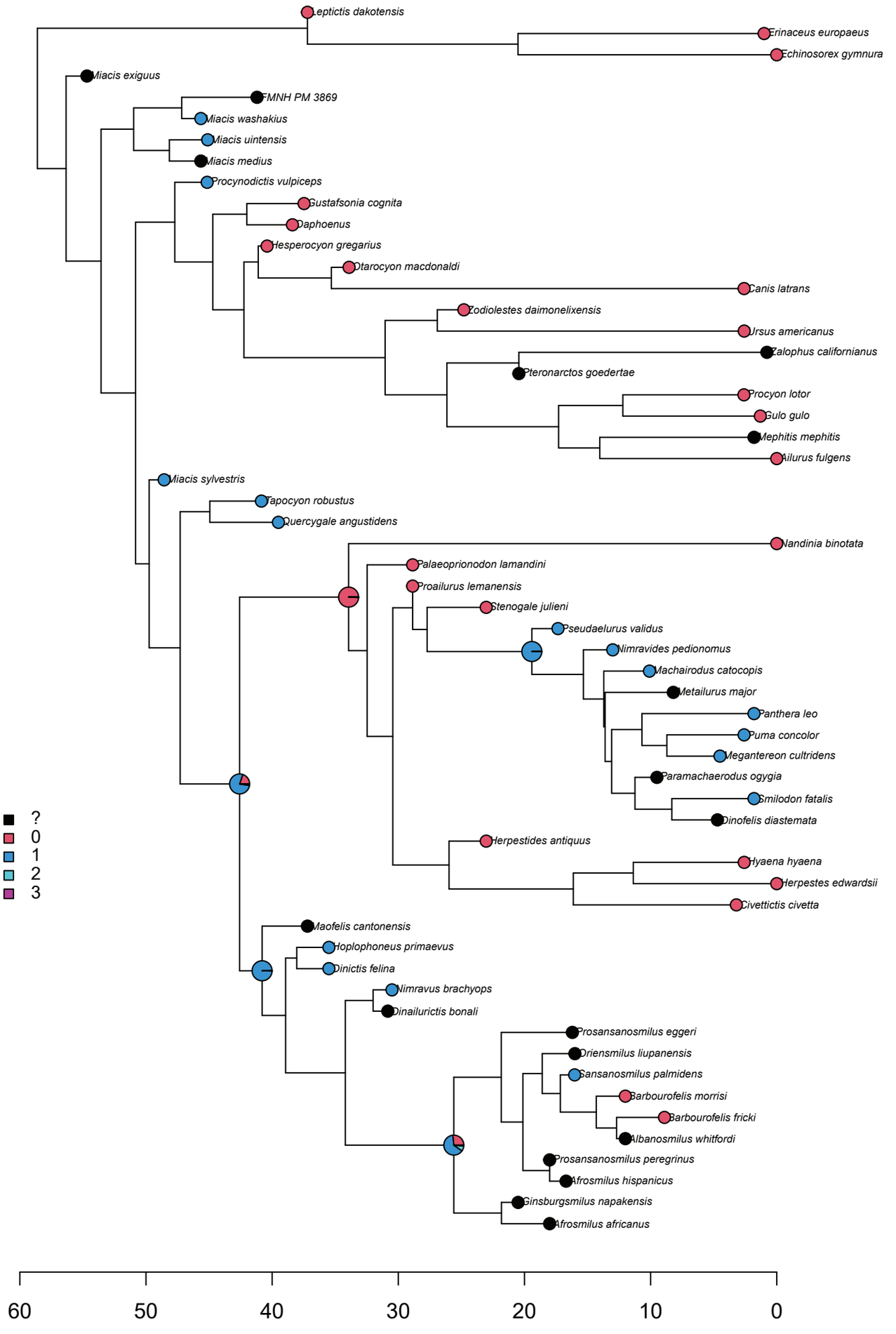

Figure S12. Synapomorphy 22

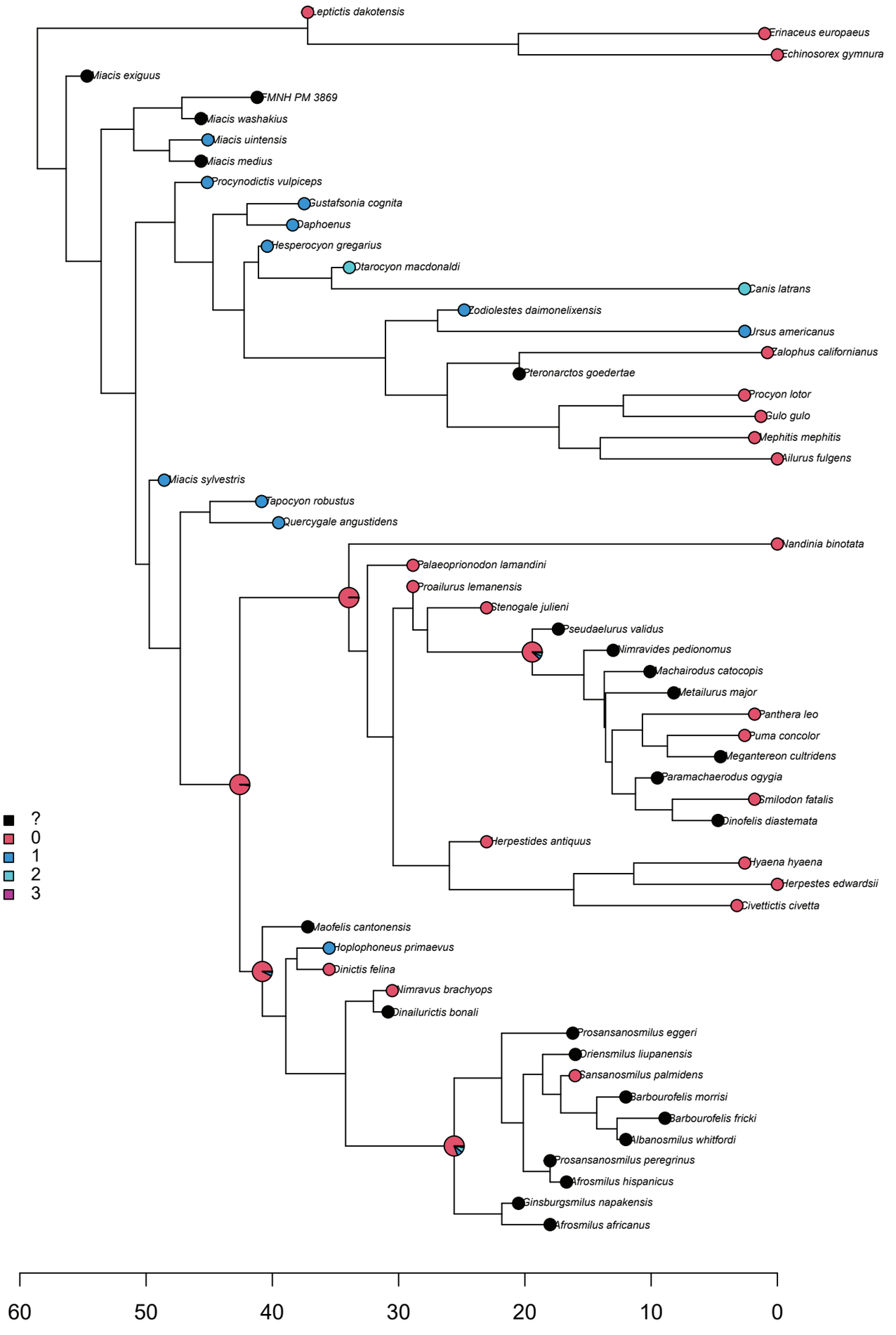

Figure S13. Synapomorphy 23

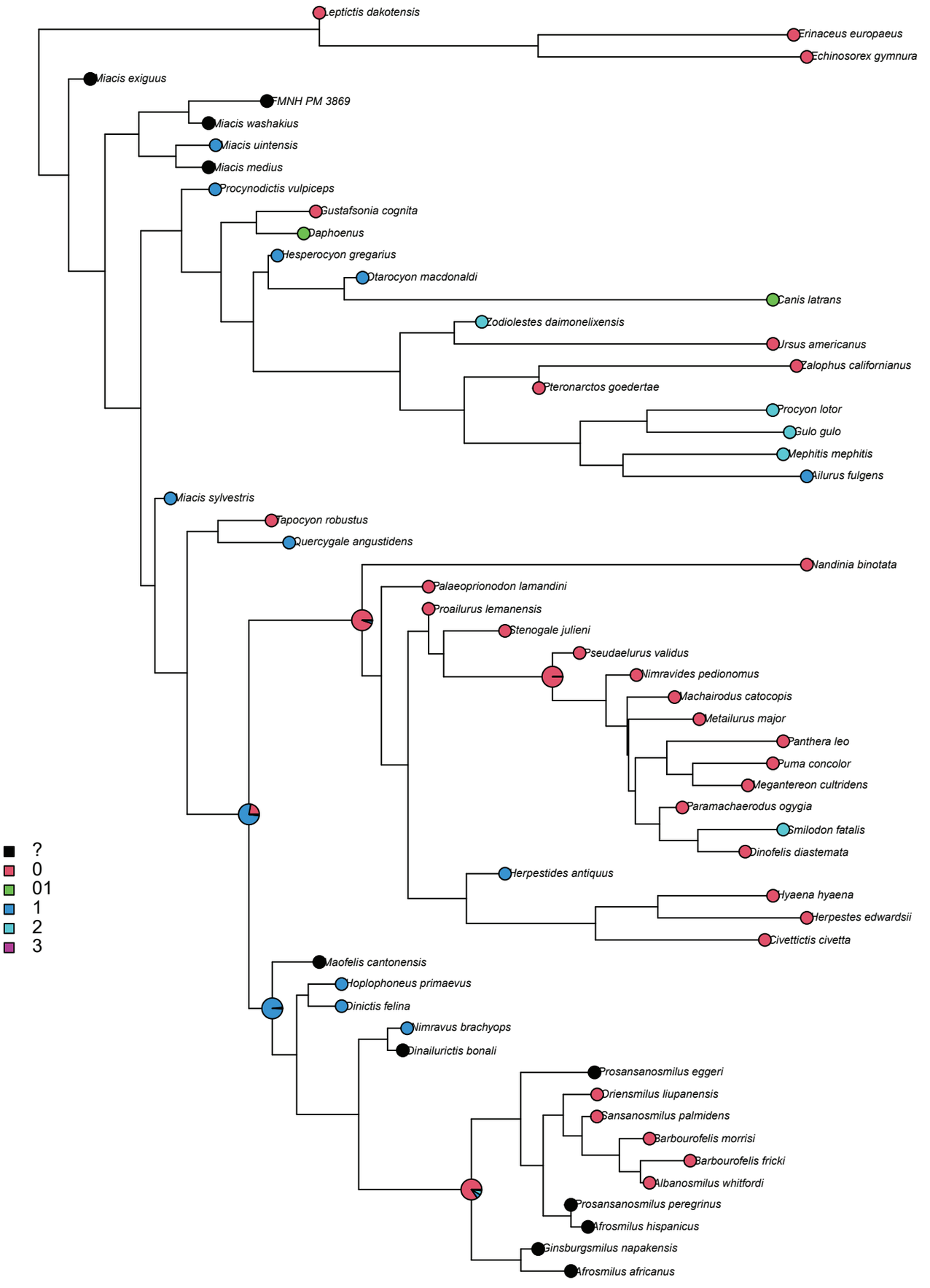

Figure S14. Synapomorphy 24

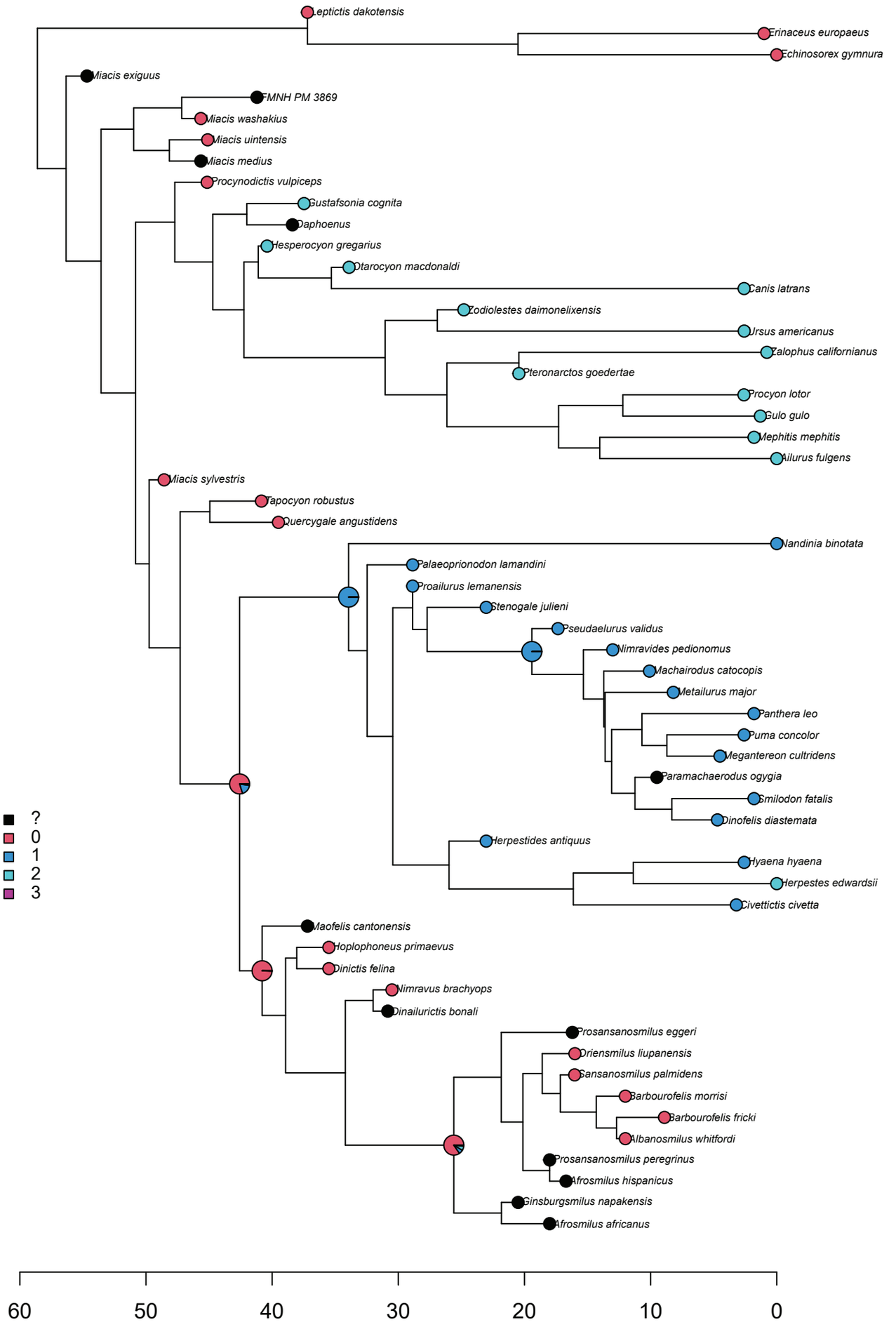

Figure S15. Synapomorphy 26

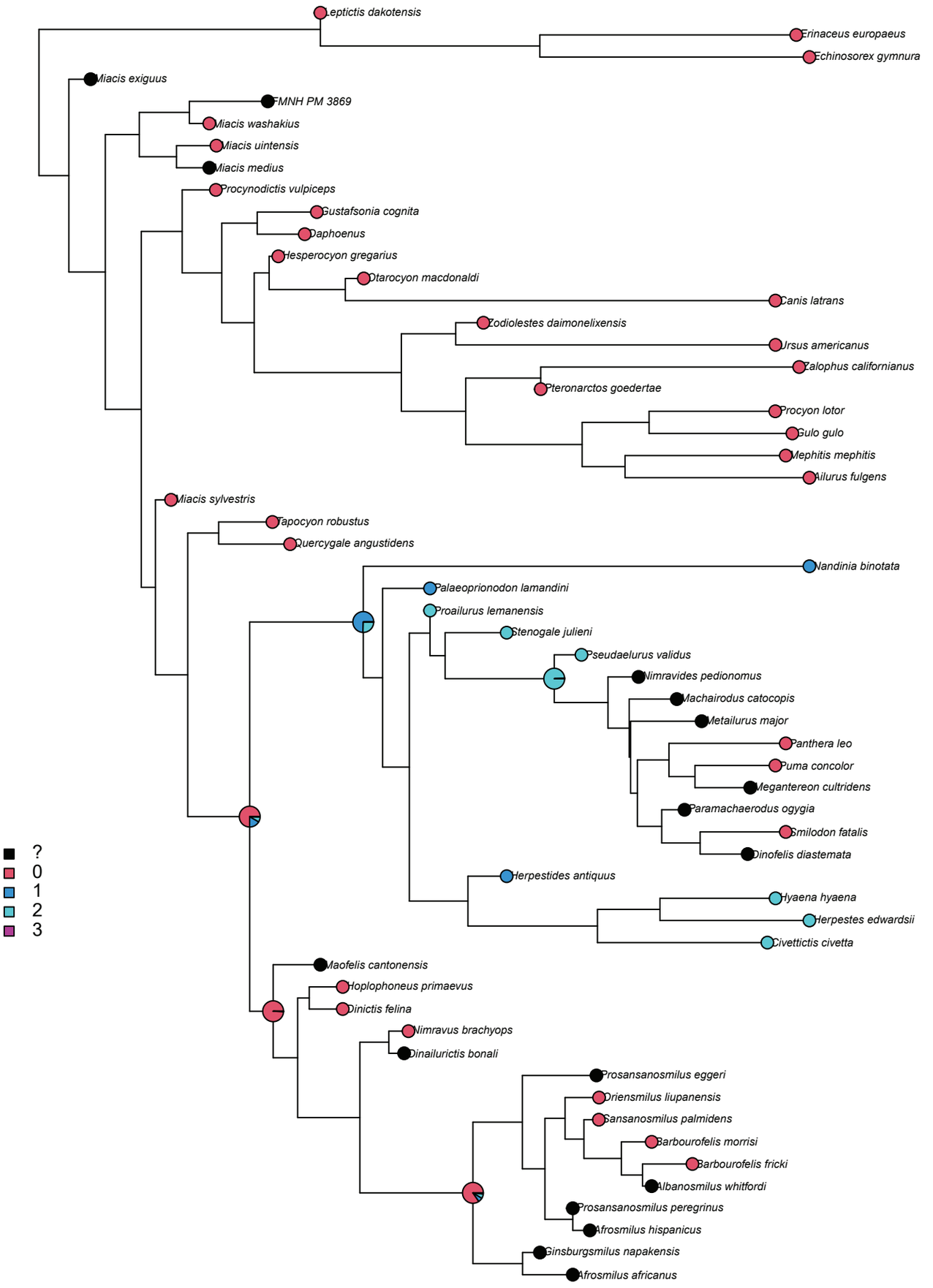

Figure S16. Synapomorphy 27

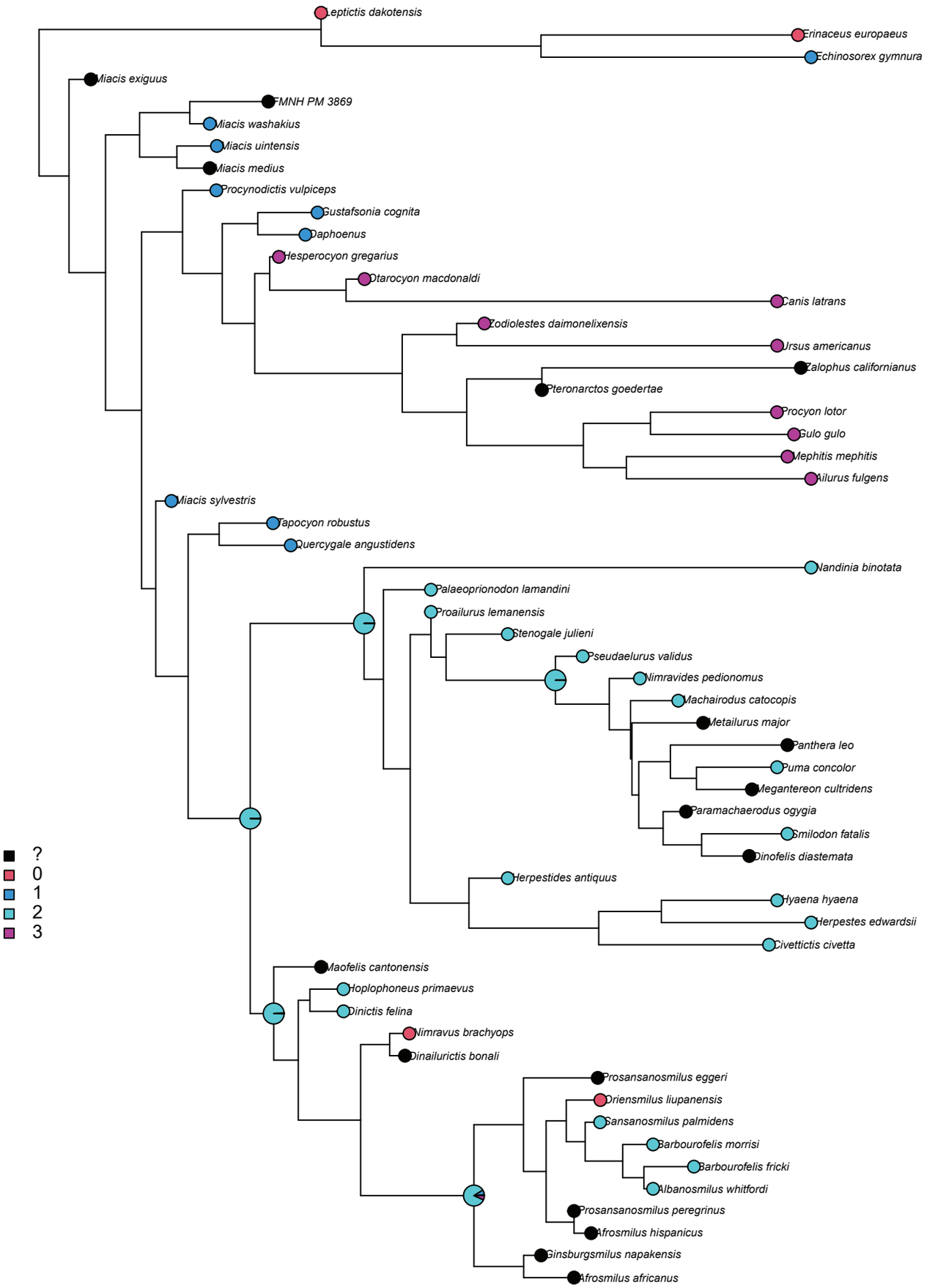

Figure S17. Synapomorphy 28

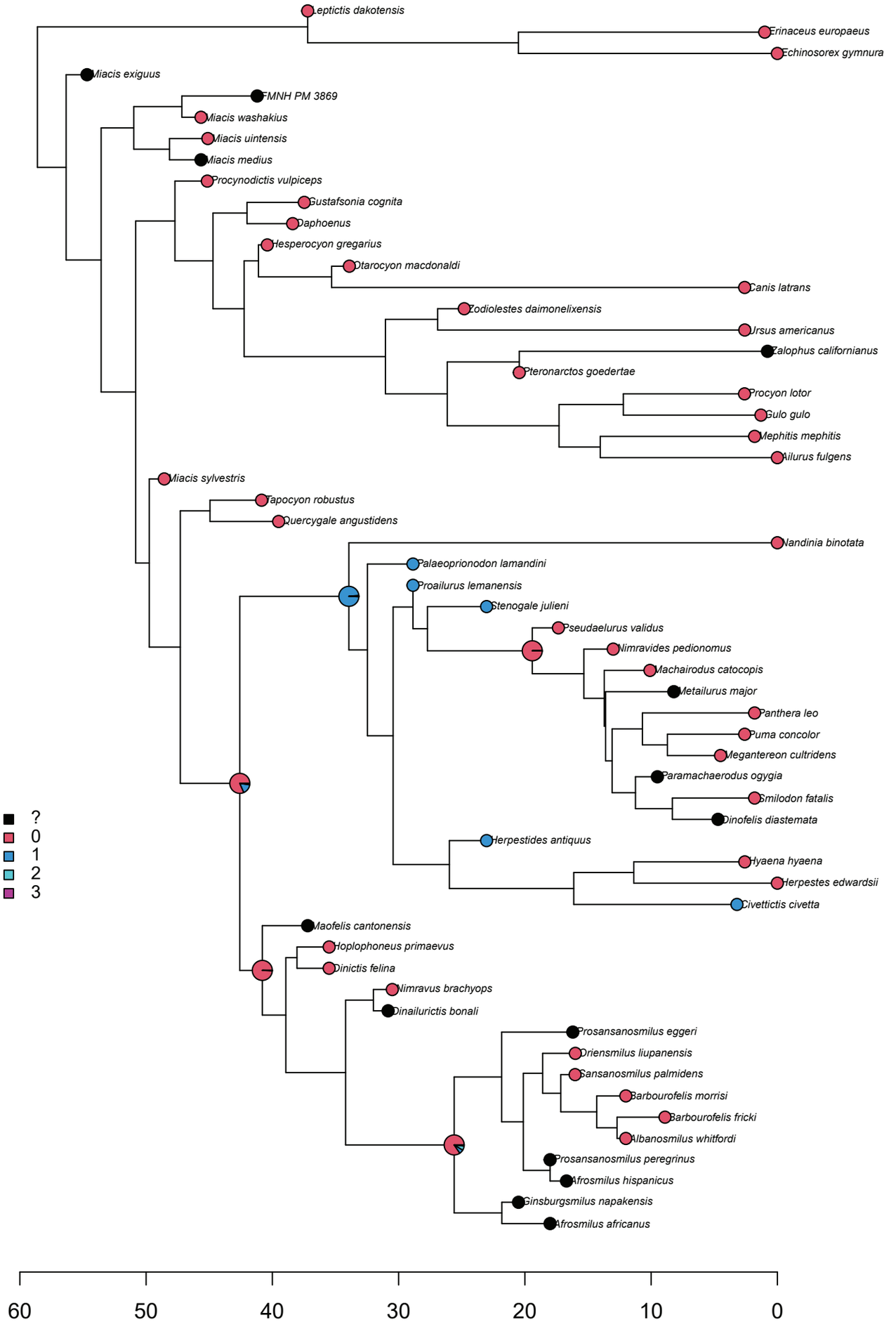

Figure S18. Synapomorphy 39

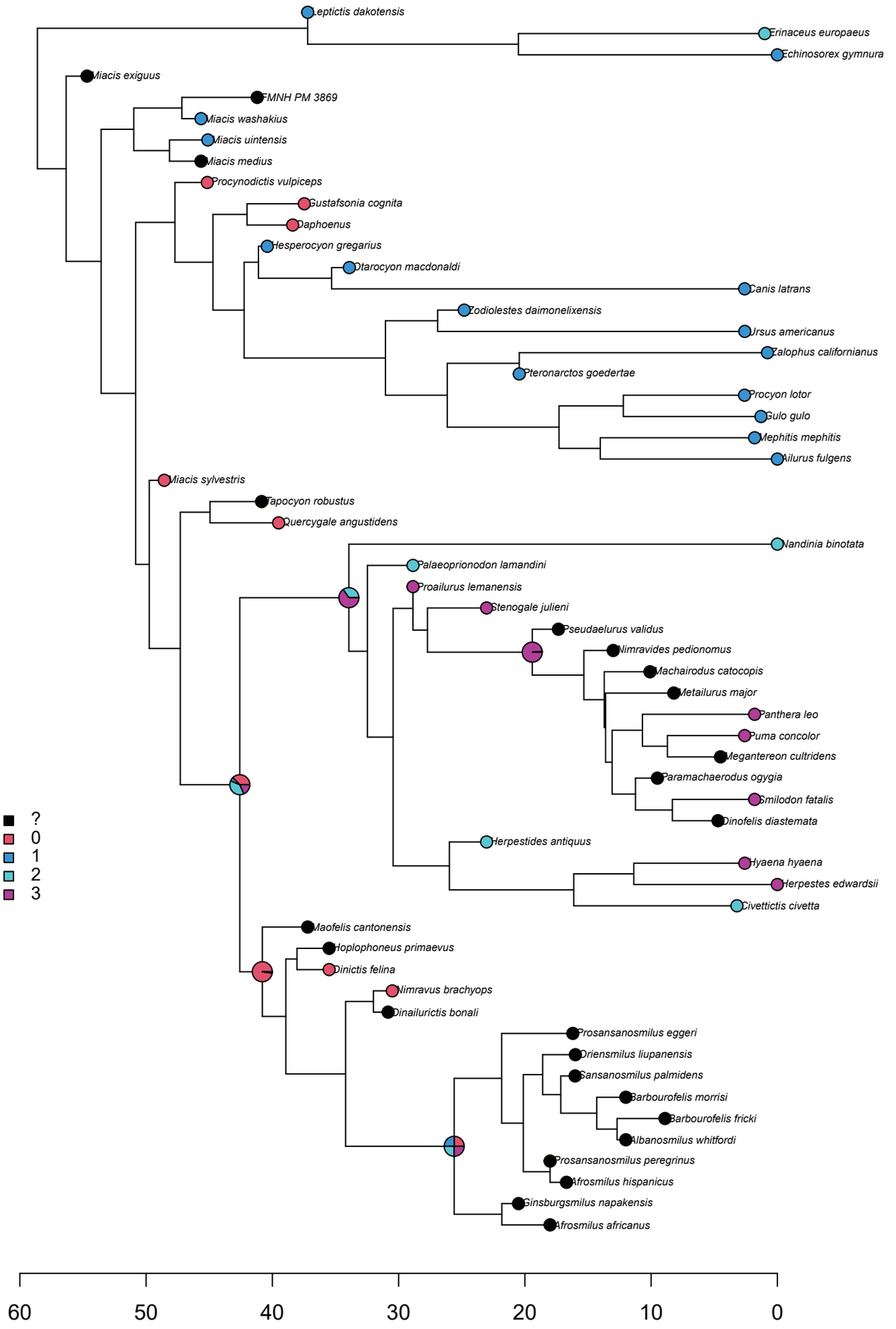

Figure S19. Synapomorphy 40

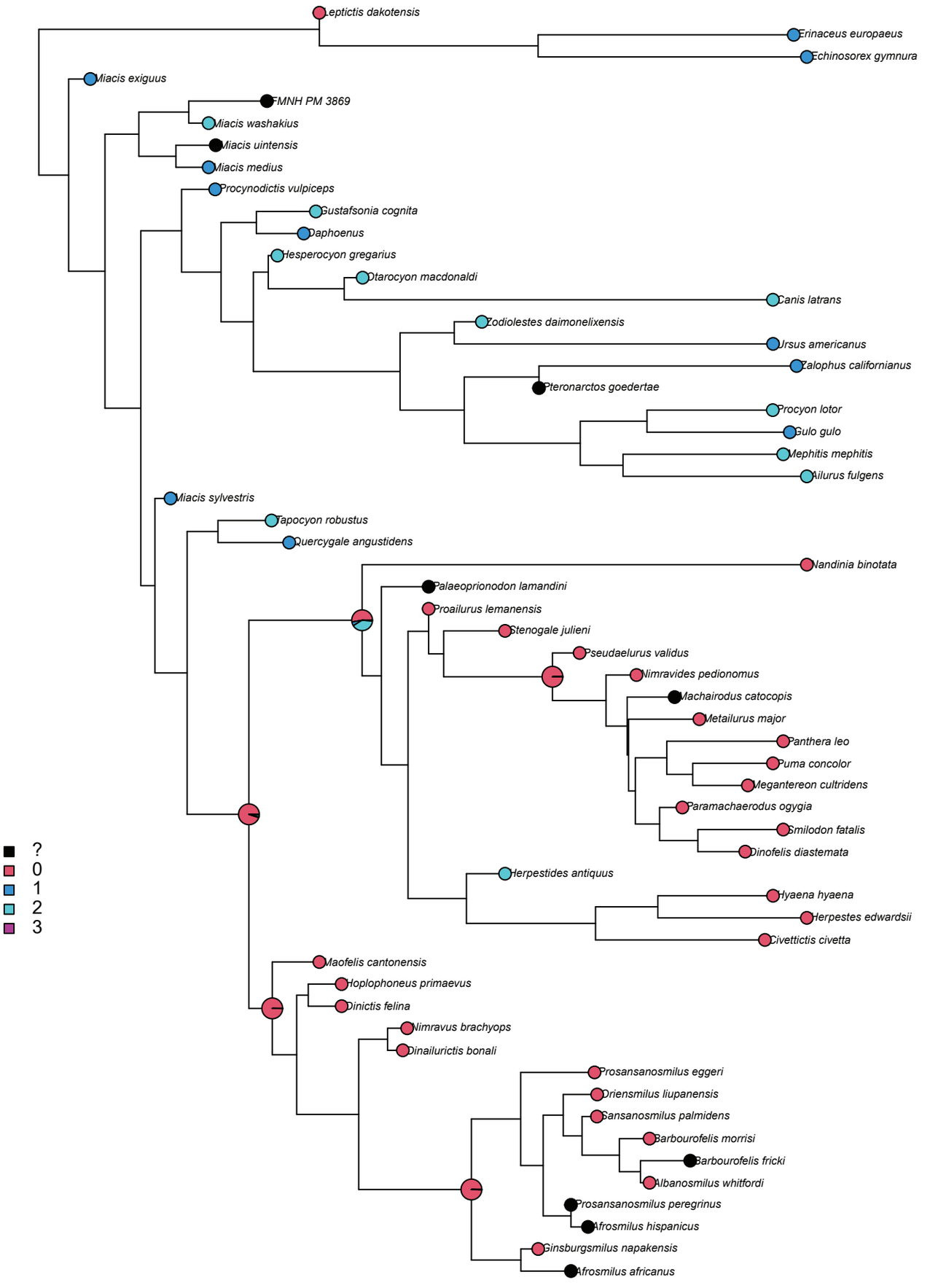

Figure S20. Synapomorphy 41

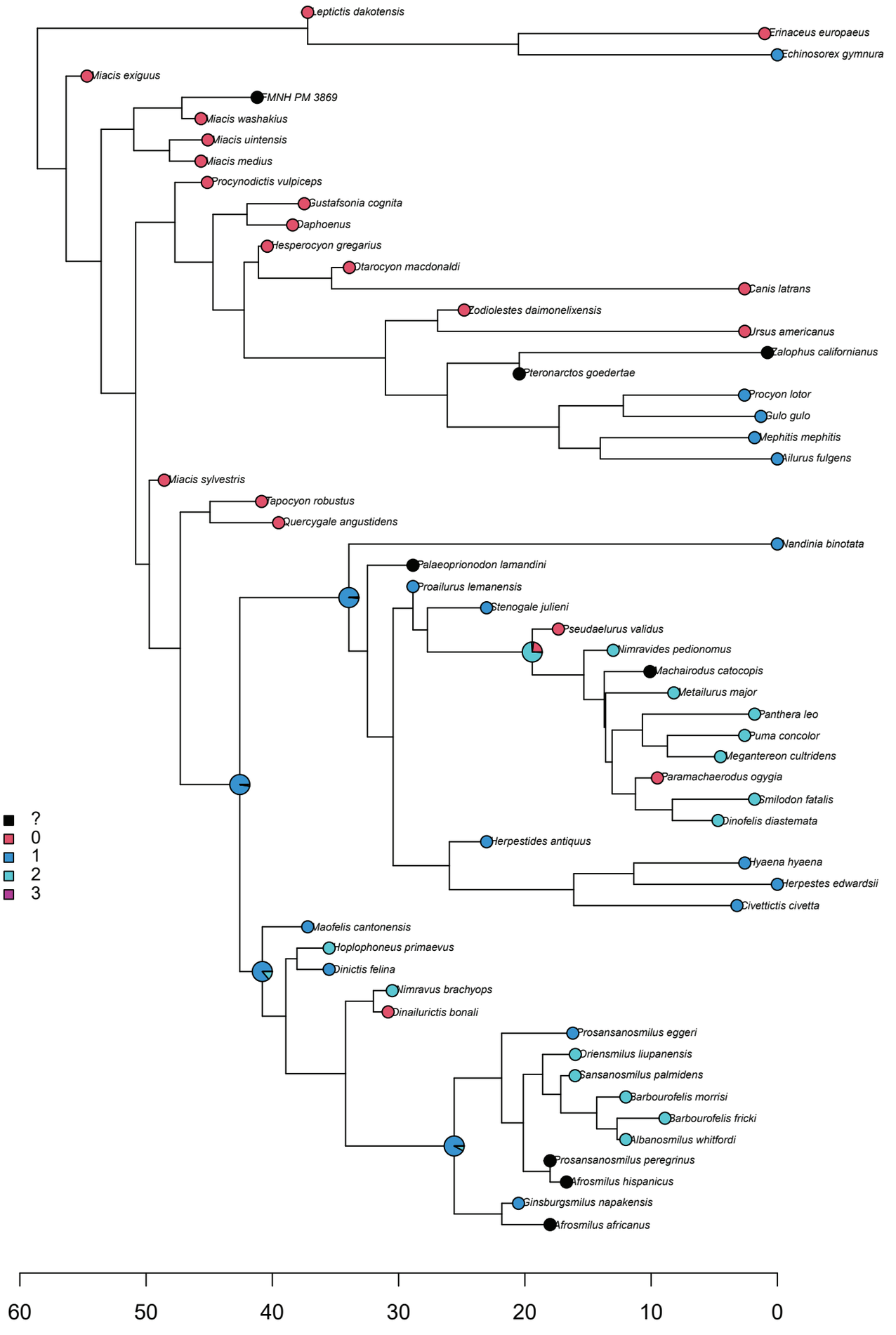

Figure S21. Synapomorphy 44

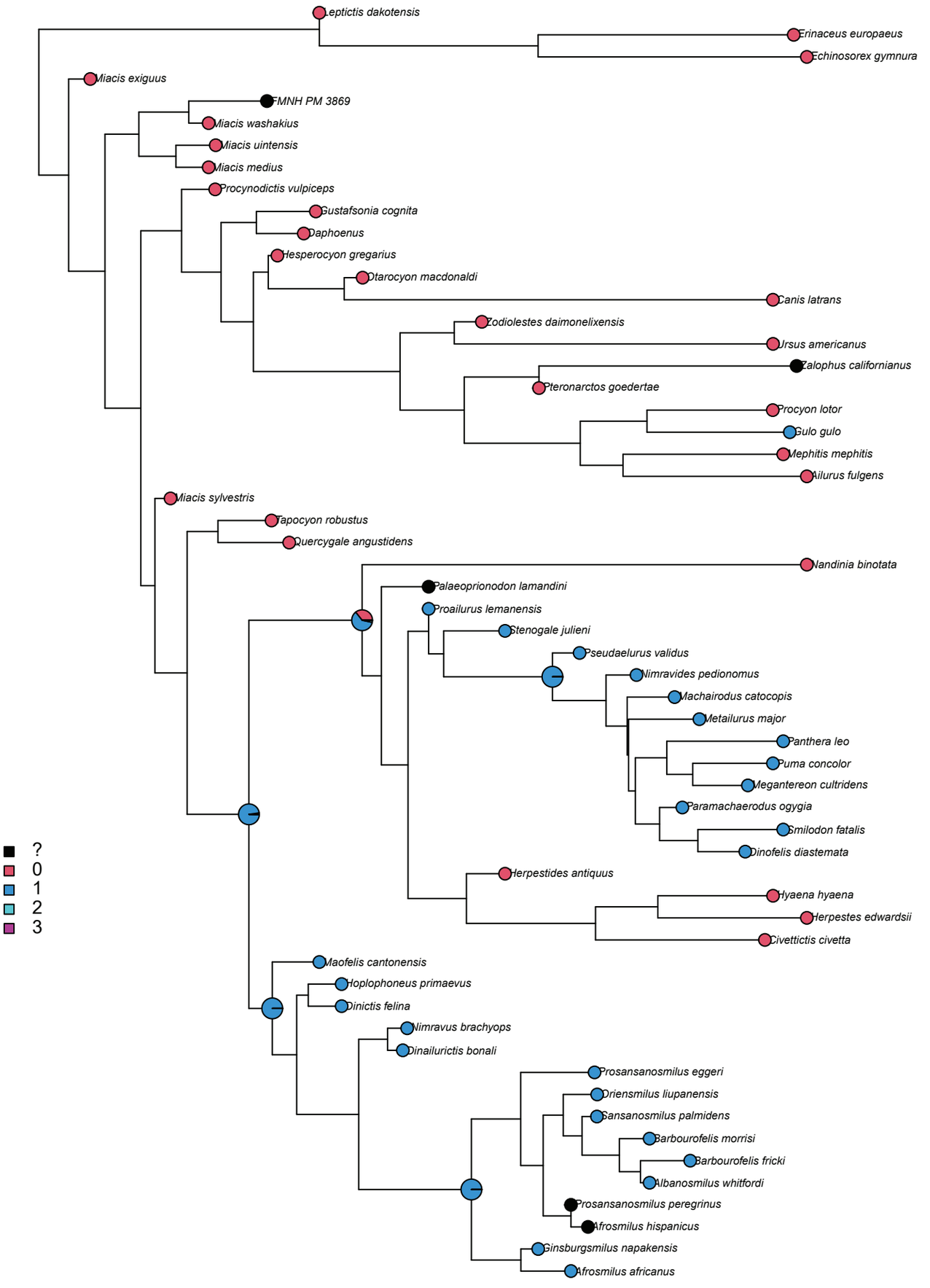

Figure S22. Synapomorphy 47

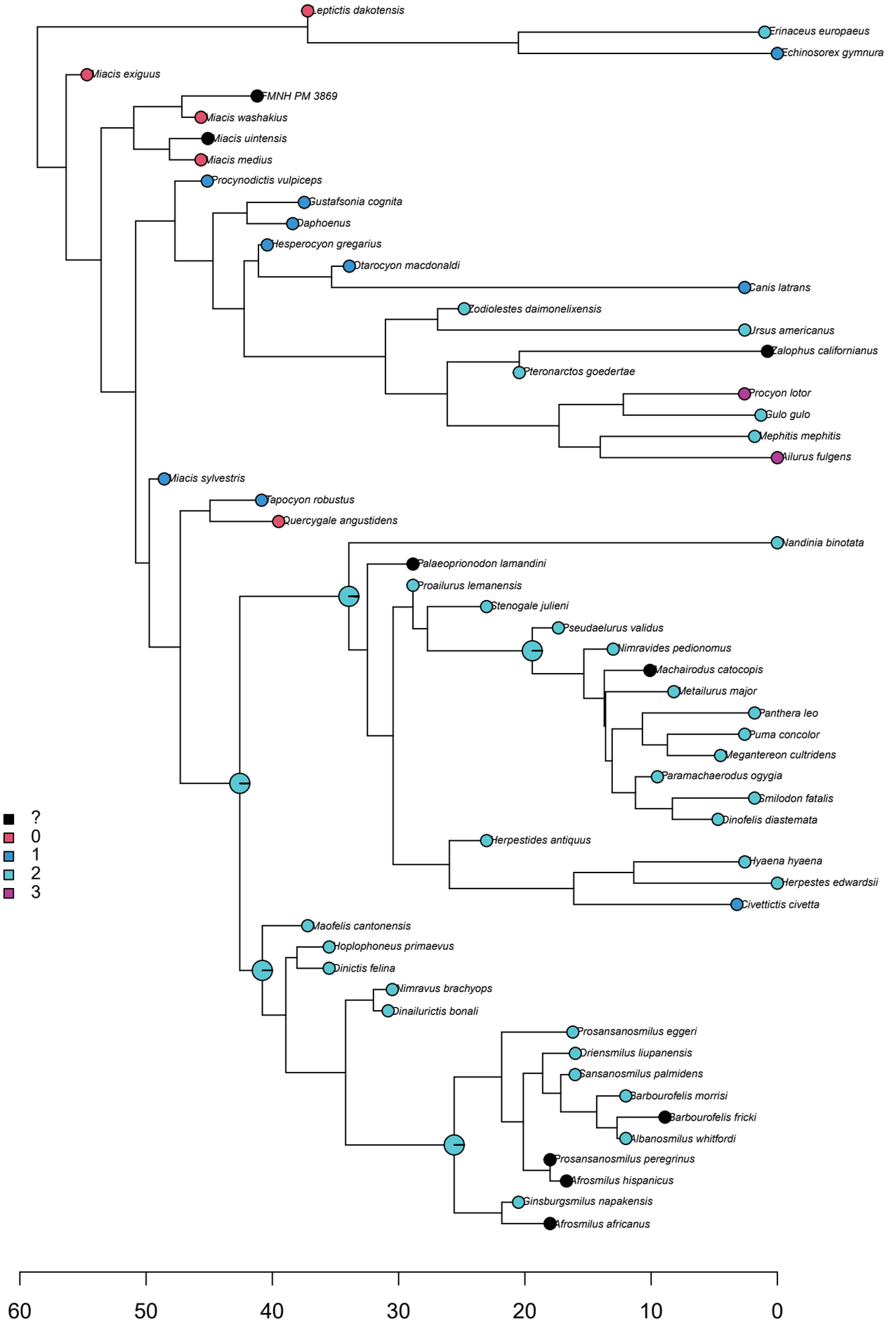

Figure S23. Synapomorphy 49

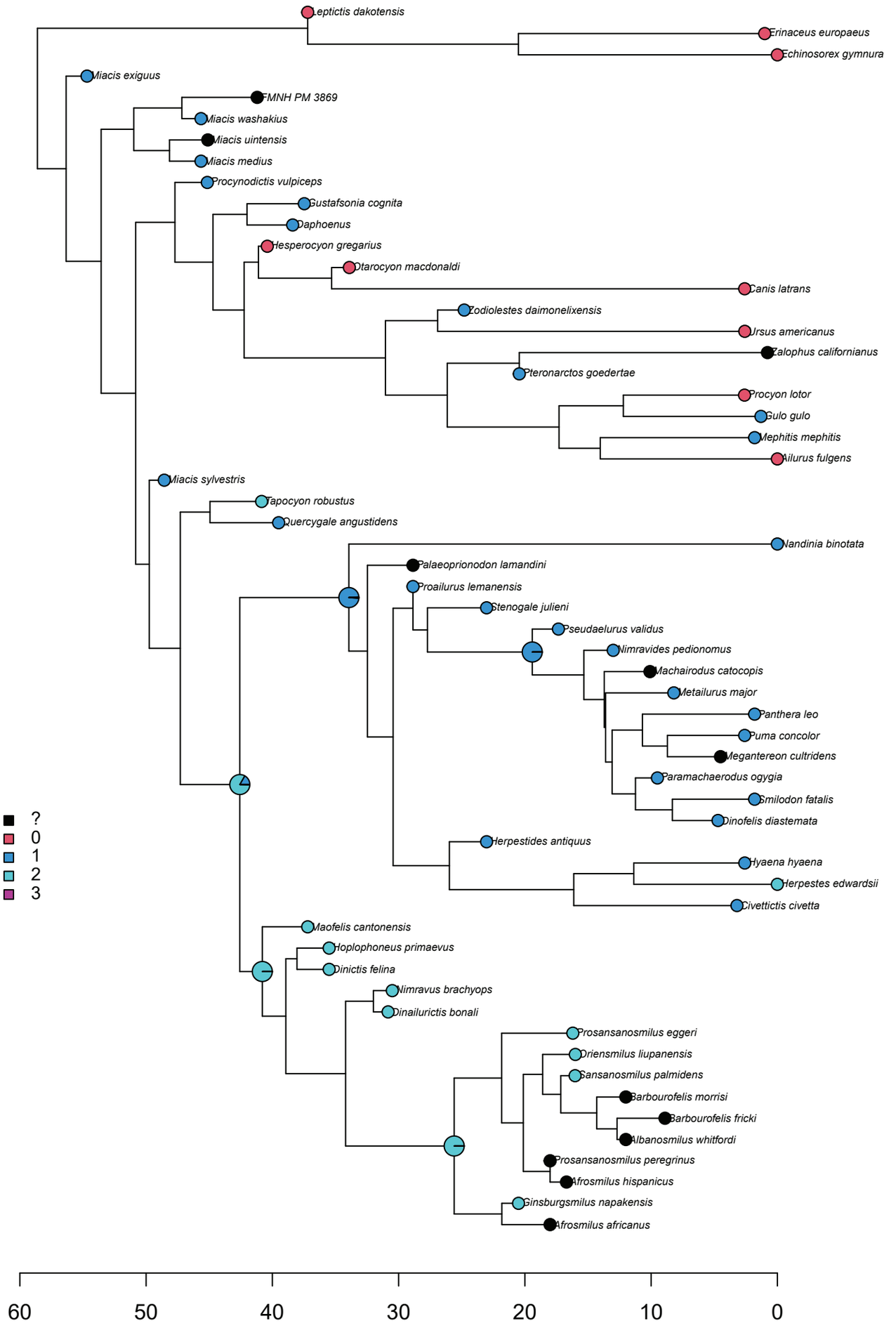

Figure S24. Synapomorphy 50

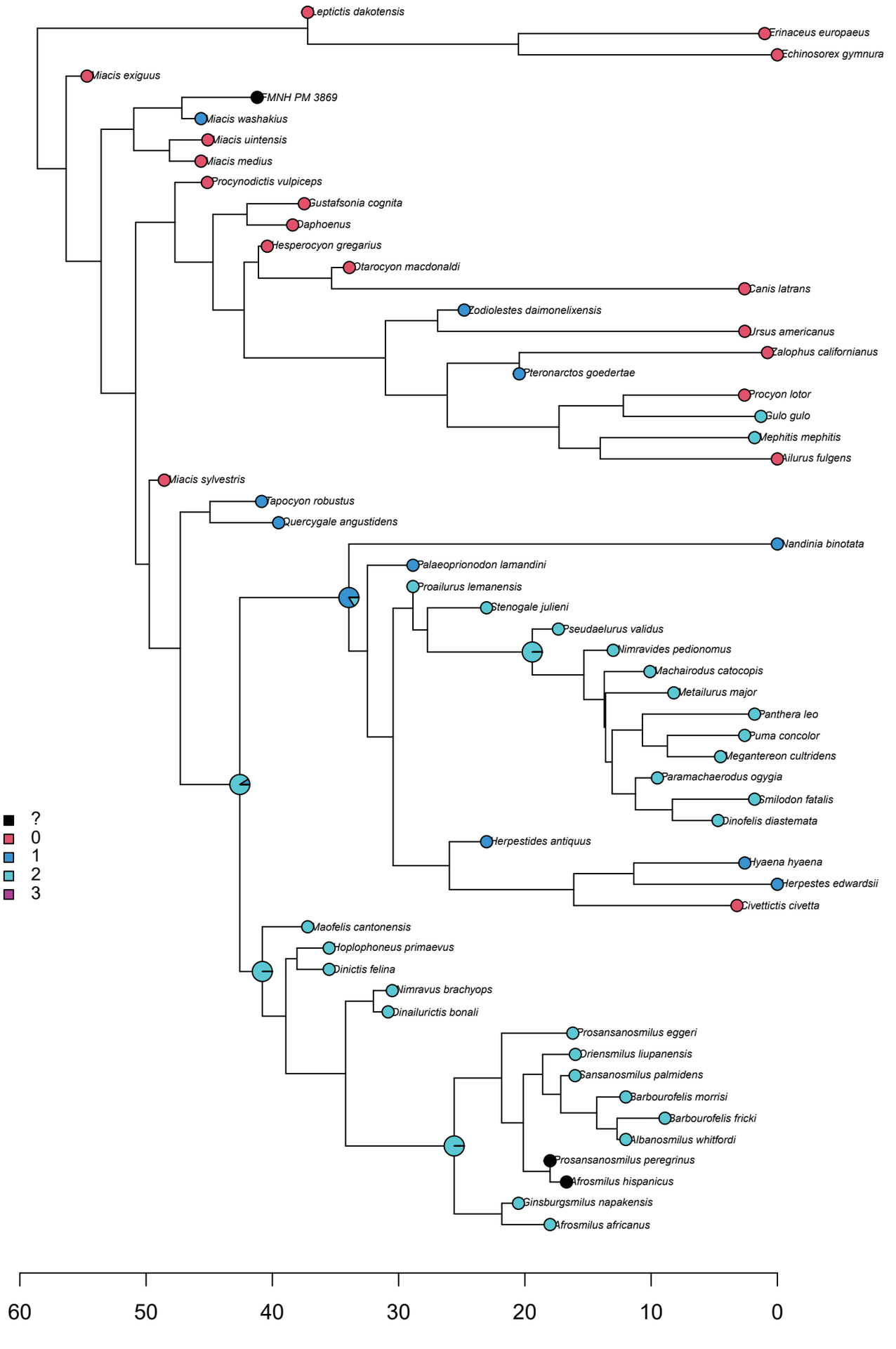

Figure S25. Synapomorphy 56

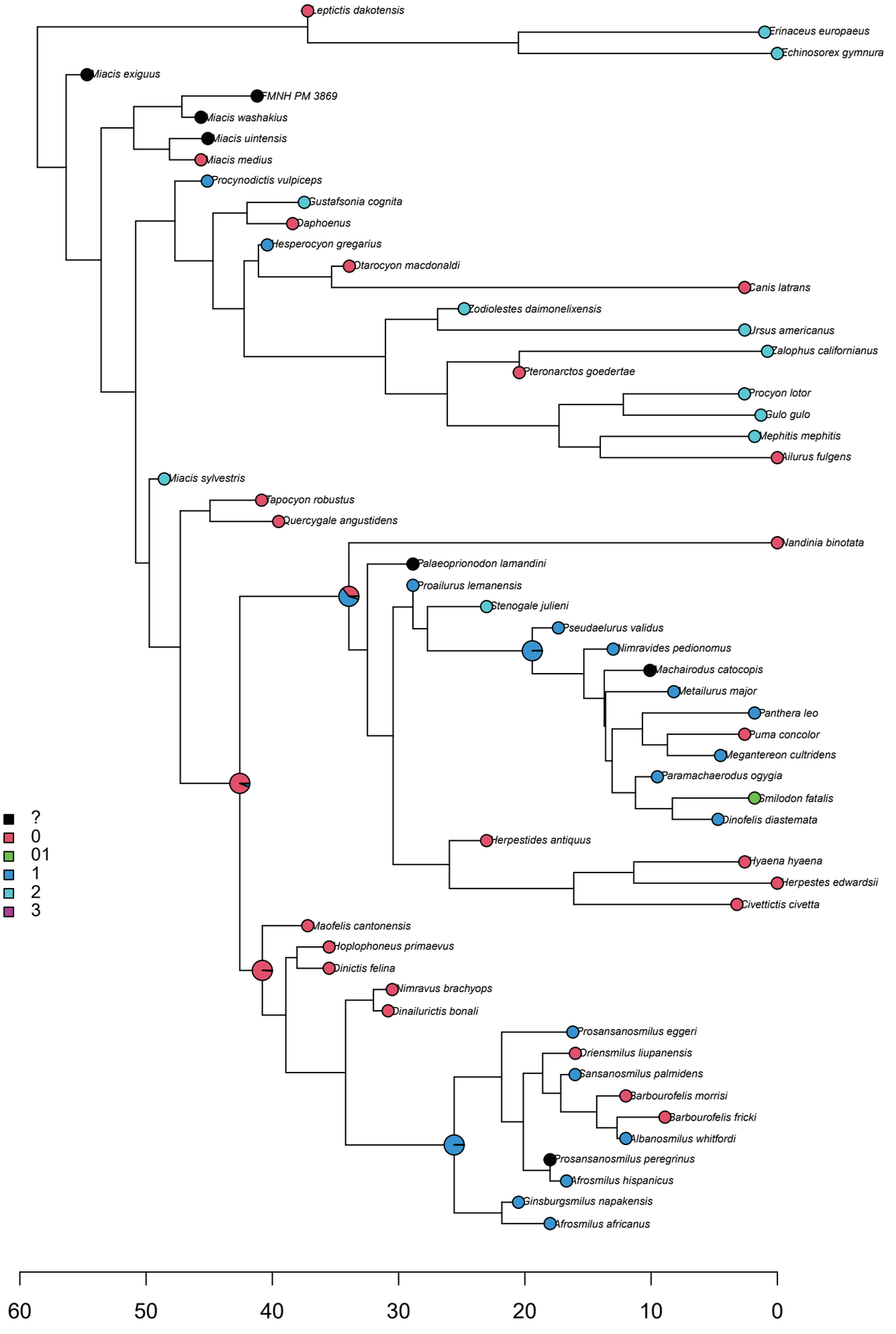

Figure S26. Synapomorphy 57

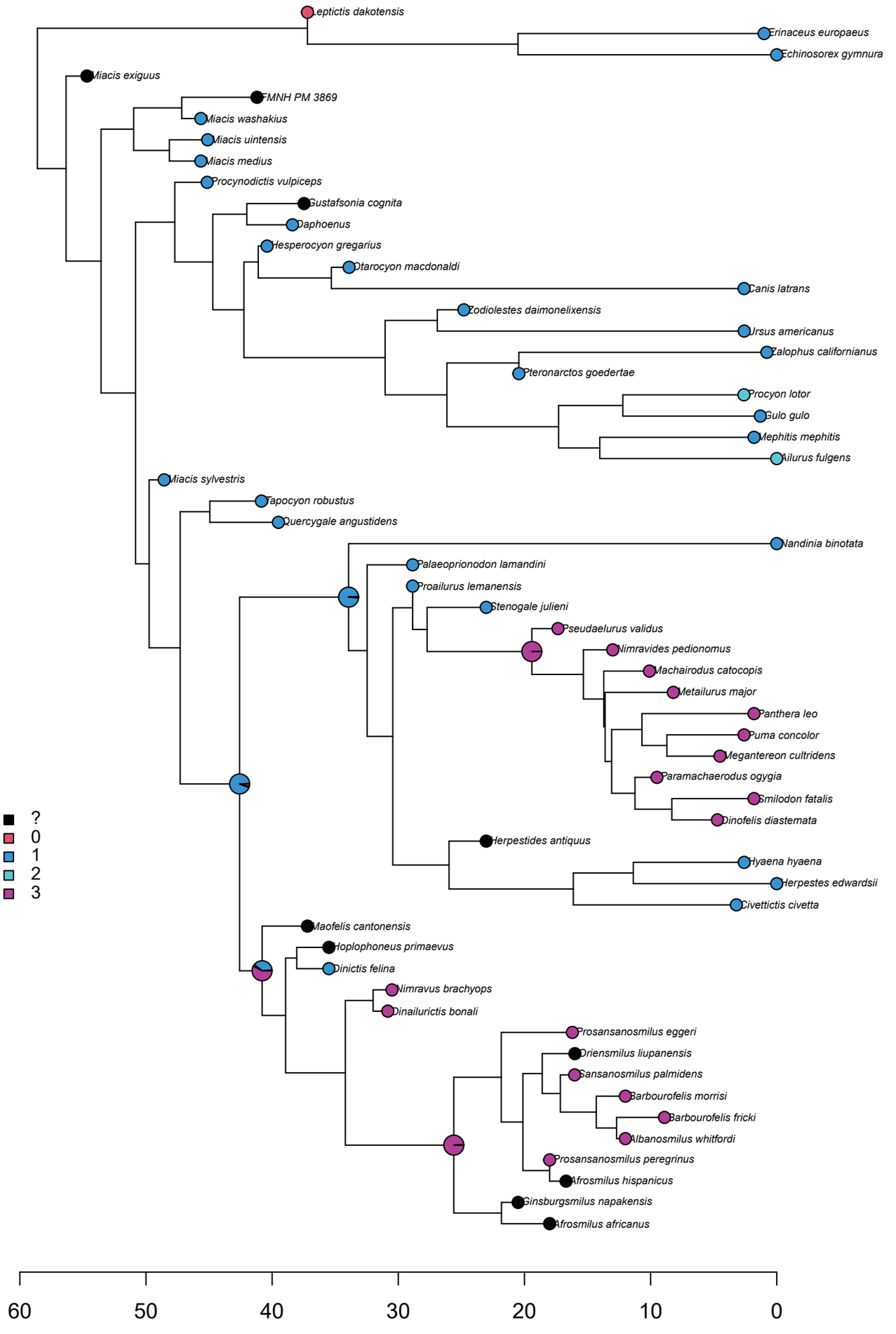

Figure S27. Synapomorphy 58

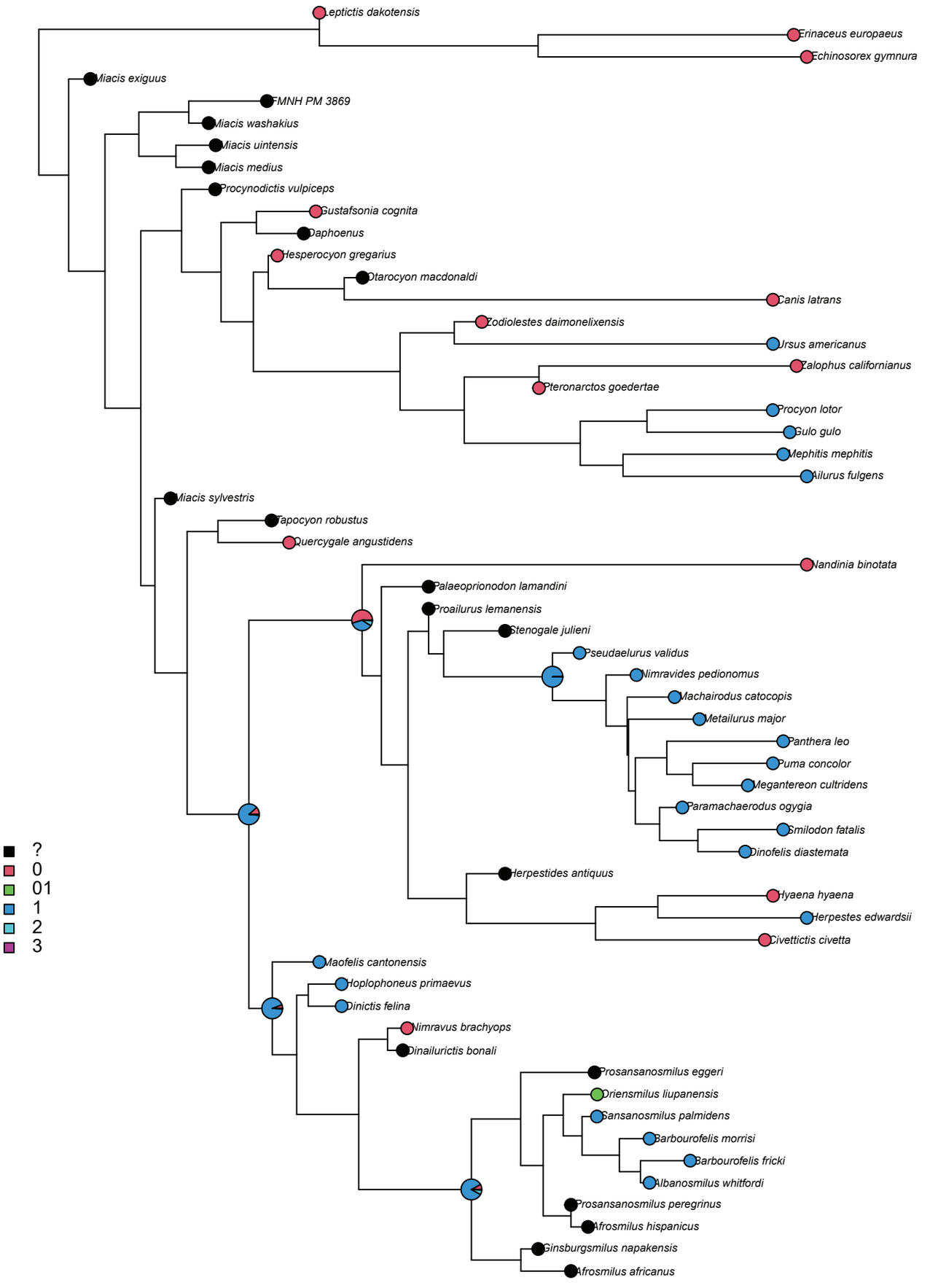

Figure S28. Synapomorphy 65

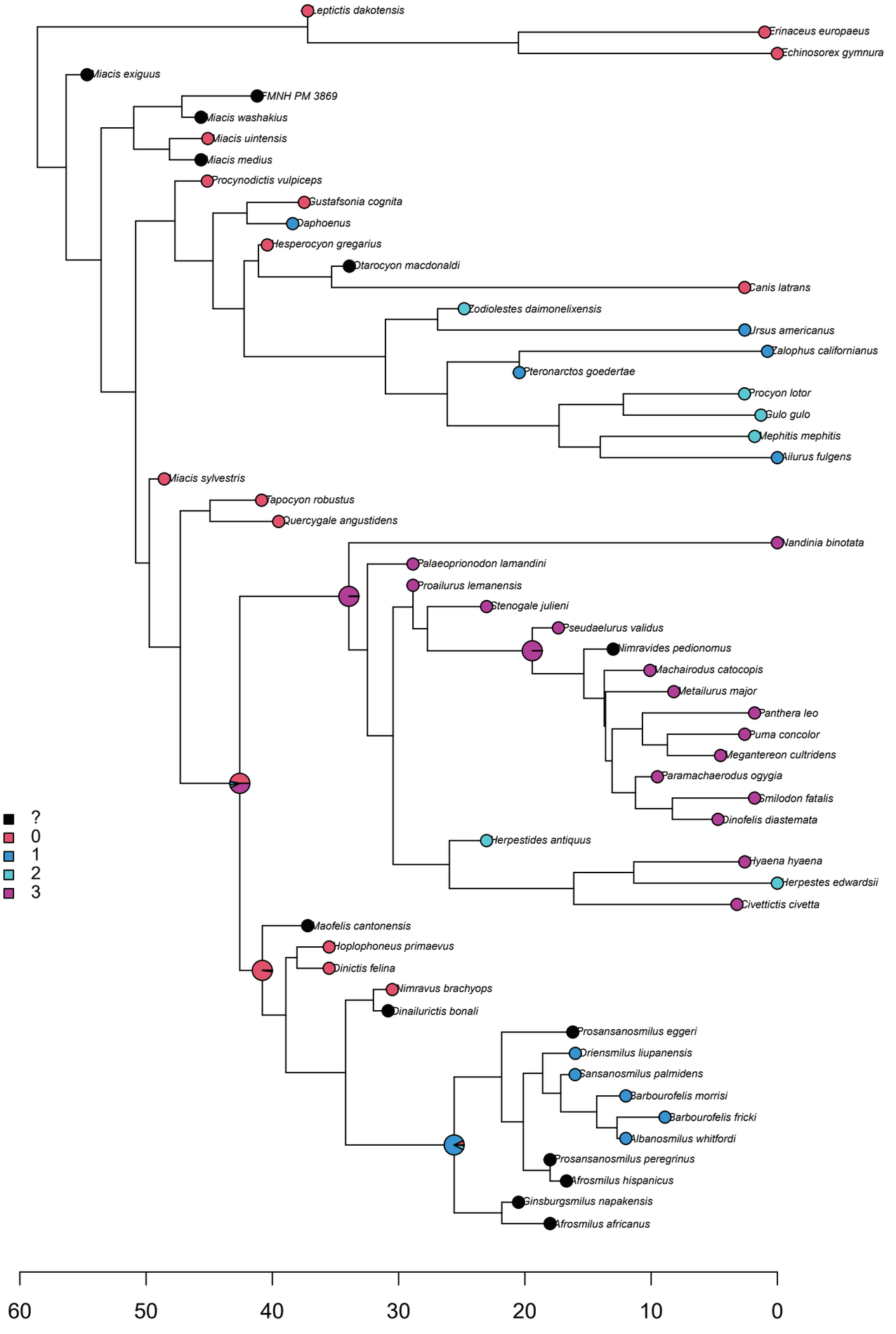

Figure S29. Synapomorphy 66

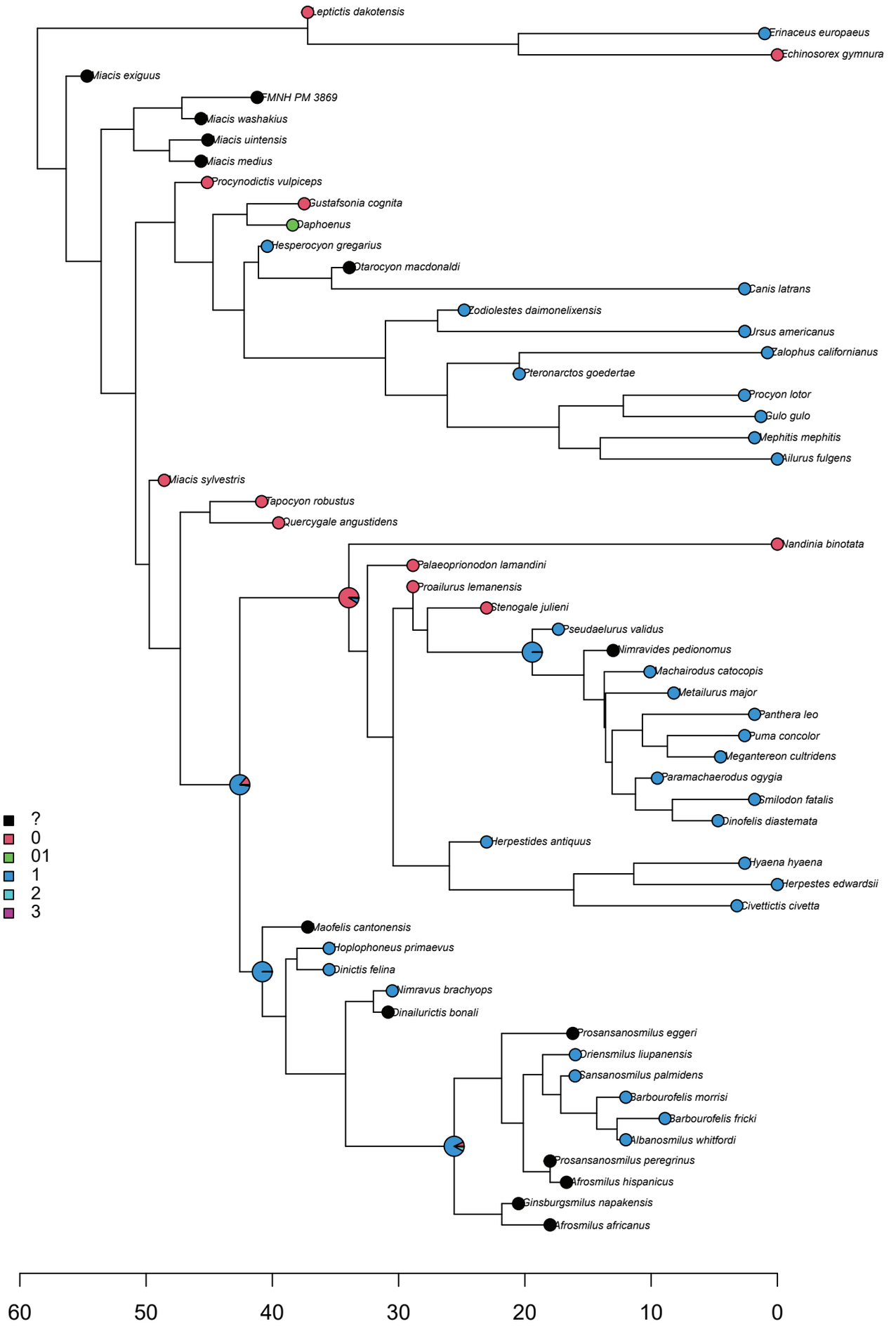

Figure S30. Synapomorphy 82

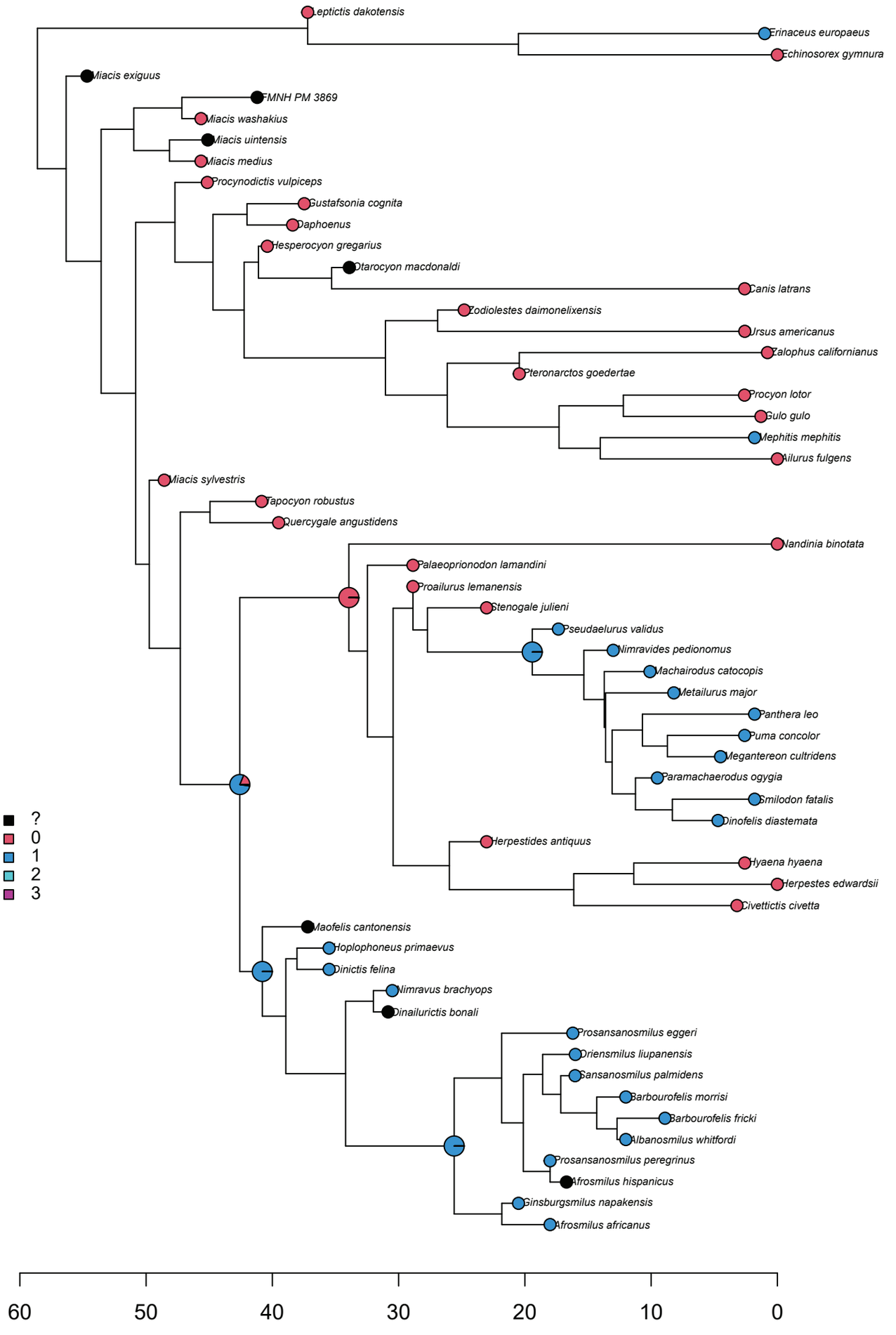

Figure S31. Synapomorphy 137

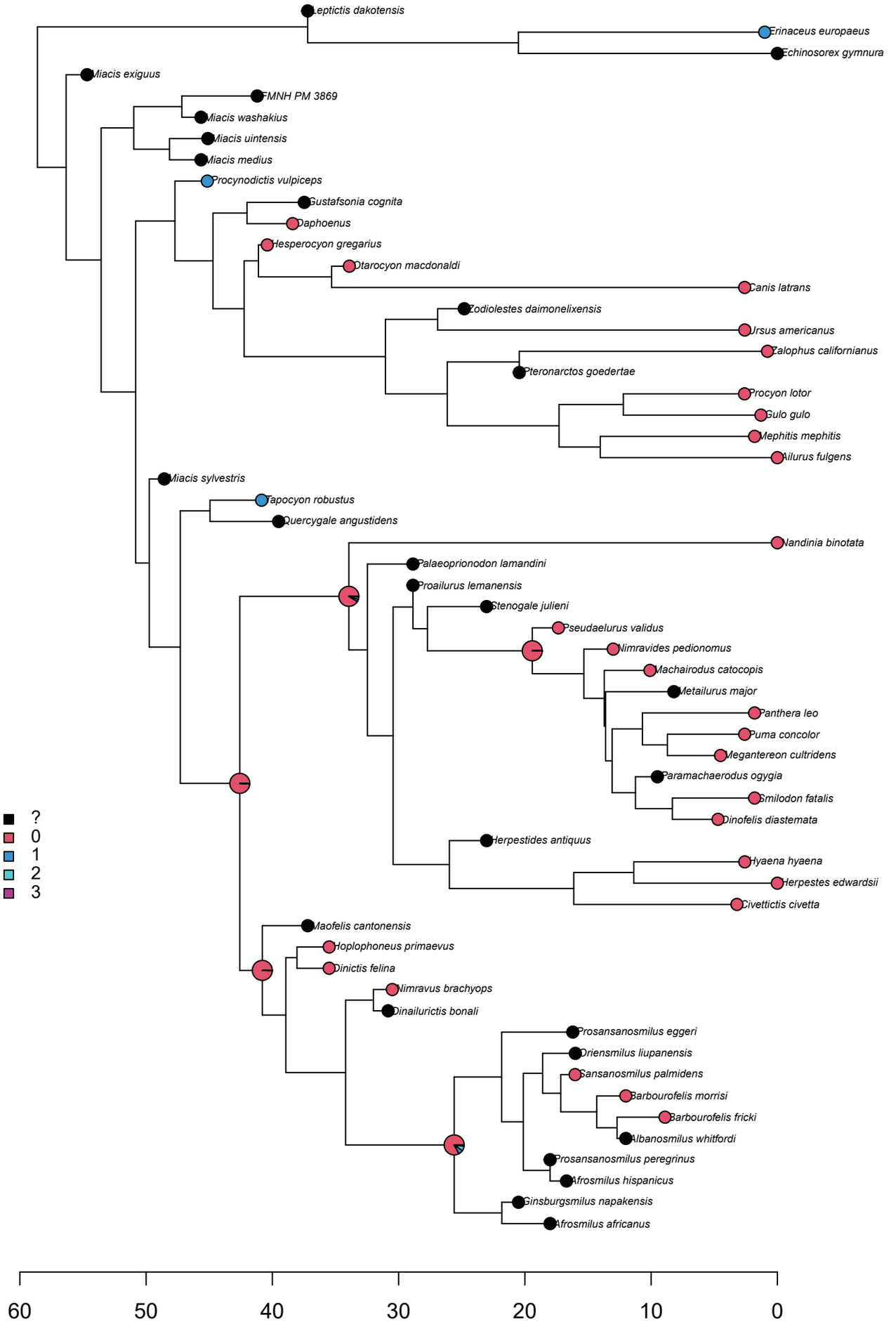

Figure S32. Synapomorphy 142

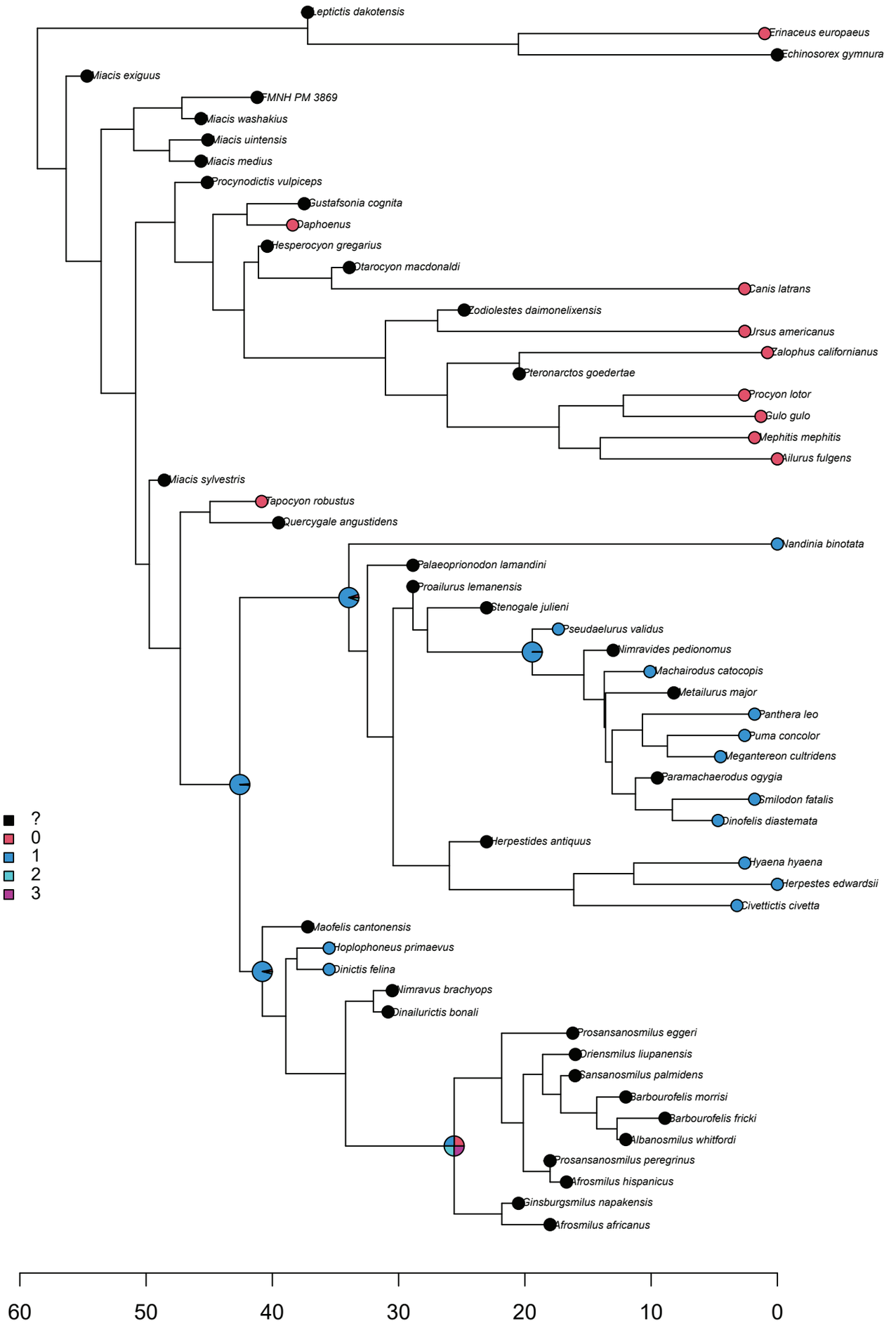

Figure S33. Synapomorphy 146

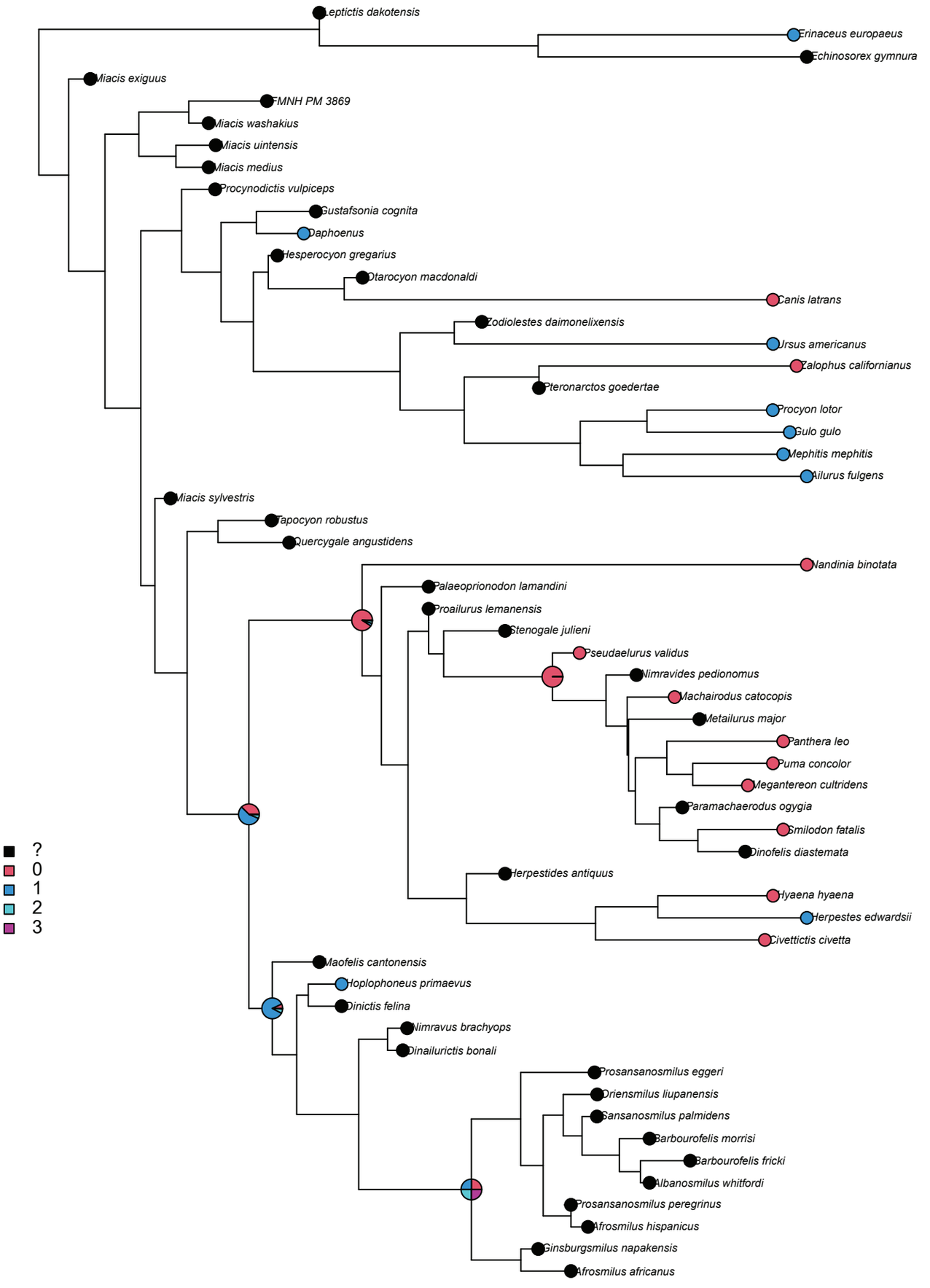

Figure S34. Synapomorphy 179

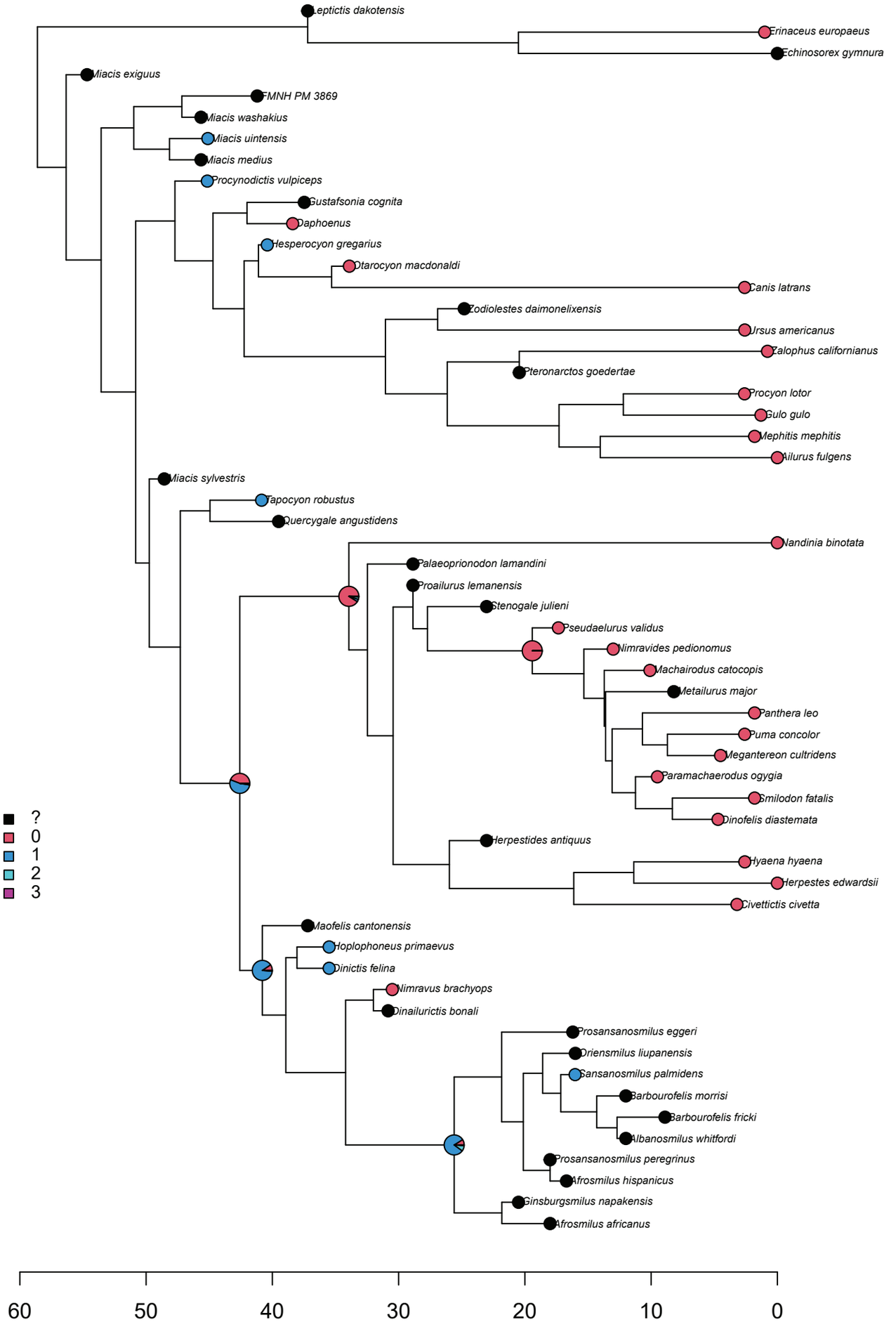

Figure S35. Synapomorphy 183

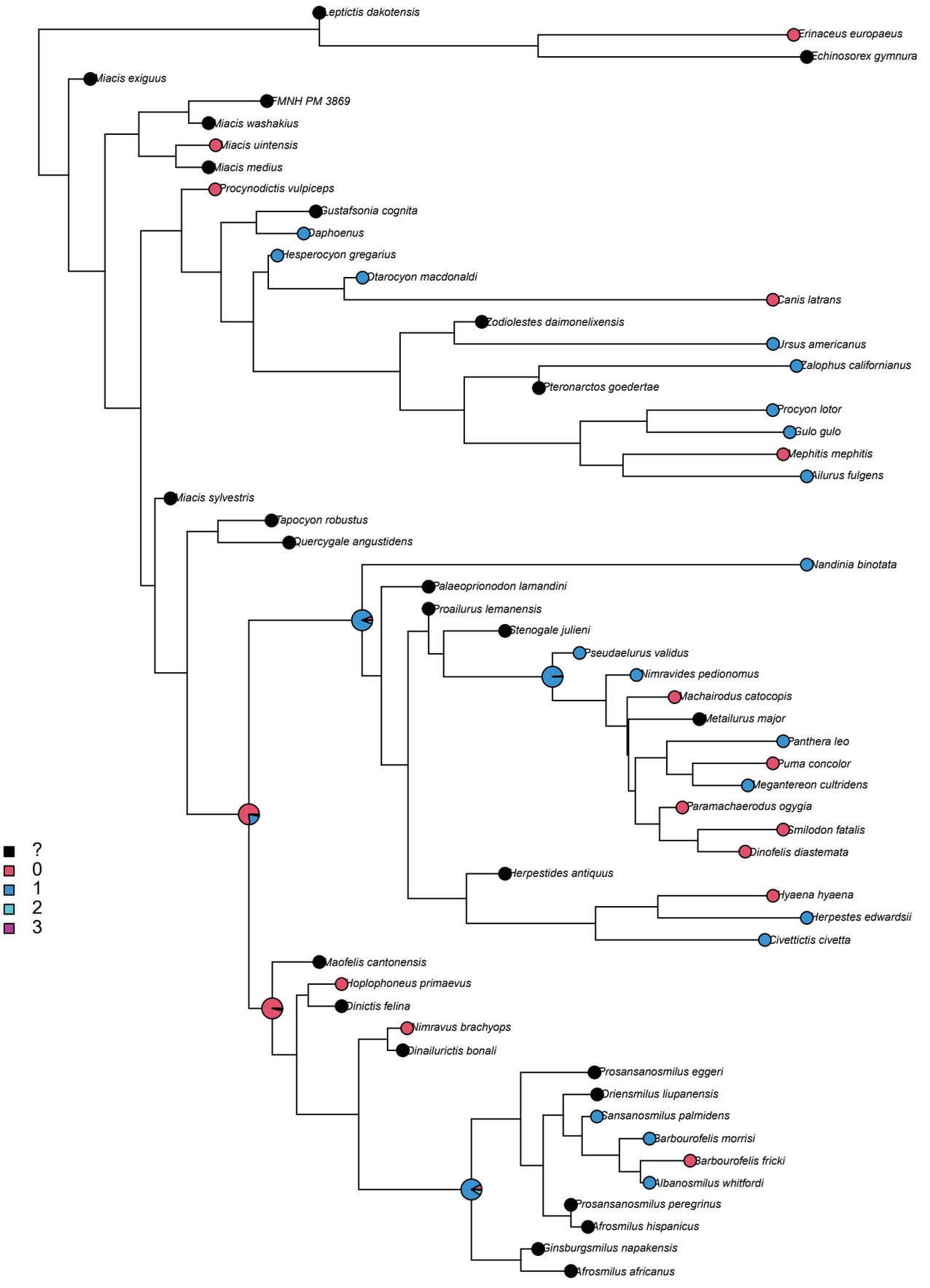

Figure S36. Synapomorphy 209

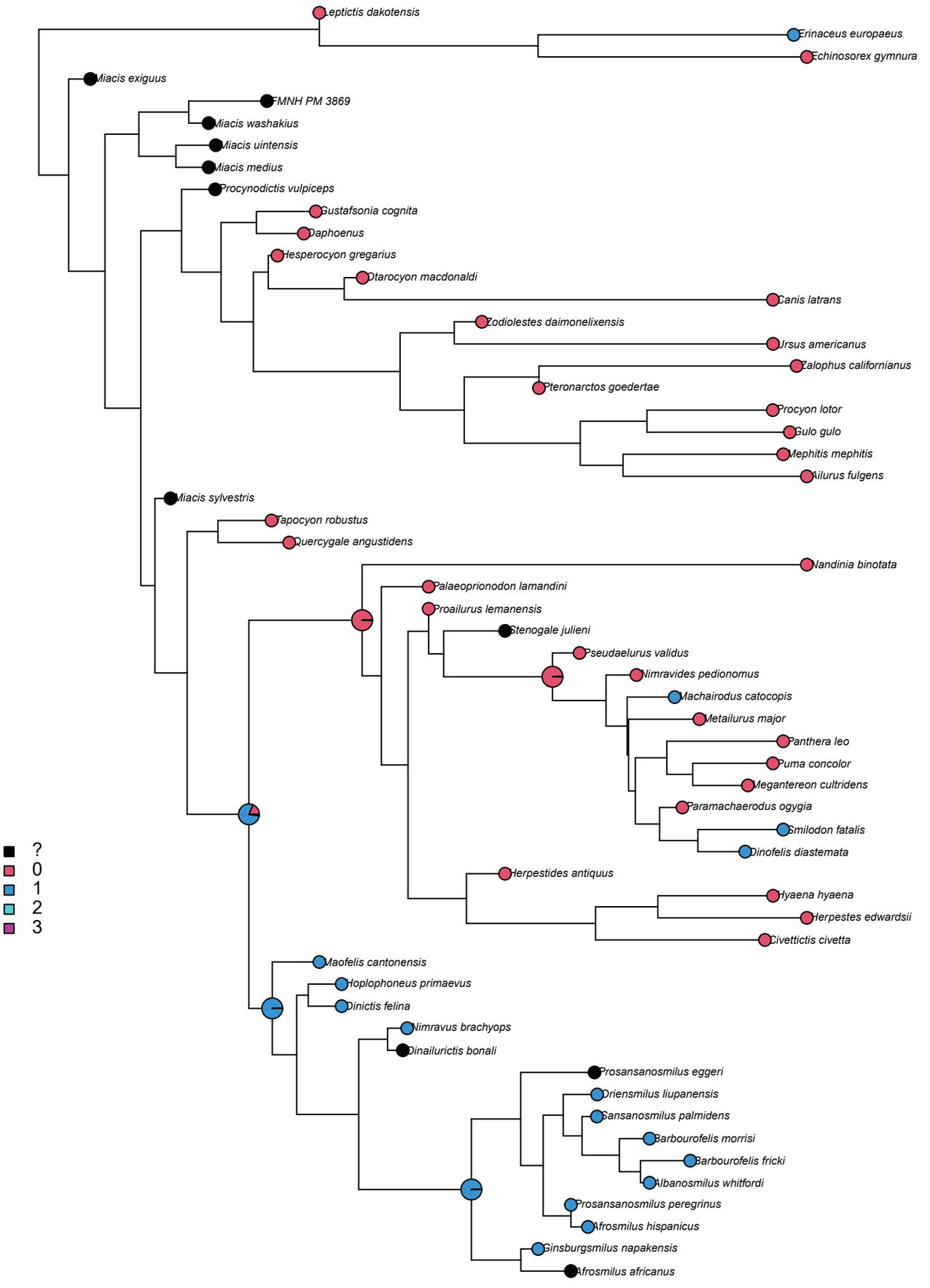

Figure S37. Synapomorphy 212

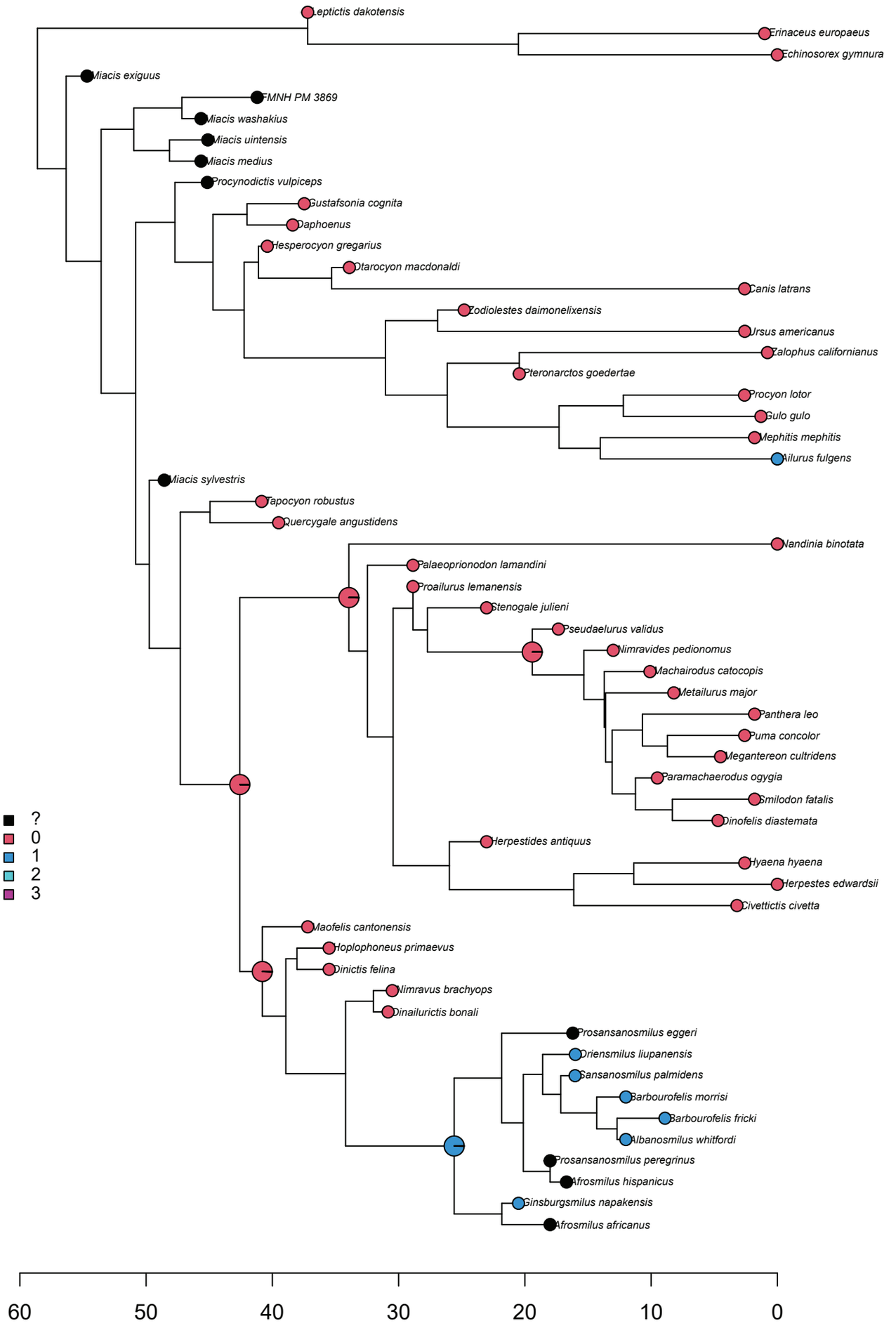

Figure S38. Synapomorphy 217

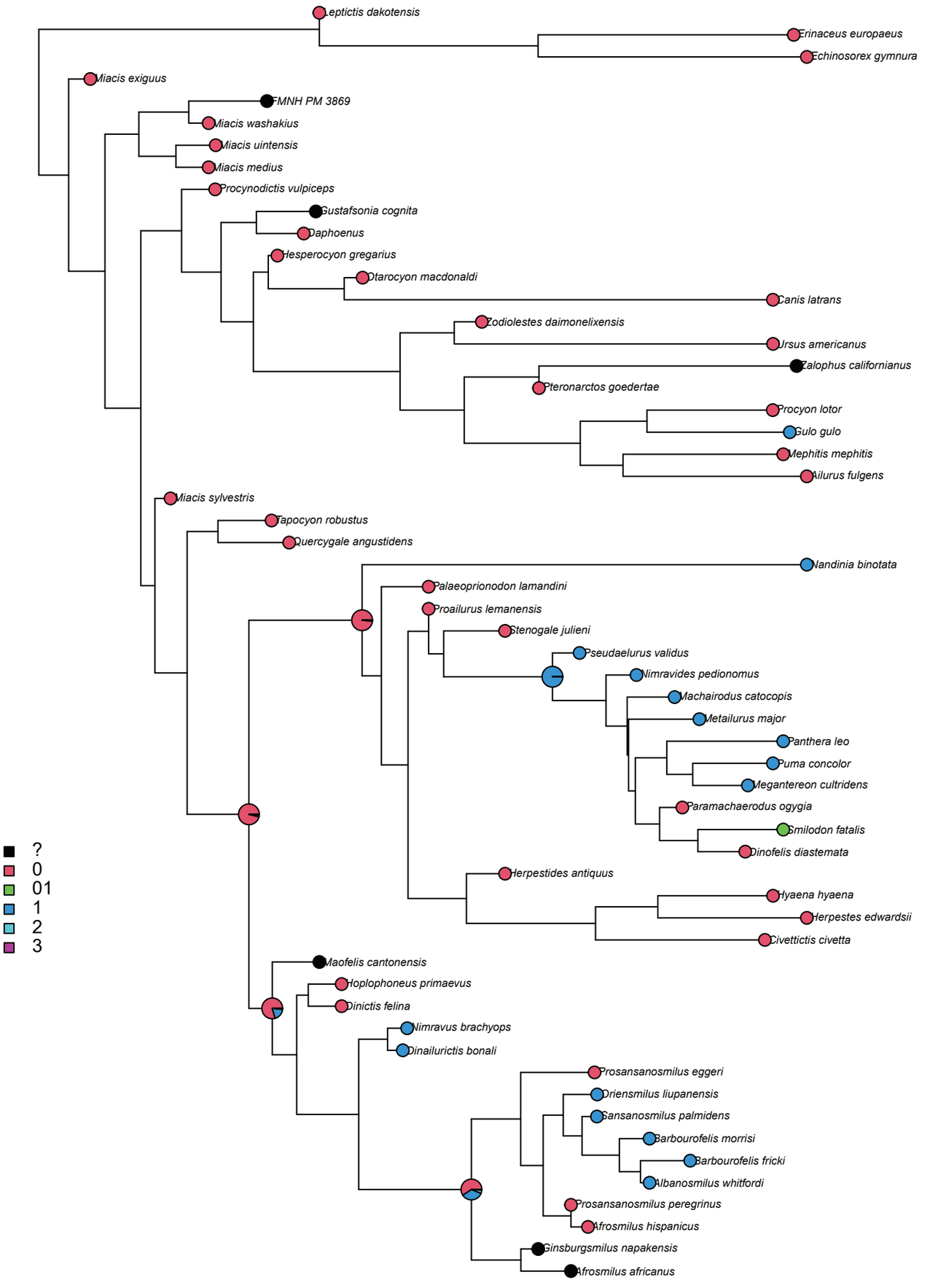

Figure S39. Synapomorphy 218

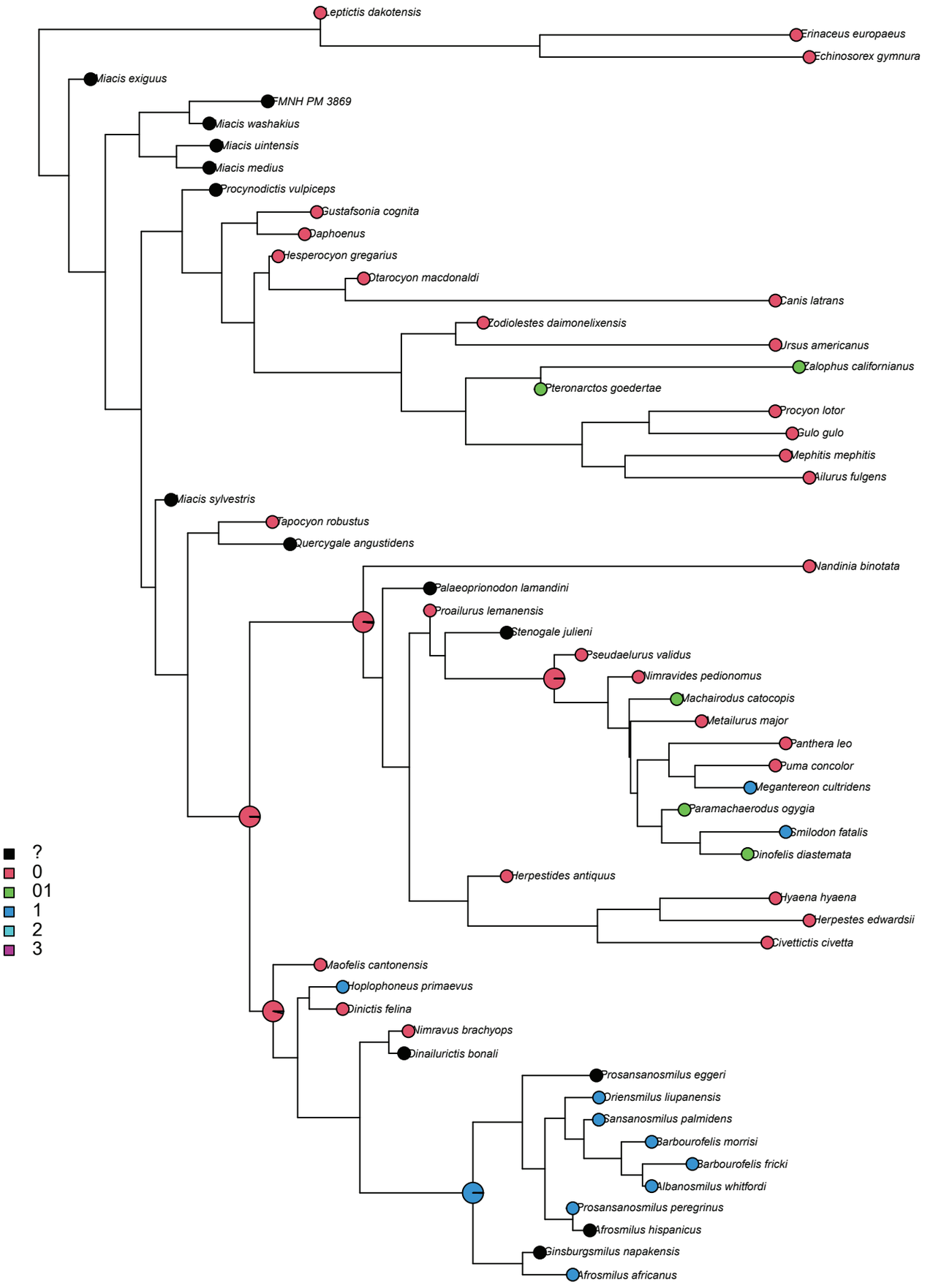

Figure S40. Synapomorphy 220

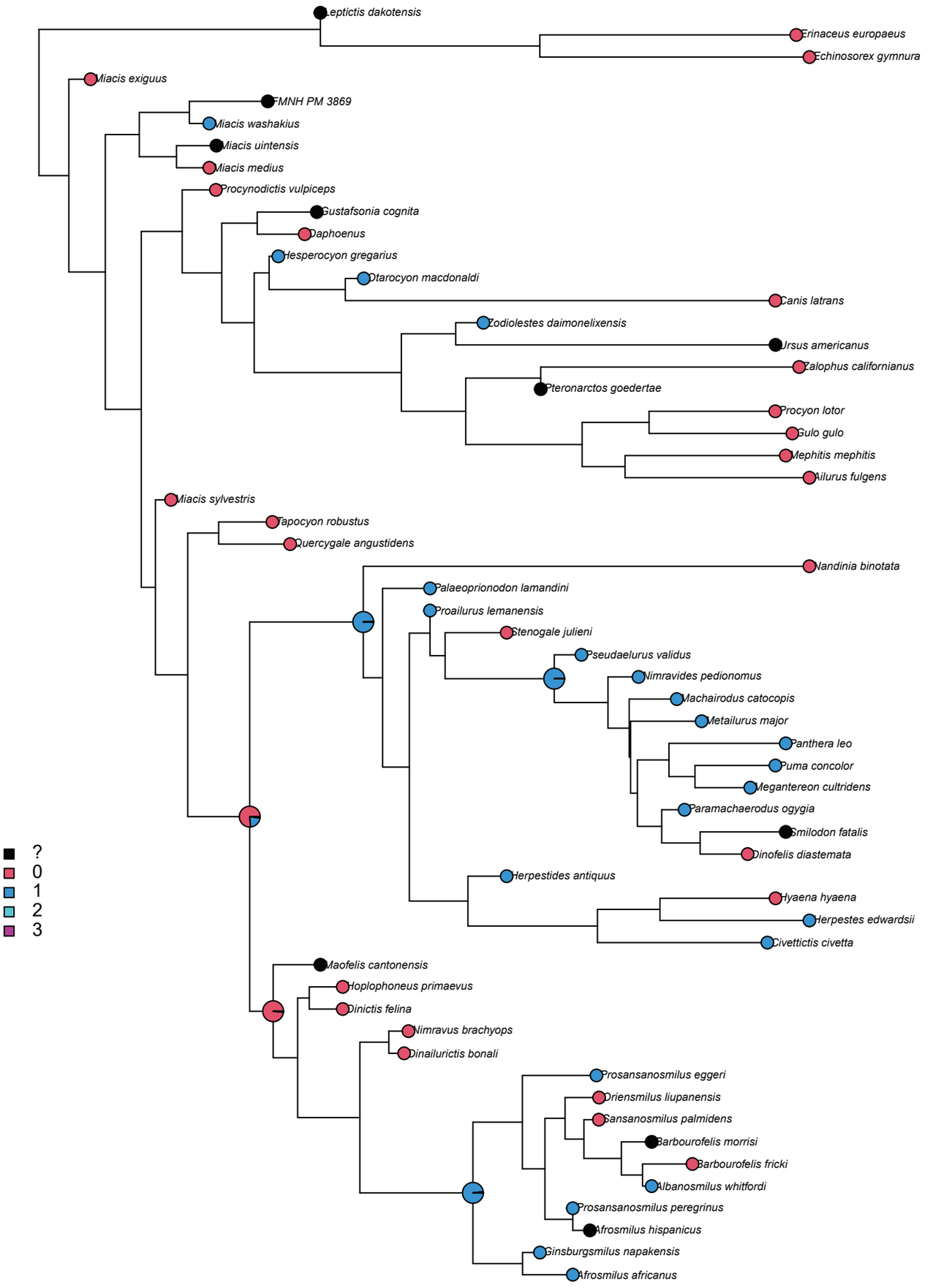

Figure S41. Synapomorphy 221

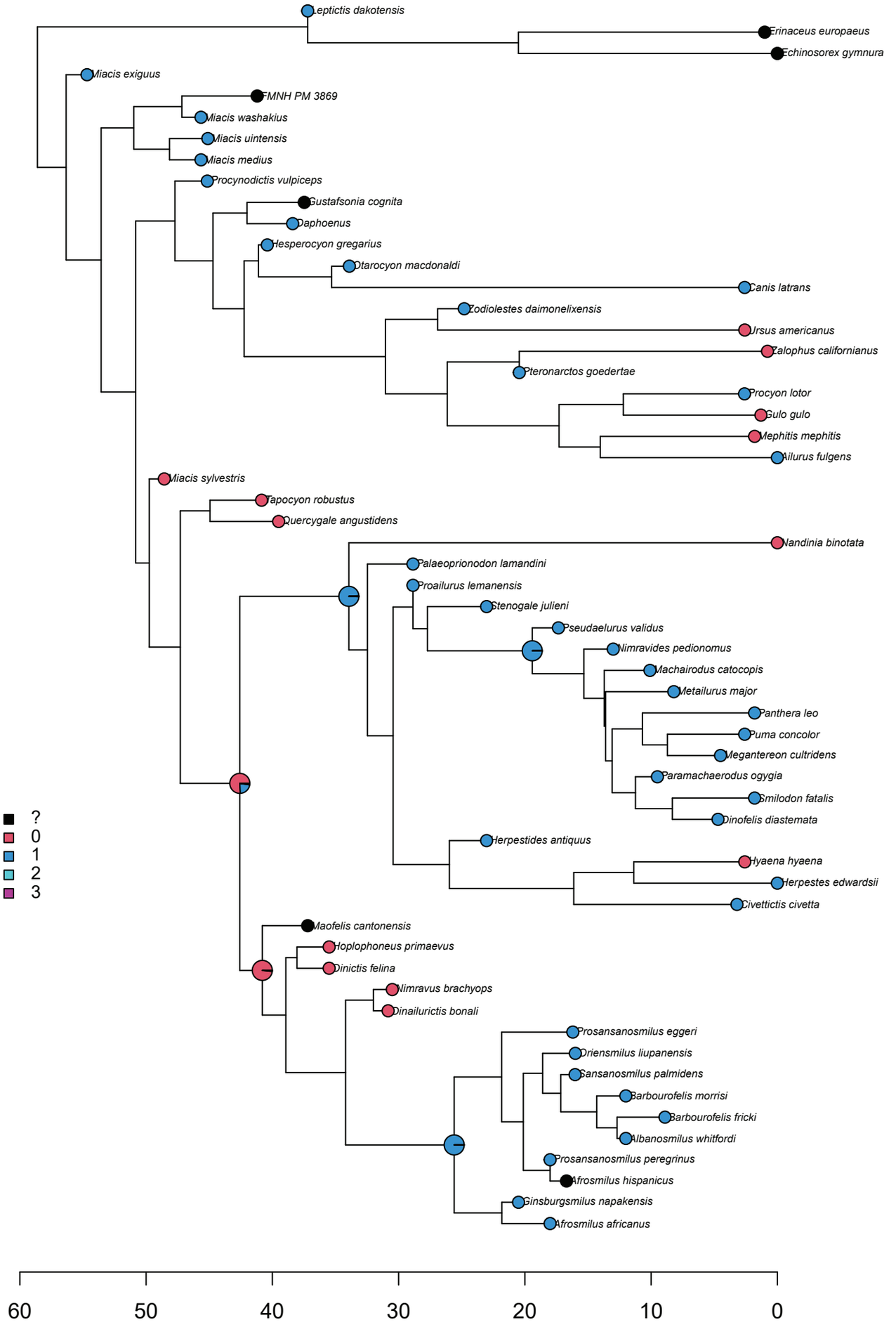

Figure S42. Synapomorphy 222

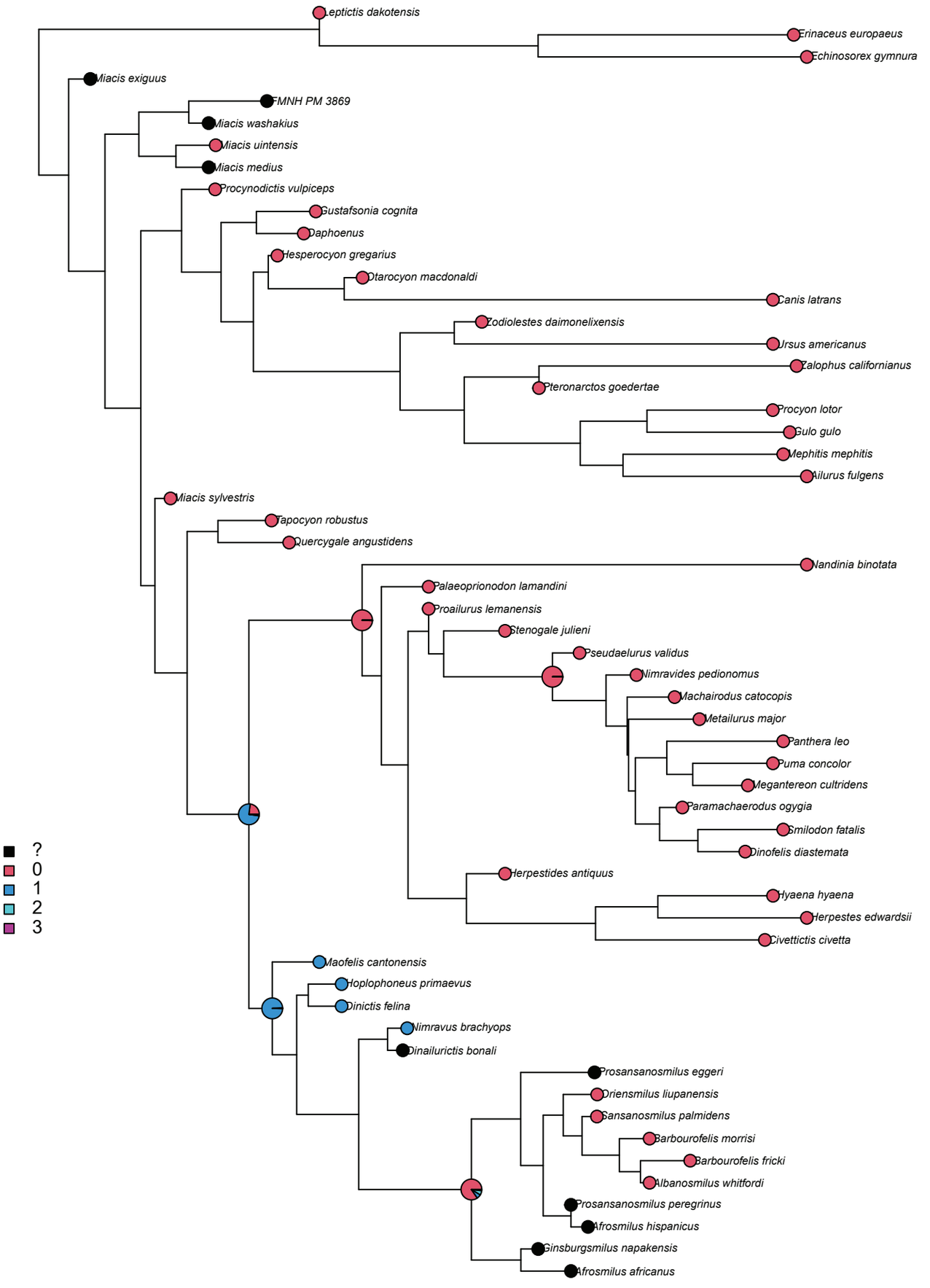

Figure S43. BioGeoBEARS DEC on Nimravidae M0_unconstrained ancstates: global optim, 4 areas max. d=0.0183; e=0; j=0; LnL=−24.55

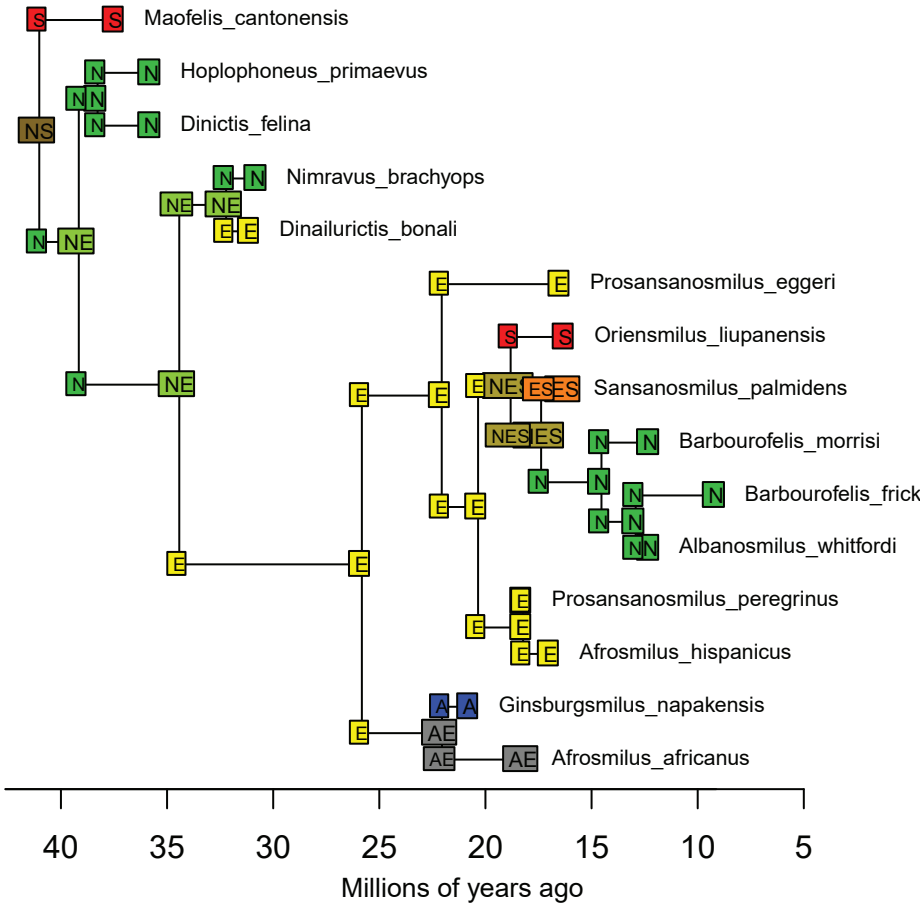

Figure S44. BioGeoBEARS DEC on Nimravidae M0_unconstrained ancstates: global optim, 4 areas max. d=0.0183; e=0; j=0; LnL=−24.55

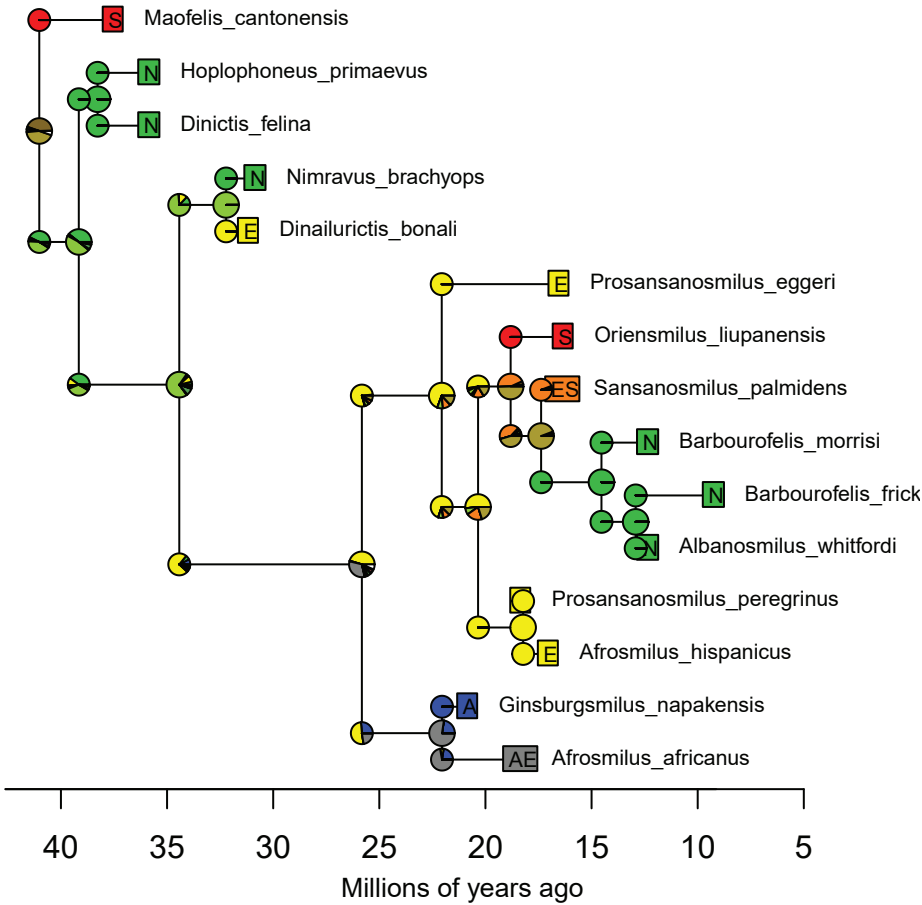

Figure S45. BioGeoBEARS DEC+J on Nimravidae M0_unconstrained ancstates: global optim, 4 areas max. d=0.011; e=0; j=0.1111; LnL=−22.52

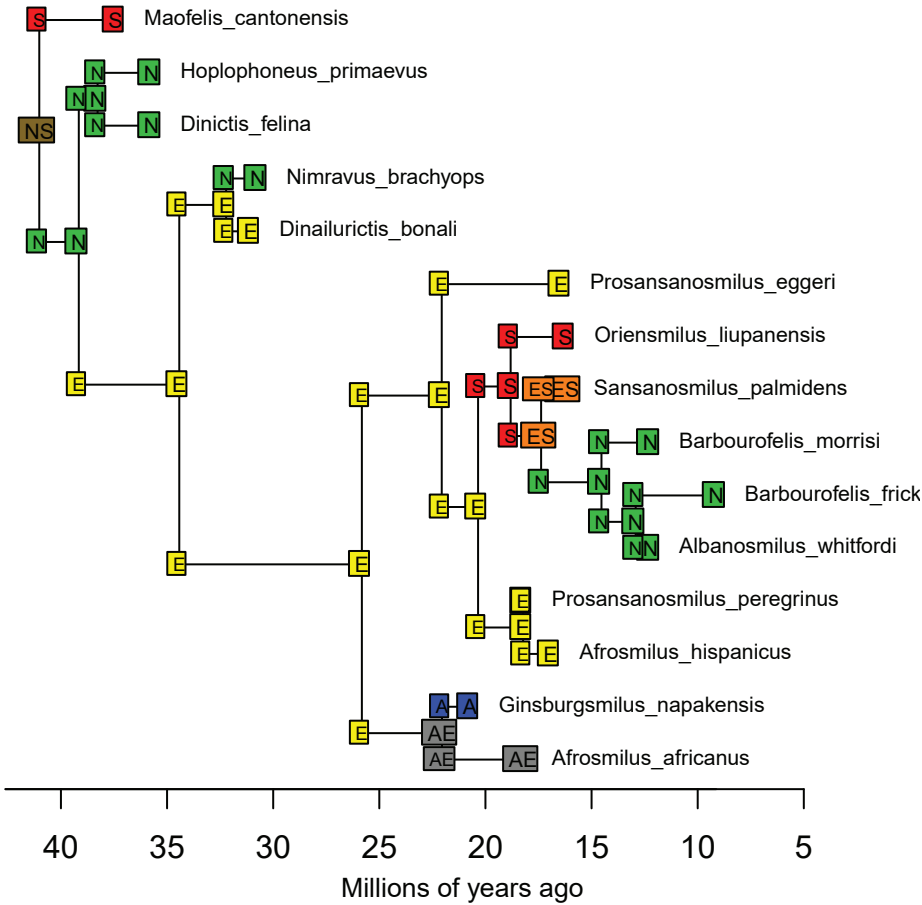

Figure S46. BioGeoBEARS DEC+J on Nimravidae M0_unconstrained ancstates: global optim, 4 areas max. d=0.011; e=0; j=0.1111; LnL=−22.52

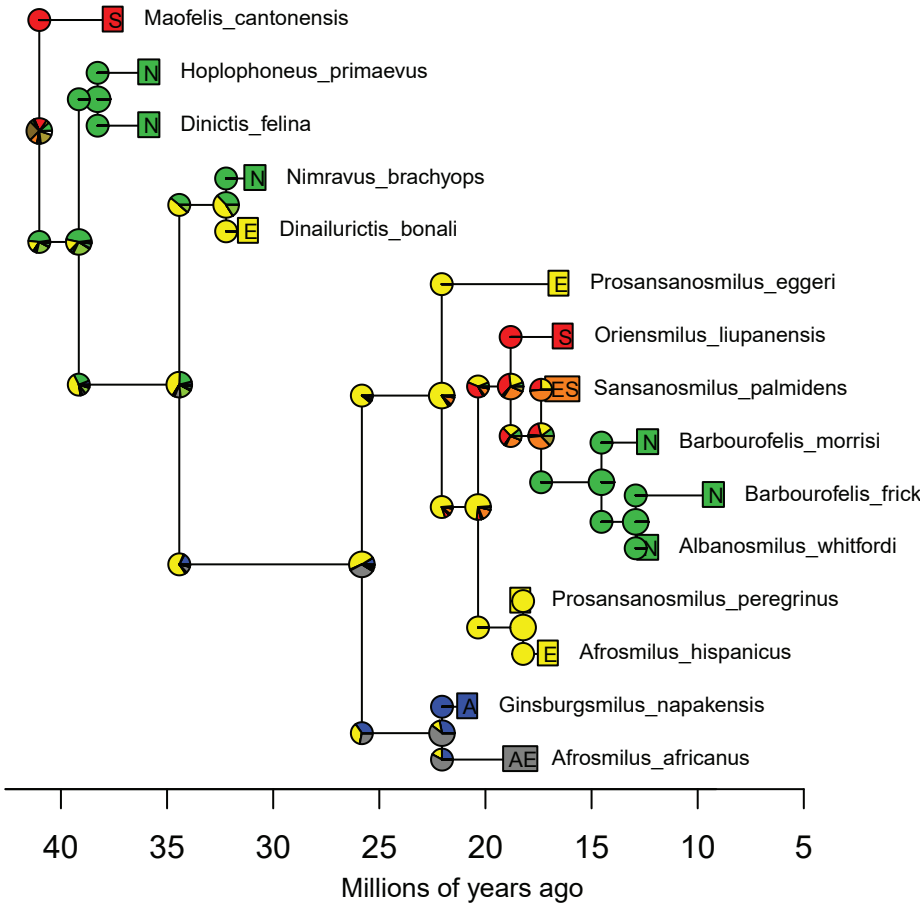

Figure S47. BioGeoBEARS DIVALIKE on Nimravidae M0_unconstrained ancstates: global optim, 4 areas max. d=0.0311; e=0; j=0; LnL=−24.38

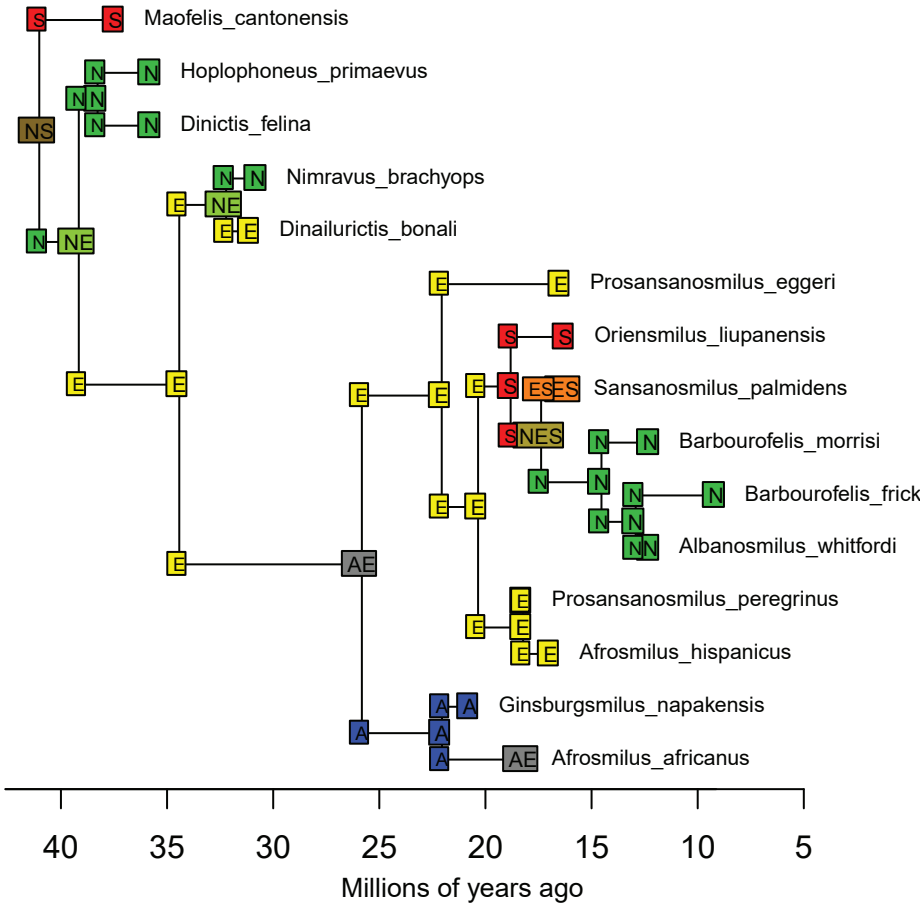

Figure S48. BioGeoBEARS DIVALIKE on Nimravidae M0_unconstrained ancstates: global optim, 4 areas max. d=0.0311; e=0; j=0; LnL=−24.38

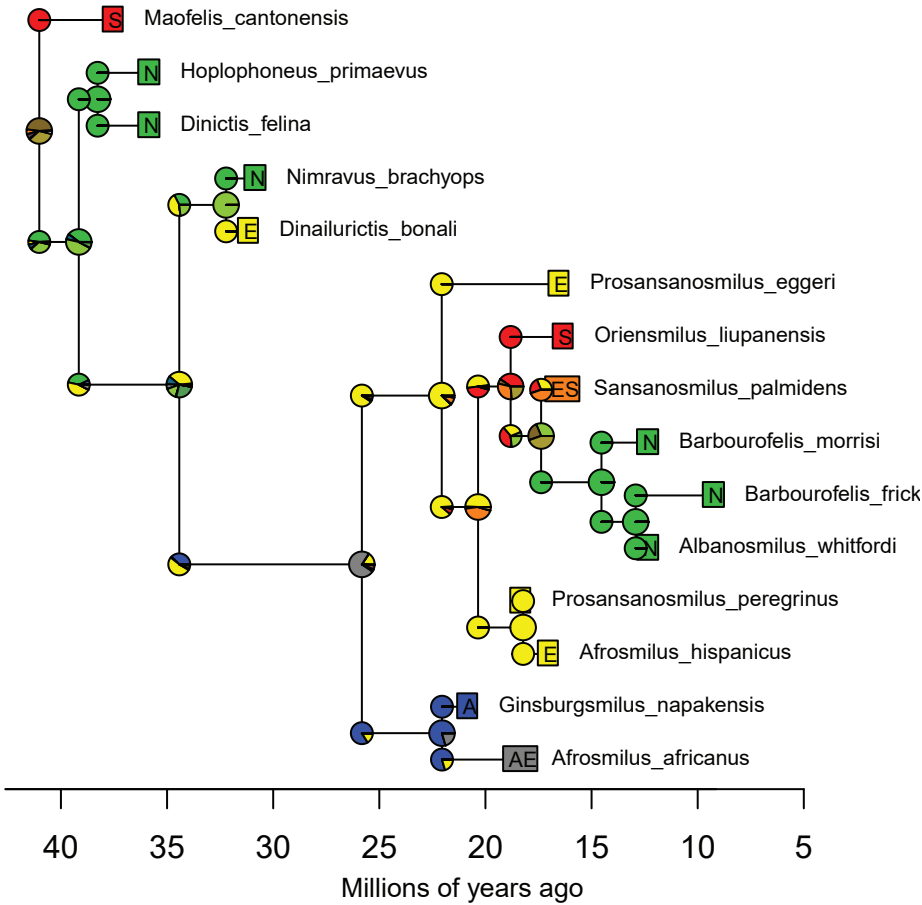

Figure S49. BioGeoBEARS DIVALIKE+J on Nimravidae M0_unconstrained ancstates: global optim, 4 areas max. d=0.015; e=0; j=0.0972; LnL=−22.21

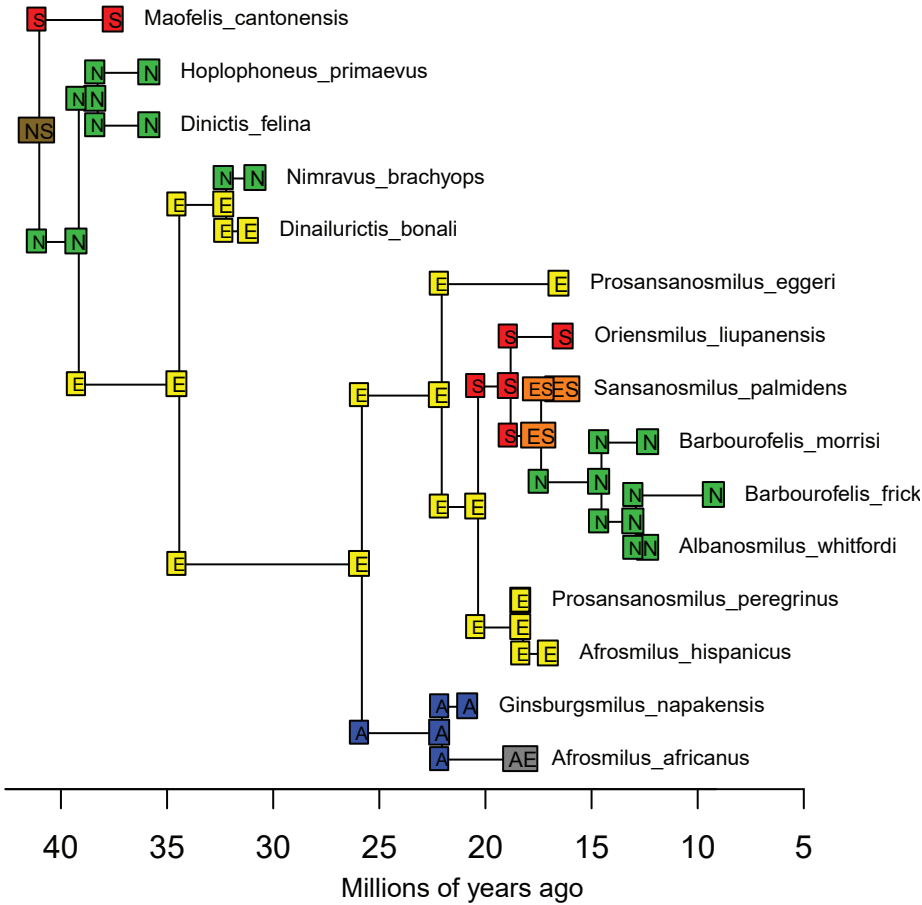

Figure S50. BioGeoBEARS DIVALIKE+J on Nimravidae M0_unconstrained ancstates: global optim, 4 areas max. d=0.015; e=0; j=0.0972; LnL=−22.21

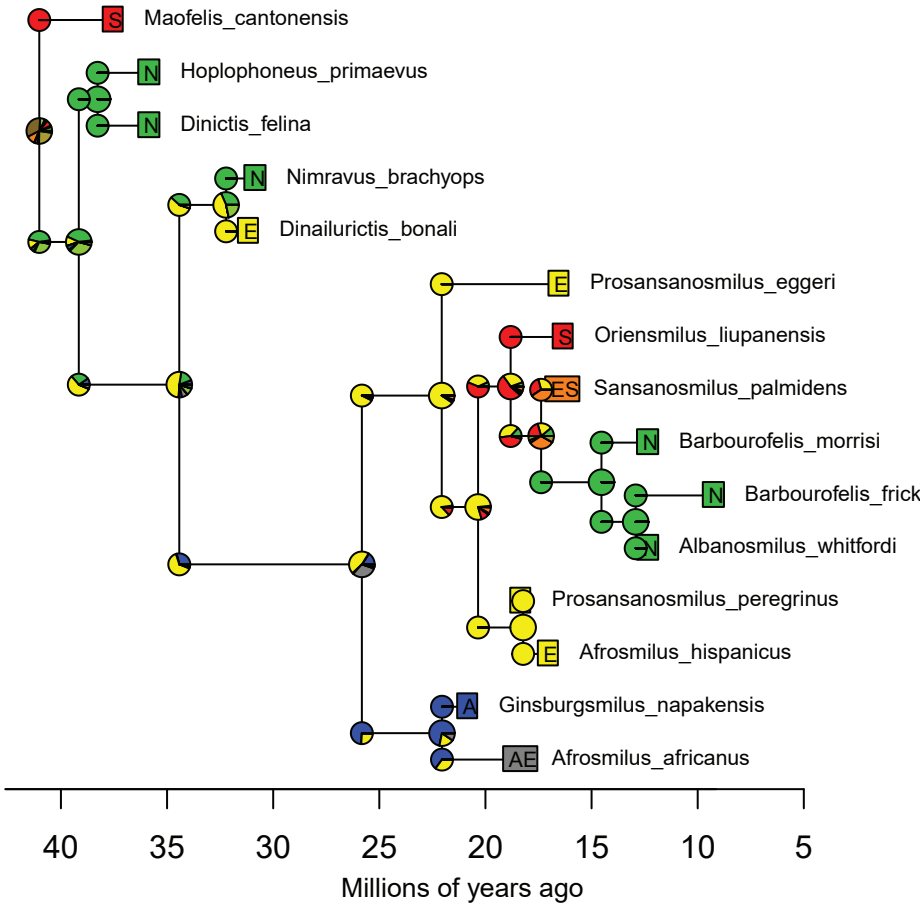

Figure S51. BioGeoBEARS BAYAREALIKE on Nimravidae M0_unconstrained ancstates: global optim, 4 areas max. d=0.0305; e=0.1352; j=0; LnL=−33.70

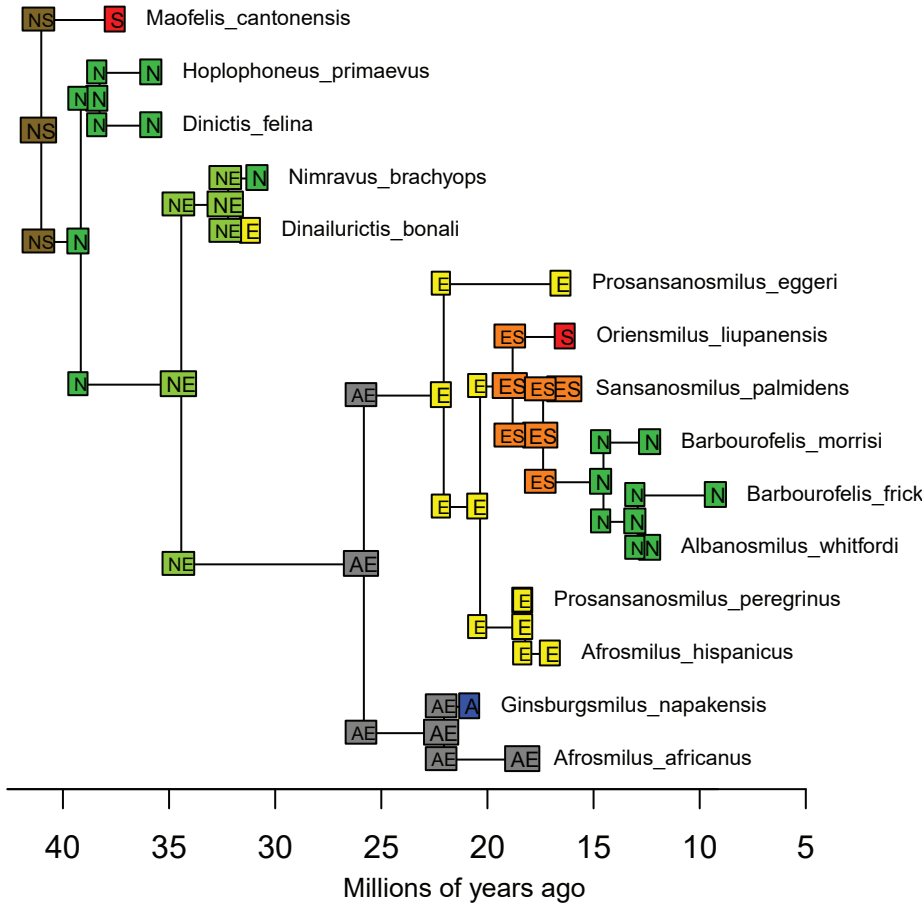

Figure S52. BioGeoBEARS BAYAREALIKE on Nimravidae M0_unconstrained ancstates: global optim, 4 areas max. d=0.0305; e=0.1352; j=0; LnL=−33.70

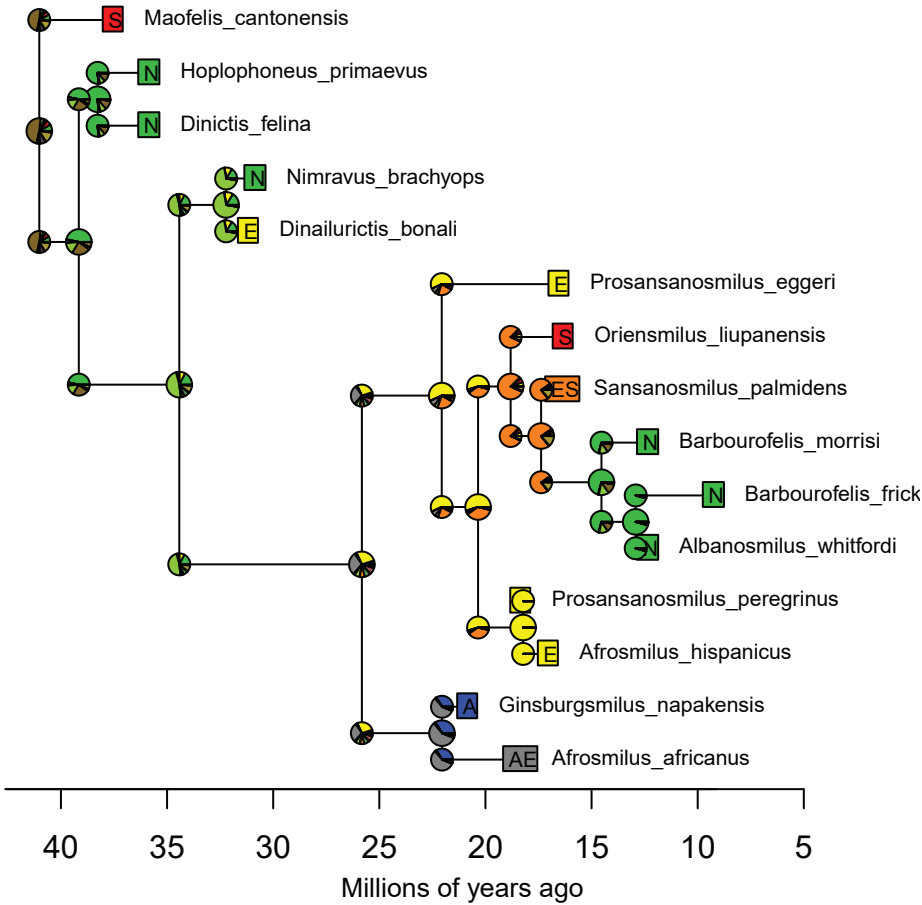

Figure S53. BioGeoBEARS BAYAREALIKE+J on Nimravidae M0_unconstrained ancstates: global optim, 4 areas max. d=0.0092; e=0; j=0.1523; LnL=−24.74

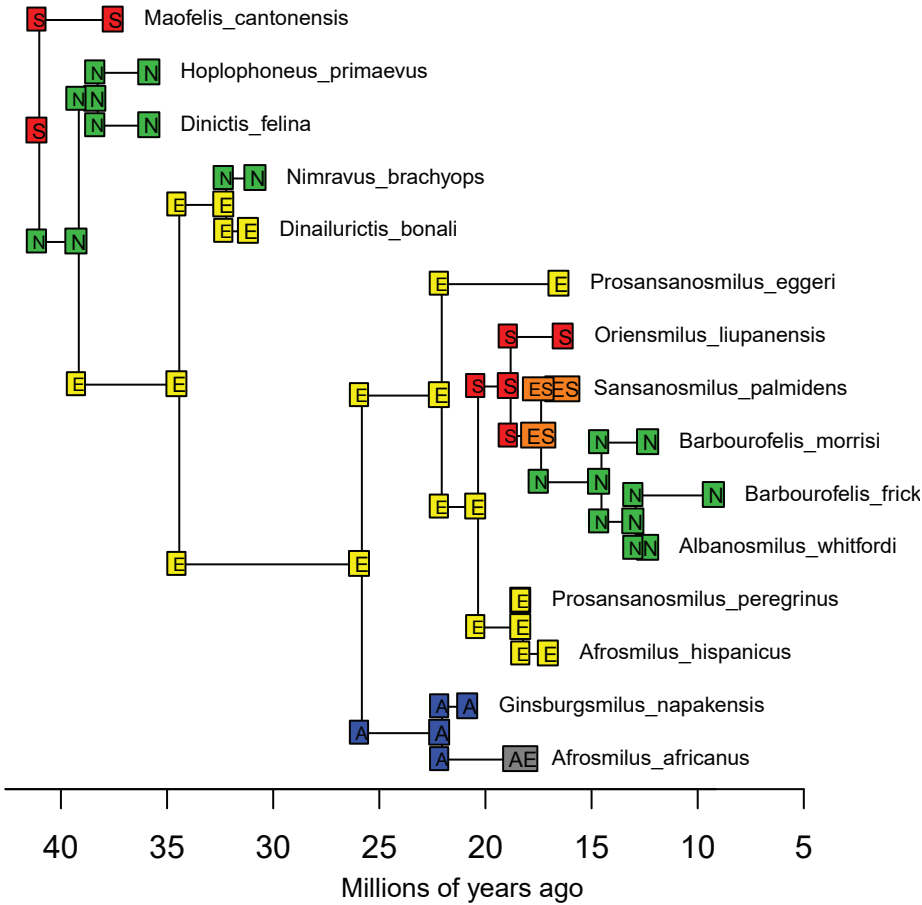

Figure S54. BioGeoBEARS BAYAREALIKE+J on Nimravidae M0_unconstrained ancstates: global optim, 4 areas max. d=0.0092; e=0; j=0.1523; LnL=−24.74

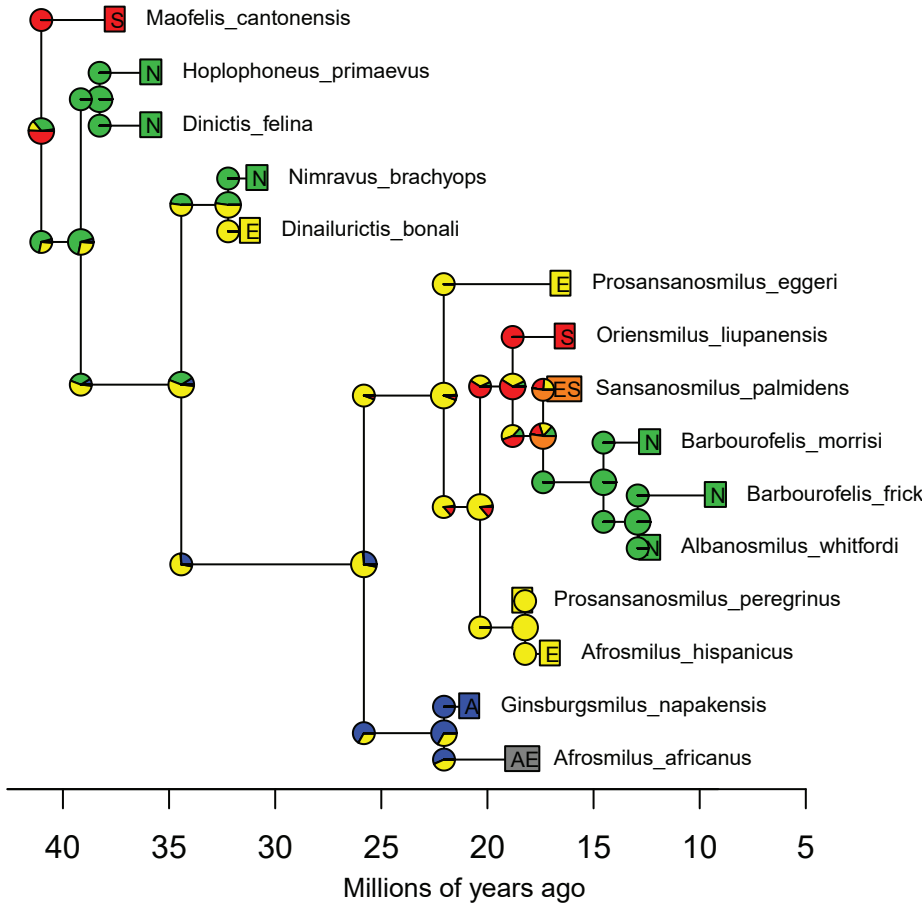

Figure S55. DIVALIKEj:
ML state probs vs. mean of BSMs